Response to reviews

We want to thank the referees for appreciating our work and for the thoughtful comments and suggestions. Most of them have been taken into account to improve the manuscript. We apologize for the difficulties associated with the length of the manuscript and excessively long sentences. We have re-worked the manuscript and addressed each comment. In the text below, the reviewerøs comments are marked in italics blue and our answers are given in normal font.

As the referee has correctly pointed out, the method itself is not new (the first author developed it in the 1990øs for TOVS), and there exist several publications, which are referenced in the article. Indeed it was a difficult task to select what should be presented and what left out, which is reflected in differing opinions of the 2 referees.

Since both referees suggested to shorten the manuscript, we have done our best to do it without losing the message we wanted to deliver to the community. Here is the list of actions performed

1) shortening section 2 ôData and methodsö and moving a shortened version of section 3.1 ôCollocated AIRS-CALIPSO-CloudSat dataö to this section

2) simplifying Table 2, taking out 5 figures / 22 figure panels (3 figures moved to supplement)

3) taking out the ENSO discussion in section 5 (together with Fig. 16) and

4) revising the remaining applications in section 5

We do not agree with the suggestion of a complete removal of section 5 ôApplicationsö, as the presented method is not new and one of the goals of this article was to present scientific applications (as indicated in the title).

Since the results similar to those presented in new Fig. 12 have recently been published for other data sets, it would be difficult to use the presented material in a separate publication. We compare our results to one of them and point out an interesting extension. We plan to work on a more complex analysis to pursue this subject further, but we think itøs important to present already these results in the current publication.

Response to Referee#1

Title: the authors should consider a better title that is punchier and emphasizes the great aspects of using sounders for cloud properties (and not have ôweaknessesö in the title)

the title was changed to : **Cloud climatologies from the InfraRed Sounders AIRS and IASI: Strengths and Applications**

Abstract: it is pretty long and not very specific. For instance, lines 24-28 has a single long sentence making multiple points about the apparent cloud top/base. Is the correction for co2 really that original and worth advertising in the abstract? On lines 23-24, the ôglobal cloud amountö is detected clouds, not effective emissivity?

We have substantially re-worked the abstract, to be more specific.

Rewritten to: The global cloud amount is estimated to 0.67 ï 0.70, for clouds with IR optical depth larger than about 0.1. The spread of 0.03 is associated with ancillary data.

It is really the amount of detected clouds; it is interesting to mention that global effective cloud emissivity of detected clouds is very similar: 0.65-0.66;

This leaves global effective cloud amount (detected clouds weighted by cloud emissivity) to about 0.46-0.48.

p. 5, lines 20-21: did the authors try (or consider) using a SST data set independent of the IR sounders, say, RTG-SST or the optimal approach using microwave made available at www.remss.com?

There are two philosophies in creating cloud climatologies : 1) ancillary data are also taken from observations, and 2) ancillary data are taken from model forecast or meteorological reanalyses. The advantage of the first is that these climatologies are independent of model input, however the problem is that the ancillary data might have biases due to faults in clear sky detection and due to interpolation when no good quality data are available.

In this article we compare these approaches; for the first one, we preferred to stay with data which include the same instrument (the ancillary data come from a combined IR sounder ï microwave retrieval). For IASI, at the time of the development, the available ancillary data did not have the quality needed. Therefore we switched to the second approach.

A separate SST data set would not help, as we also need surface temperature over land, and both are needed at the satellite observation times. I addition they also should be coherent with the retrieved atmospheric profiles.

p. 5, lines 23-24: ózquite differentôz is not quantitative and not useful in the context of this discussion. How different were they?

Rewritten to: The comparison with collocated temperature profiles of the Analyzed RadioSoundings Archive (ARSA, available at the French data centre AERIS) has shown that, while AIRS-NASA and ERA-Interim (section 2.3) temperature profiles do agree in general with the ARSA profiles within 1 K, differences between IASI-NOAA and ARSA profiles were often larger than 1 K in the lower troposphere (not shown).

In the following plots we present differences in T profiles between NASA AIRS V6 and ARSA, ERA Interim and ARSA and NOAA IASI and ARSA, separately for different latitude bands over land (above) and ocean (below). Whereas AIRS and ERA agree in general within 1K, NOAA IASI differs from ARSA often more than 1 K in the lower troposphere.

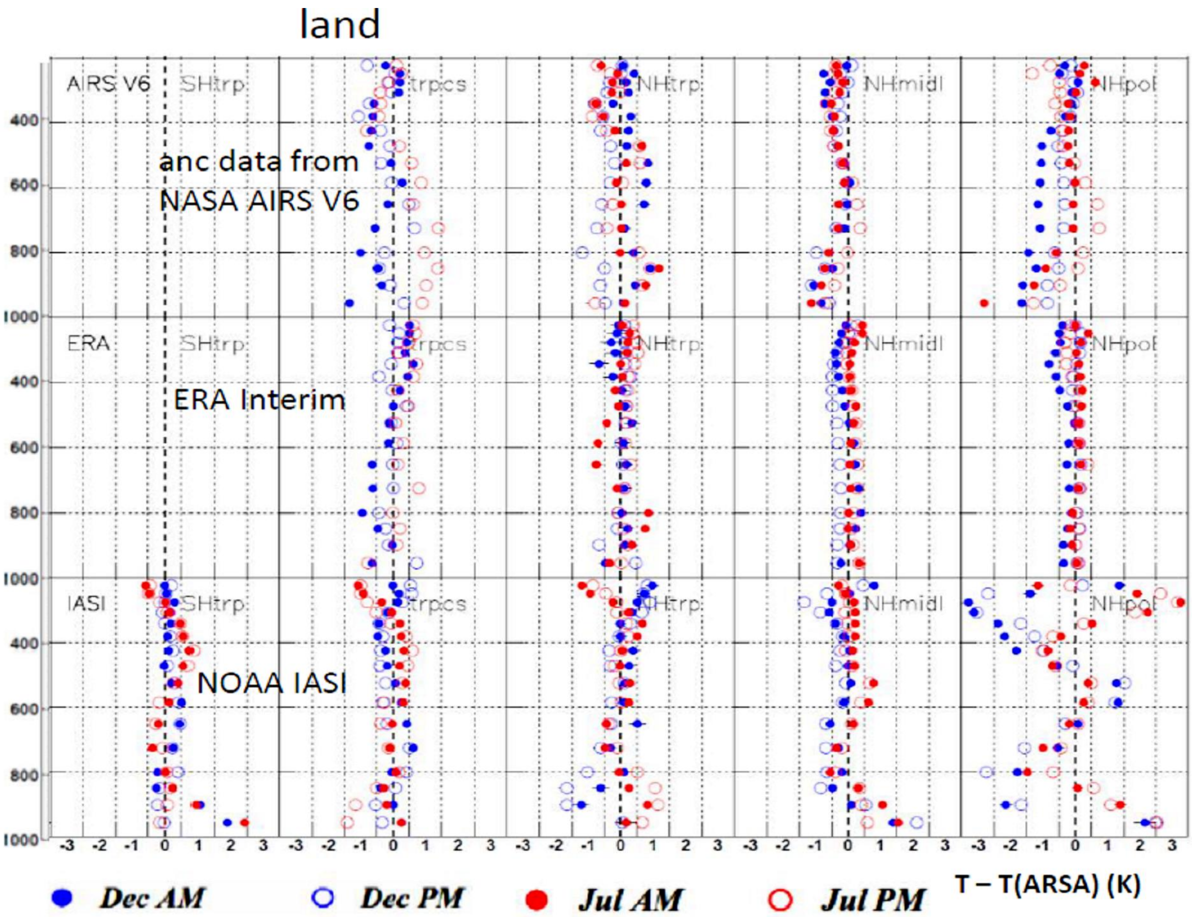

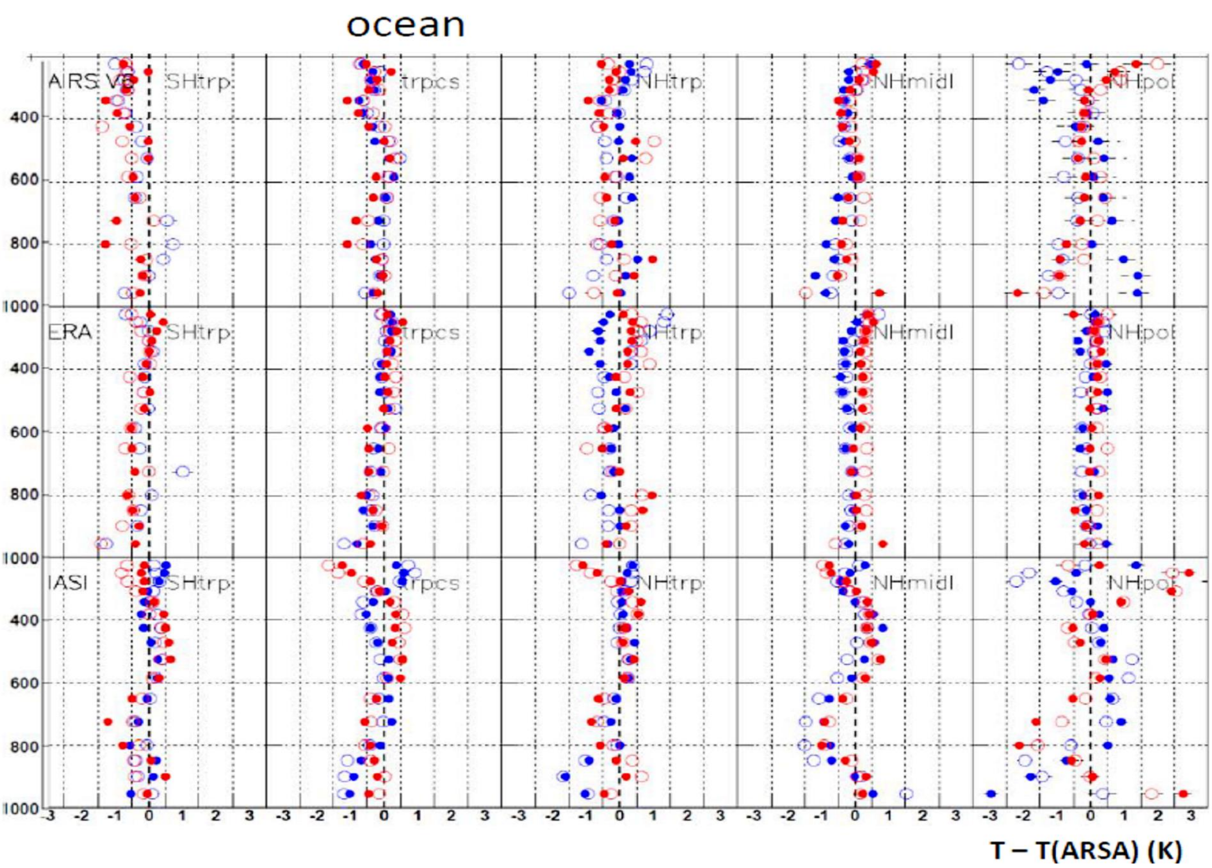

Line 25: the IASI and AIRS sounders will not resolve the diurnal cycle but will capture aspects of it.

We agree that the diurnal cycle is difficult to resolve with data given in temporal intervals with 4h ï 8h ï 4h ï 8h, but as one can see in the cited conference proceeding (publication is under preparation), by using appropriate analysis techniques, both the amplitude and phase of the diurnal cycle of upper tropospheric clouds can be obtained, especially due to the fact that IR sounders provide unbiased day-night results.

Rewritten to :

This brought us to the conclusion, that ancillary data from the same source are necessary to make use of the AIRS ï IASI synergy for exploring cloud diurnal variability in a coherent way.

Lines 26-27: if it is of any help, there is a paper that describes cloud type comparisons between AIRS and ECMWF T/q:

Yue, Q. et al. (2013), Cloud-state dependent sampling in AIRS observations based on

CloudSat cloud classification, J. Climate, 26, 8357ï8377.

Unfortunately this very interesting article refers to NASA AIRS L2 data of Version 5 ;

We have used in our revised cloud climatology NASA AIRS L2 data of Version 6

p. 6, lines 9-12: the variables should be listed here (e.g., T, q, emissivity, sfc T, etc.)

the whole paragraph was taken out, as this issue was already partly discussed in 2.2.

p. 7, lines 11-12: here is a good example of over explaining. Why should ófor which temperature first increases with height before decreasingô be included? This is technically only true if ascending in the atmosphere. Line 12: ómoved to the inversion layerô is not clear. Is the cloud placed at the base of the inversion? Hopefully not the top because that would be impossible in reality. Line 14: ó . .about 7 to 15% of the time.ô

Text improvements taken into account.

In the case of an inversion, the cloud height is set to the level at which the temperature starts to decrease with height.

p. 8, lines 20-23: this statement is unclear. How can óclear skyô be ónot too cloudyô?

text in parentheses taken out; the synergy of IR sounder and microwave also leads to retrievals for party cloudy scenes. In that case, a ócloud clearingô is performed before the retrieval.

p. 9, line 7: there is a specific QC approach that filters based on a PBest or PGood pressure level. Was this done on a per profile basis? Or were the Level 3 gridded AIRS Team products used?

We used the quality criteria on a per profile basis, as we work with L2 data ; reference added

p. 9, lines 8-9: there is a paper that describes AIRS surface temperature biases with respect to ship observations:

Dong, S., S. T. Gille, J. Sprintall, and E. J. Fetzer (2010), Assessing the potential of the Atmospheric Infrared Sounder (AIRS) surface temperature and specific humidity in turbulent heat flux estimates in the Southern Ocean, J. Geophys. Res., 115, C05013, doi:10.1029/2009JC005542.

Again, the problem is that this paper refers to AIRS V5 ; we had problems to find published results for the AIRS V6 version, apart from the V6 L2 Performance and Test Report.

p. 9, line 11: with respect to what is the land more complex?

We meant that there was not a clear bias found as over ocean ; clarified in the text to :

Since differences over land might be positive or negative (Fig. 2), we left the AIRS-NASA surface temperature (T_{surf}) values as they are.

p. 10, line 23: is the artifact in cloud amount causing more clouds? Less clouds? Higher clouds? Lower clouds?

Global cloud amount is increasing, when the CO2 increase is not taken into account in the computation of atmospheric spectral transmissivities (new Fig. 10);

When splitting into low-level and high-level cloud amounts, the artefact led to increasing CAL and slightly decreasing CAH.

p. 11, line 3: base of the inversion?

In the case of atmospheric temperature inversions, the cloud height is moved to the level at which the temperature starts to decrease with height, and ε_{cld} is scaled accordingly.

p. 11, line 25: is ónot cloudyô the same as ócleará? or something else?

As the IR sounder footprint size is large, it is difficult to distinguish between completely clear sky and cloudy. Even the evaluation with CALIPSO-CloudSat stays approximate as the sampling is only about 1.5 km x 2.5 km, which corresponds to a sampling of about 2 %.

p. 12, line 10: óexplainableô should be óexplainedâ The paper could use a good thorough editing for clarity of English.

Unfortunately, all authors are non-native English speakers; we tried however to improve the readability of the present version to the best of our abilities.

p. 12, lines 14-16: are there three different sigmas for the three different emissivity_i values? It appears that some of the clear will be selected as cloudy, and vice-versa. Is this correct?

The thresholds were chosen separately for 1) ocean, 2) land and 3) snow/ice, as the distributions in new Fig S1 (original Fig. 2 moved to the supplement) showed slightly different distributions. Indeed, all methods using thresholds include misidentifications. These are difficult to estimate because of the sampling (2% of CALIPSO-CloudSat per AIRS footprint). The cloud detection includes 80 (over ice) to 92% (over ocean) cases for which CloudSat-lidar GEOPROF and CALIPSO at 5 km resolution (excluding subvisible cirrus) have identified at least one cloud layer, and 30% cases for which the samples did not include a cloud layer. The latter might look at first as a large misidentification of clear sky as cloudy, but the very small coverage of the CloudSat-CALIPSO samples (2%) certainly includes partly cloudy fields.

Results in section 3 show that by using these thresholds the overall agreement with CloudSat-CALIPSO is 70% (over ice) to 85% (over ocean), given as hit rates.

p. 12, lines 20-21: the emis < 0.1 threshold is very conservative. The IR sounders will capture a lot of optically thinner clouds than that. Are the authors arguing the point that below that threshold some clear values could leak in? The paper by Kahn et al. (2008) seems to argue that the emis threshold could be lower than that:

Kahn, B. H. et al. (2008), Cloud-type comparisons of AIRS, CloudSat, and CALIPSO

cloud height and amount, Atmos. Chem. Phys., 8, 1231ï1248.

Indeed, the AIRS-LMD climatology (Stubenrauch et al. 2010) went down to an ε_{cld} of 0.05.

Considering the large footprint and a comparison of ε_{cld} distributions for cloudy and clear sky CloudSat-CALIPSO scenes (see below), we decided to exclude scenes with $\varepsilon_{cld} < 0.1$.

We made the sentence more explicit : To reduce misidentification of clear sky as high-level clouds, only clouds with ε_{cld} Ó0.10 are considered.

Indeed, this came out of a study with CALIPSO-CloudSat :

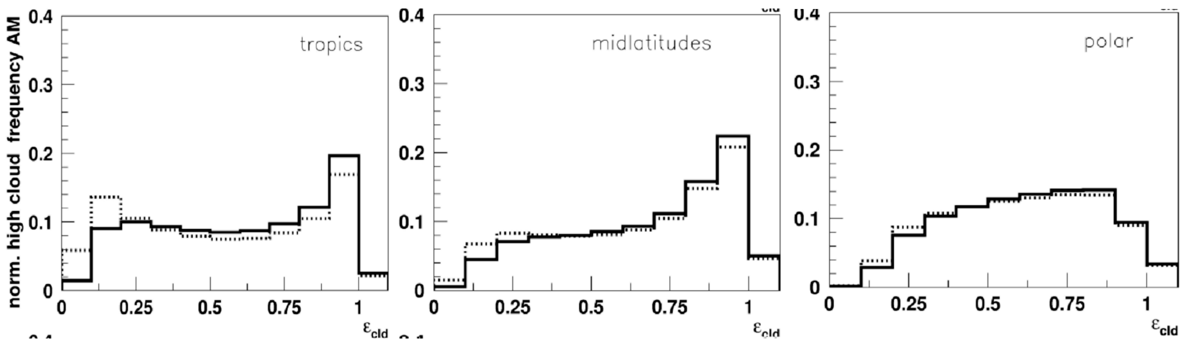

The above figures present normalized ε_{cld} distributions of high-level clouds, after multi-spectral cloud detection, but leaving clouds with $0.05 < \varepsilon_{cld} < 0.10$ as clouds, separately for cloudy scenes defined by GEOPROF and CALIPSO (full line) and for all scenes (dotted line). The first bin includes scenes with $0.05 < \varepsilon_{cld} < 0.10$; in the tropics this bin has more clear sky than high-level clouds. Therefore we have moved the threshold to 0.1. As the contribution of the first bin is small compared to the integral, this seemed a reasonable choice.

p. 12, section 3.1: this is where the paper starts to be a real grind. Wasnât the methodology of the AIRS and C/C comparison described in a previous paper(s) by the lead author? There must be a way to tighten this up and make it more concise, but I am lacking any good suggestions for that.

Indeed, part of the description of the collocated dataset was already published before, though not the computation of the cloud height corresponding to a specific optical depth. Referee #2 finds that this section is not detailed enough.

We have rewritten this section and moved it to section 2.4, hoping that in this way the paper gains clarity. It also allows the reader who is only interested in the results, directly to go to sections 3-5.

p. 14, start of Section 3.2: it is really nice to see that the level of agreement is very similar to the AIRS Team cloud retrievals in Kahn et al. (2008) with a finer breakdown of surface type and ancillary data.

We donôt completely agree with the statement about the level of agreement with the AIRS cloud data from NASA V5: one important difference is that while the AIRS NASA V5 cloud data agree well for high-level clouds, they have a very large height bias for low-level clouds. This is stated by the Kahn paper: a bias which reaches about 5 km ! Actually, this was the reason for adapting the χ^2 retrieval method to AIRS. Our comparison with the NASA V5 AIRS cloud height was published (Fig. 12) in 2008. Our goal was to build a cloud climatology which is reliable for all clouds. If this is not the case, there will be many cloud type misidentifications. Though the retrieved properties of low-level clouds might be noisier, it was important that their height is not biased, so that they are not confounded with higher level clouds.

Kahn et al. have published a new version of the NASA AIRS cloud climatology, but as unfortunately the team does not yet participate in the GEWEX cloud assessment (though invited), a direct comparison is difficult.

Is the fact that the percentage is slightly higher over ice/snow indicative of a loss of skill at sounding T/q over these surfaces, and Era-Interim is superior? What is different about these profiles over ice/snow? Better detection of inversions and isothermal layers in ERA-Interim?

The frequency of retrievals with good quality decreases over ice/snow, probably also because clouds over these surfaces are more difficult to detect. In addition, polar regions might oft be covered by clouds (especially in SH ocean). We show a map of relative frequency of good quality retrievals of T_{surf} for December 2007, at 1:30AM LT (criteria described in 2.5.1). When only 10% of the time during a month, data are available and the meteorological situation is very variable during the month, the interpolation gets to its limits, whereas ERA-Interim data are always available. ERA-Interim also detects twice more inversions than AIRS (though we do not know which of the dataset is closer to the reality).

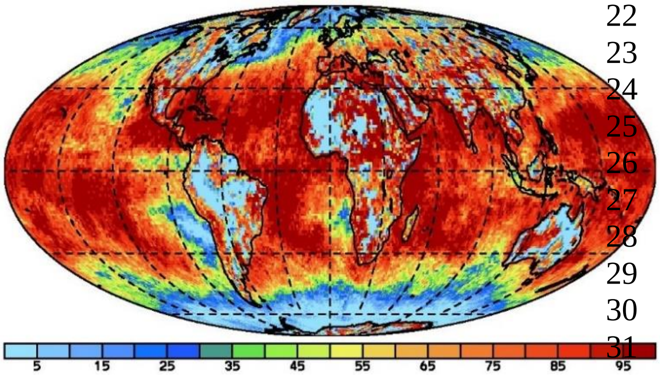

Rel. frequency of good quality Tsurf, Dec 2007, 1:30AM

p. 14-16: section 3.3: this section is extremely long and detailed. A lot of it seems consistent with previous paper by the first author. Around lines 31-32 on p. 15 there is one quite interesting point about opaque clouds and a reduced geometrical thickness. Could this be because the IWC is larger in these clouds and thus leads to a smaller difference between the sounders and CALIOP?

This reminds me of a paper by Sherwood et al. discussing these types of discrepancies:

Sherwood, S. C., J.-H. Chae, P. Minnis, and M. McGill (2004), Underestimation of

deep convective cloud tops by thermal imagery, Geophys. Res. Lett., 31, L11102,

doi:10.1029/2004GL019699.

We have substantially shortened this section, also by taking out Fig. 6 and taking out 3 panels of Fig 4 and moving 3 panels of Fig 5 to the supplement. We also tried to be more concise. Compared to Stubenrauch et al. 2010, the estimation of the height at which the cloud reaches a COD of 0.5 is new, though one has to keep in mind that it depends on several assumptions (section 2.4). Concerning the slight drop in difference between z_{cld} and z_{top} for ε_{cld} close to 1, it probably means that for these clouds opacity is reached within a smaller vertical extent, as for those clouds z_{cld} also corresponds to the mean between top and height at which clouds gets opaque. We cited the Sherwood paper in Stubenrauch et al. 2010, where we had already shown that z_{top} - z_{cld} increases with z_{top} -$z_{(app\ base)}$, reaching up to 3 km.

p. 17-21, Section 4: another really long section with figures 8-14 that have a combined total of over 80 sub-panels. A lot of these figures are known from previous papers or are common knowledge. Some of these panels appear to show some redundant information. I would suggest trying to trim this down as much as possible and try and keep the information to the most interesting and novel bits.

We took out 16 panels of Fig. 10-13 and 6 panels of Fig. 14, which we also moved to the supplement. This leaves 5 Figs, and we shortened the discussion. On the other hand, we want to show the quality of the new climatologies, so we have to show some comparisons, even if they might not be novel.

p. 19, lines 25-27: I donôt see why ówhich might have important consequences on radiative feedbacksô should be there. Since the SW and LW budgets are not shown with respect to the different cloud types described in the paper, this is speculative. I would further emphasize that there are many other interesting things about these particular clouds, including the hydrological cycle, not just radiation and its feedbacks.

We agree with this suggestion so we took this part out and shortened the sentences to:

The independent use of p_{cld} and ε_{cld} made it possible to build a climatology of upper tropospheric cloud systems, using ε_{cld} to distinguish convective core, cirrus anvil and thin cirrus of these systems. These data have revealed for the first time that the ε_{cld} structure of tropical anvils is related to the convective depth (Protopapadaki *et al.*, 2017).

p. 20, lines 27-28: Are the authors suggesting that the global cloud amount should be related to the global surface temperature? Is there a previous reference that argues for this? Most studies show a relationship of the patterns of global cloud distributions, height, types, etc. can change with respect to global averaged surface temperature, but Iôve never seen an argument for an average global cloud amount. Also, another point here regarding surface temperature that it did not increase much. If the authors are referring to the alleged óhiatusô, I think that is basically proven that there was no hiatus (a recent paper by T. Karl at NOAA).

http://science.sciencemag.org/content/348/6242/1469

Thank you for the interesting article. We just wanted to make the point that global cloud amount stays stable during this period; we have removed the sentence about surface temperature.

p. 21, lines 28-29: what is the justification to relate infrared derived cloud amount to SW reflected radiation? Are there any previous papers that have shown a correlation? The infrared derived cloud amount saturates around an optical depth of 5 or so, but the SW does not. How can the infrared derived cloud products be used to infer consistency with SW results?

We talk here about total CA, which we have shown in section 4 to be consistent with all other climatologies. Also CAH, CAM and CAL are reliably identified, as all discussions in section 4 have shown ! Indeed the effective cloud emissivity saturates at 1 (corresponding to visible COD of about 10), while VIS COD continues to increase. However, the paper of Stephens et al. 2015 is relating the planetary albedo to cloud amount.

p. 22, lines 1-3: how can the CAH be used as a proxy for precipitation rate? Because the ITCZ is narrower in the CIRS data, one can infer a more intense precipitation rate? I'm not sure I understand the logic used here.

We understand the InterTropical Convergence Zone as the zone with strong convection which then produces large cirrus anvils. The latter stay longer in the atmosphere than the convective towers themselves. It is also seen in all maps that the ITCZ has a strong occurrence of high-level clouds (which are mostly cirrus anvils, see for example (Protopapadaki *et al.* 2017)). Hence, we assume that the ITCZ can be determined by the latitude with a peak in CAH (new Fig. 8). We have partly rewritten this section and hope that the motivation and analysis are easier to follow.

p. 22, first paragraph of Section 5.2: there is no reason to have a basic tutorial on ENSO in the paper. The authors should just get to the results and describe what is novel and delete that part.

we have taken out the introduction and Figure 16 and its discussion.

Figure 3: numbers are too small and blurry for reading

fixed in new Figure 2

Figure 4: why bother with the right column? Weren't these differences previously described by the lead author?

Right column taken out

Figure 6: three figures in a row describing apparent cloud top and biases with CALIOP. Need to emphasize the novel results and parts of figures that support them. The numbers are overlapping on the x-axis at the edges of the subpanels too.

Figure taken out and added quartiles to Fig 4, so that the width of the distributions are shown together with the medians; this makes the discussion more concise

Figure 13: can't tell the difference between open and closed red circle, red square, and red dashed line

fixed in new Figure 10

Figure 14: the seasonal variability in latitude bands is well understood. What is new in this figure? Are there new insights between different instruments and inferences of the seasonal cycle?

Panels with CAM taken out and Figure moved to supplement (new Figure S4); there is nothing new, it is just to show the quality of the new cloud climatologies, compared to other datasets.

Response to Referee #2

5 particular issues that need further explanation:

- the role of CALIPSO-CALIOP data for tuning the method

The cloud property retrieval was originally developed for TOVS data (Stubenrauch et al. 1996, 1999, 2006); at that time the cloud detection, which indeed was applied before the cloud retrieval, was essentially based on interchannel regression tests using a combination of IR sounder and microwave (MSU) brightness temperatures.

When we adapted the cloud retrieval to AIRS, channel 7 of AMSU did not work, so we could not adapt the cloud detection. However the retrieval itself provides cloud pressure and emissivity for each measurement (only about 5% of the data do not give a solution, these are declared immedeately as clear sky). We then considered it more interesting to develop a cloud detection which could be applied after the retrieval. The idea was to test the reliability of the results to decide if a footprint is cloudy. By comparing clear sky and cloudy scenes determined within time synchroneous samples from CALIPSO L2 5km cloud data, provided by NASA, we found that the relative spectral spread of cloud emissivities determined at atmospheric window wavelengths is small if the footprint contains a cloud for which the cloud height and emissivity are well determined (both are used in the computation of the spectral emissivities), while most clear sky scenes lead to very large values. These distributions have been published in Stubenrauch et al. 2010, and for the retrievals with new ancillary data in Fig. S1. These distributions show a nice distinction between clear and cloudy, but the thresholds themselves have been determined by examining many different aspects, like maps and comparison with other datatsets, distributions separately over tropics, midlatitudes and polar regions. One important aspect was also to test that AIRS, using two different ancillary data sets, together with IASI gave coherent answers, day and night.

So, the CALIPSO-CloudSat data have been essential to guide us in the cloud detection, but they were not used to tune it.

- the exact description of the used CALIPSO dataset for tuning and for evaluation of cloud properties

Again we want to stress that we did not use CALIPSO for tuning.

We have moved the section of the collocated AIRS-CALIPSO-CloudSat data forward, so that the description is placed before the description of the cloud detection. It was well written that we used version 3 of the NASA CALIPSO L2 cloud data averaged over 5 km (Winker et al. 2009) ; and we explained the procedures how we used the data (for example excluding subvisible cirrus). By the way, we published comparisons with lidar already in 2005, when we compared TOVS Path B cloud properties with LITE (Stubenrauch et al. 2005) where we also investigated subvisible cirrus. In this paper we just wanted to show that the CIRS cloud data are of slightly better quality than the AIRS-LMD cloud climatology, and the effect of ancillary data, which in our opinion has not been stressed with other cloud climatologies.

- the consequence of using some unphysical assumptions in the retrieval

We accept cloud emissivities up to a value of 1.5, due to noise. This is explained in the reference Stubenrauch *et al.* 1999, which is cited :

As in Eq 2 the denominator includes two terms (Icld and Iclr) which get very close to each other in the case of low-level clouds, the cloud emissivity can get larger than 1 when taking into account uncertainties. In Stubenrauch et al. (1999), it was shown that the original method, which excluded values larger than 1, underestimated the amount of low-level clouds considerably.

The limit larger than 1 has been chosen to compensate for radiation noise and ancillary data uncertainties and this leads to a better identification of low-level clouds.

- the balance between finding spectral coherence in the solutions and still maintain physically reasonable emissivity differences

The multi-spectral cloud detection is indeed based on wavelengths in an interval which is sensitive to thermodynamical phase and ice crystal sizes. As can be seen in Fig. 3 of Guignard et al. (2012), the relative cloud emissivity difference between 9 µm and 12 µm can go up to 0.3 for small IWP and ice crystal size. However, instead of using a spectral difference, we use a standard deviation between 6 wavelengths, divided by retrieved cloud emissivity. This should be always smaller than 0.15, even in the case of small IWP and ice crystal sizes which produce the largest slope (we have studied that in detail when developing the method in 2010). In this empirical method, the error one makes, if the used cloud pressure does not correspond to the real pressure, is larger, and Fig. S1 (of the supplement) illustrates nicely, that this relative standard deviation is larger than 0.3 for clear sky scenes, while for cloudy scenes distributions the distributions are really narrow, using CALIPSO-GEOPROF to separate cloudy and clear sky scenes.

- justification of the statement of achieving successful cloud detection down to IR cloud optical thicknesses of 0.1

optical thickness can be deduced from cloud emissivity as COD = - ln(1-ε_{cld})

As we present clouds with ε_{cld} > 0.1, this corresponds to clouds with IR COD > 0.1 (or with VIS COD > 0.2 as VIS COD = -2ln(1-ε_{cld}).

To reduce misidentification of clear sky as high-level clouds, only clouds with ε_{cld} Ó0.10 are considered.

Indeed, this came out of a study with CALIPSO-CloudSat :

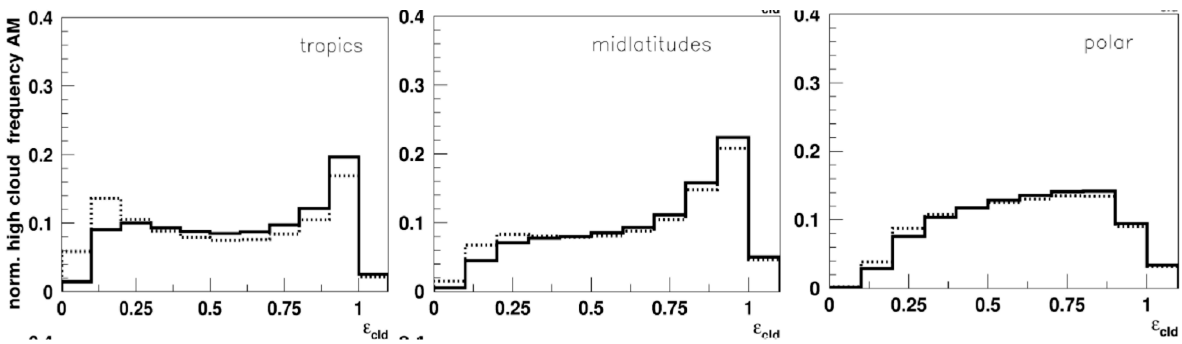

The above figures present normalized ε_{cld} distributions of high-level clouds, after multi-spectral cloud detection, but leaving clouds with 0.05 < ε_{cld} < 0.10 as clouds, separately for cloudy scenes defined by GEOPROF and CALIPSO (full line) and for all scenes (dotted line). The first bin includes scenes with 0.05 < ε_{cld} < 0.10; in the tropics this bin has more clear sky than high-level clouds. Therefore we have moved the threshold to 0.1. As the contribution of the first bin is small compared to the integral, this seemed a reasonable choice.

Specific comments

1. Page 1, Abstract, line 19, ñto evaluateò:

The term ñto evaluateò should be changed to ñto design and evaluateò. You used A-train data to find your óa posterioriô cloud masking thresholds, right? Then you should be clear in your description that A-train data is not completely independent from your data/method. This is important for the reader to know.

We do not quite agree with this comment; the cloud retrieval was originally developed for TOVS data (Stubenrauch et al. 1996, 1999, 2006); at that time the cloud detection, which indeed was applied before the cloud retrieval, was essentially based on interchannel regression tests using a combination of IR sounder and microwave (MSU) brightness temperatures.

When we adapted the cloud retrieval to AIRS, channel 7 of AMSU did not work, so we could not adapt the cloud detection. However the retrieval itself provides cloud pressure and emissivity for each measurement (only about 5% of the data do not give a solution, these are declared immedeately as clear sky). We then considered it more interesting to develop a cloud detection which could be applied after the retrieval. The idea was to test the reliability of the results to decide if a footprint is cloudy. By comparing clear sky and cloudy scenes determined within time synchroneous samples from CALIPSO L2 5km cloud data, provided by NASA, we found that the relative spectral spread of cloud emissivities determined at atmospheric window wavelengths is small if the footprint contains a cloud for which the cloud height and emissivity are well determined (as both are used in the computation), while most clear sky scenes lead to very large values. These distributions have been published in Stubenrauch et al. 2010, and for the retrievals with new ancillary data in Fig. S1. These distributions show a nice distinction between clear and cloudy, but the thresholds themselves have been determined by examining many different aspects, like maps and comparison with other datatsets, distributions separately over tropics, midlatitudes and polar regions. One important aspect was also to test that AIRS, using two different ancillary data sets, together with IASI gave coherent answers, day and night.

So, the CALIPSO-CloudSat data have been essential to guide us in the cloud detection, but they were not used to tune it.

2. Page 1, Abstract, line 23, ñcoincidesò:

To use the term ñcoincidesò here is a too strong conclusion from your results. Figure 6 (lower right panel) clearly shows a rather broad distribution of results where frequencies at the two extremes (0 and 1) are still about 20-25 % of the frequency for the value 0.5 (representing the middle of the defined layer).Therefore you can possibly only state that the cloud height can be ñapproximatedò by the middle of the defined layer. Also ñmiddleò could possibly be replaced by ñthe mean layer heightò to make the description scientifically stricter.

3. Page 1, Abstract, line 27, ñapparent vertical cloud extentò:

The explanation here is confusing, indicating that upper level clouds generally have higher cloud emissivities than lower level clouds. This cannot be true. I guess the authors mean something else. Please clarify!

Rewritten as :

CIRS cloud height can be approximated by the mean layer height (for optically thin clouds) or the mean between cloud top and the height at which the cloud reaches opacity. For high-level clouds, especially in the tropics, this height lies on average 1 km to 3 km below cloud top.

4. Page 2, Abstract, lines 5-8, ñresponse to climate changeò + Page 3, Section 1, lines 23- 25 and the entire section 5: The last sentence in the abstract, the sentence about Section 5 in Section 1 and the entire section 5 could possibly be removed for shortening the paper (see also comment 25!).

We have considerable shortened section 5, but have left two main studies, which have been described in a more concise manner. The latter study is also compared to recent results using other data.

Changed last part of abstract to :

The 5% annual mean excess in high-level cloud amount in the Northern compared to the Southern hemisphere has a pronounced seasonal cycle with a maximum of 25% in boreal summer, in accordance with the moving of the ITCZ peak latitude, with annual mean of 4°N, to a maximum of 12°N. This suggests that this excess is mainly determined by the position of the ITCZ. Considering interannual variability, tropical cirrus are more frequent relative to all clouds when the global (or tropical) mean surface gets warmer. Changes in relative amount of tropical high opaque and thin cirrus with respect to mean surface temperature show different geographical patterns, suggesting that their response to climate change might differ.

5. Page 2, Section 1, line 11, ***ñ****70 % cloud cover* ***ò****:*

Although this is a widely used and accepted figure for global cloudiness, I would like to point out that a value of global cloud cover cannot be stated without first defining what you mean by a cloud. The figure 70 % is kind of representing clouds which have a significant impact on radiation budgets and it could possibly be relevant if you define that clouds should have at least a cloud optical thickness of approximately 0.2. But if including also the thinnest clouds (often called sub-visible clouds and so far only observed by high sensitive instruments like CALIPSO-CALIOP) the figure may increase to values well above 80 %. I think it would be appropriate to at least make a short statement on what clouds are considered when stating that global cloudiness is about 70 %.

Indeed, in the GEWEX Cloud Assessment we found out that global cloud amount is about 0.68±0.03 when considering clouds with VIS optical depth of larger than 0.2, and additional 0.06 arise from subvisible clouds detected by CALIPSO (Stubenrauch et al. 2013), which brings it to 0.74. This is written in Section 4.

It seems for us appropriate to leave the about 70%, as this sentence is the first in the introduction and is just meant to bring up the importance of clouds because of their large coverage. 7 lines further the reader finds more detail on the threshold (IR optical depth > 0.1).

6. Page 3, Section 1, line 3: ***ñ****optical depth less than 3* ***ò***

My impression is that the capability is better than that, i.e., the capability of having reasonable cloud optical depth estimations from CALIOP data covers the interval 0-5. Please check that the value of 3 is really justified.

The optical depth at which clouds are opaque is difficult to determine. In an earlier publication (Lamquin *et al.* 2008), we wrote that the upper limit lies between 3 and 5. One should not forget that the uncertainty is easily 20% due to uncertainty in multiple scattering contributions (Lamquin *et al.* 2008).

We have rewritten this in accordance :

Whereas the lidar can detect sub-visible cirrus, its beam can only penetrate the cloud down to optical depth of about 3 to 5 (in visible range). For optically thicker clouds, the radar provides the cloud base.

7. Page 7, Section 2.4, line 4, ***ñ****emissivities larger than 1* ***ò****:*

I must say that it is quite disturbing to ***ñ****be forced* ***ò*** *to use unphysical values in the retrieval. I understand that uncertainties can lead to this but I am not sure that this is then the best way of handling these* *uncertainties. Why not restrict emissivities to 1 in the optimization/minimization process when knowing that this is physically correct? I canôt see why your present method gives better uncertainty descriptions of the retrieved cloud pressures than when using a restricted emissivity value. Donôt inconsistencies give rise to new inconsistencies? Please explain and motivate.*

The reason is explained in the reference Stubenrauch *et al.* 1999 which is cited:

As in Eq 2 the denominator includes two terms (Icld and Iclr) which get very close to each other in the case of low-level clouds, the cloud emissivity can easily get unphysical when taking into account uncertainties. In Stubenrauch et al. (1999), it was shown that the original method, which excluded values larger than 1, underestimated the amount of low-level clouds considerably.

The limit larger than 1 has been chosen to compensate for radiation noise and ancillary data uncertainties and this leads then to a better identification of low-level clouds.

8. Page 7, Section 2.4, lines 22-28, ña posteriori cloud detectionò:

The ña posteriori cloud detectionò has already been briefly introduced (page 4, lines 7- 11). Why repeating this information here? Delete these lines or move part of this to the relevant section 2.5.

deleted

9. Page 9, Section 2.4.1, lines 18-20, ñocean cloud amounts larger during nightò:

To find larger ocean cloud amounts at night than during day is found in many regions (e.g. over marine stratocumulus areas). What made you think this was a problem specifically for ERA-Interim? Please explain.

The problem is not that the cloud amount is larger during night than during day, but that results are different when using two different sets of ancillary data ; we had to find out which dataset had a problem, and after some time we found that the amplitude of the ERA-Interim SST diurnal cycle is not in agreement with observations. It is reassuring that after applying a correction, this had a positive effect on the cloud amounts, as now the diurnal variation of cloud amount is more similar.

Rewritten to : Without this correction, the cloud amount (CA) at night / early afternoon was 78% / 71%, compared to 71% / 71% when using AIRS ancillary data. The correction led to 76% / 73%, closer to the results using AIRS ancillary data.

10. Page 10, Section 2.4.2:

The CO2 correction appears to be a very relevant change (also visualized nicely in Figure 13. This appears to be one of the most important improvements of the methodology. Should become mandatory in all sounding-based retrievals for climate datasets, in my opinion.

Thank you for the compliment ☺ In our case this was necessary, as the spectral transmissivities came from look-up tables computed for a fixed CO2 concentration.

Actually, Menzel *et al.* (2016) also use a varying CO2 concentration adjustment, for a 35-year HIRS cloud climatology.

11. Page 11, Section 2.5, general comment on the ña posteriori cloud detectionò:

The methodology appears a bit awkward compared to many other cloud retrieval methods in that cloud properties are first derived and then a determination whether a FOV is cloudy is carried out as a second *step. Most common otherwise is that a cloud screening is done first and then followed by a cloud property retrieval. So, could you confirm that after having performed the cloud property retrieval, all FOVs are still assumed to be cloudy? Does it mean that you will always find a solution to Equation 2? You have already mentioned some problems in finding a distinct minimum for lowlevel clouds (page 7, lines 2-3) but what happens in obviously cloud-free situations?*

Actually, we see this method as an advantage, because the method tests if the retrieved values are coherent, whereas most cloud detection methods use many different threshold tests, mostly based on brightness temperatures. We would have liked to adapt the cloud detection which was based on the comparison of temperatures (after correction for water vapour effects) obtained from HIRS to those of the microwave sounding unit MSU (developed for TOVS) to AIRS. Unfortunately, the AMSU channel which sounded closest to the surface did not work from the beginning. Therefore we have developed this method. Indeed, the χ^2 method provides in most cases (95%) a solution. The cloud detection is based on the coherence of spectral emissivities which are calculated using the retrieved cloud pressure. If the retrieved cloud pressure does not correspond to reality (as for clear sky or partly cloudy situations), the spectral variability gets large, as illustrated in Fig. S1.

We have now moved section 2.5 to section 2.4.3 and have rewritten part of the text.

12. Page 11, Section 2.5, line 16 + lines 20-21, ñmeaning of spectral coherenceò:

I am a bit concerned about the concept indicating that, for a cloud to be identified, the differences between emissivities in the six infrared channels should be small. In this wavelength region we know that the refractive indices of water and ice, respectively, varies considerably. For example, this is one of the fundamental properties that allows separating water clouds from ice clouds in passive imagery (e.g. as introduced by Pavolonis et al., 2005, J. Appl. Meteorol.). This fact would also certainly introduce considerable differences in cloud emissivities depending on if it is a water or ice cloud in addition to variations in optical thickness or partial coverage within each FOV. So, isnôt there a risk that the demand on spectral coherence is in conflict with reality? Or are you able to find a balanced and optimized method based on reference observations from CALIPSO-CALIOP data and still retain reasonable resulting emissivity differences? I guess that the access to CALIPSO-CALIOP data here is essential since it would be difficult otherwise (e.g. through detailed cloud model simulations) to find an optimal way here. Please comment.

The multi-spectral cloud detection is indeed based on wavelengths in an interval which is sensitiv to thermodynamical phase and ice crystal sizes. As can be seen in Fig. 3 of Guignard et al. (2012), the relative cloud emissivity difference between 9 μm and 12 μm can go up to 0.3 for small IWP and ice crystal size. However, instead of using a spectral difference, we use a standard deviation between 6 wavelengths, divided by retrieved cloud emissivity. This should be always smaller than 0.15, even in the case of small IWP and ice crystal sizes which produce the largest slope (we have studied that in detail when developing the method in 2010). In this empirical method, the error one makes, if the used cloud pressure does not correspond to the real pressure, is larger, and Fig. S1 (of the supplement) illustrates nicely, that this relative standard deviation is larger than 0.3 for clear sky scenes, while for cloudy scenes distributions the distributions are really narrow, using CALIPSO-GEOPROF to separate cloudy and clear sky scenes.

13. Page 11, Section 2.5, line 25, ñstandard deviationò:

How do you calculate the standard deviation here? Do you use all values in the ñAIRS golf ballò (i.e., 9 values) for the calculation for each wavelength? The current description is not clear enough on this.

It is a standard deviation over all 6 emissivities per AIRS footprint.

14. Page 11, Section 2.5, line 27, ñCALIPSO samplesò:

Unfortunately, here you introduce the use of CALIPSO data without having described what data you actually used (this description comes later in Section 3.1). More clearly, it is not obvious to the reader that you will get three CALIPSO samples in the AIRS golf ball. For this, you need to know that you use 5 km CALIPSO data. Because of the importance of A-train data for your method and study, I am of the opinion that you should have introduced them already in Section 2 on ñData and Methodsò. Can you consider changing this?

Section 3.1 now moved to section 2.4

15. Page 12, Section 2.5, lines 18-19, ñminimum optical depthò:

In the introduction section you mention that with IR vertical sounding data ñreliable detection of cirrus with IR optical depths as low as 0.1ò is possible indicating that this is much better than what can be achieved from other sensors (except from active sensors). I wonder what this restriction in order ñto reduce noiseò means in this context? Have you estimated further the minimum cloud optical depths being detected after introducing this restriction? CALIPSO-CALIOP offers the possibility to do such in-depth studies.

We made this sentence more explicit : To reduce misidentification of clear sky as high-level clouds, only clouds with ε_{cld} Ó0.10 are considered.

Indeed, this came out of a study with CALIPSO-CloudSat :

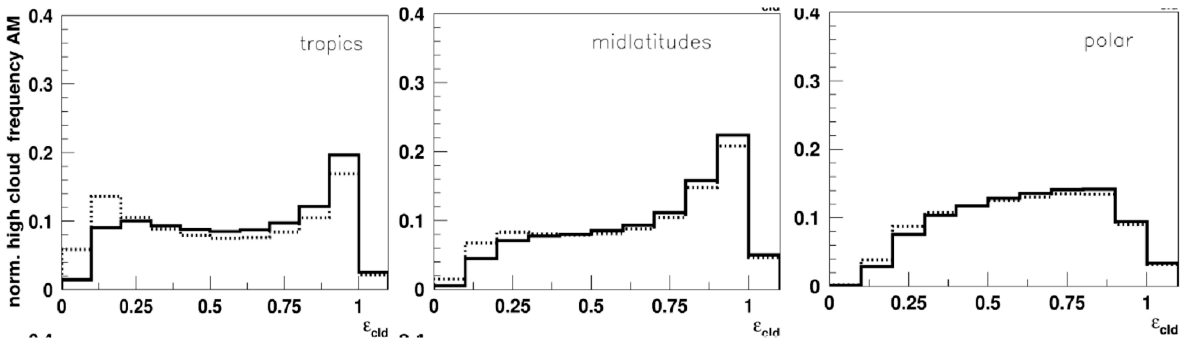

The above figures present normalized ε_{cld} distributions of high-level clouds, after multi-spectral cloud detection, but leaving clouds with $0.05 < \varepsilon_{cld} < 0.10$ as clouds, separately for cloudy scenes defined by GEOPROF and CALIPSO (full line) and for all scenes (dotted line). The first bin includes scenes with $0.05 < \varepsilon_{cld} < 0.10$; in the tropics this bin has more clear sky than high-level clouds. Therefore we have moved the threshold to 0.1. As the contribution of the first bin is small compared to the integral, this seemed a reasonable choice.

16. Page 13, Section 3.1, lines 16-19, ñCALIPSO and CloudSat dataò:

This requirement should mean (?) that you require that both CloudSat and CALIPSO say it is cloudy. But what about the fact that CALIPSO sees much more of the very thin cirrus clouds being available? Does it mean that these cirrus cases are not included in your evaluation study despite the fact that you several times have emphasized the capability of your method to detect very thin cirrus? Or is it different for studies of cloud amount (as indicated by description in lines 7-15) and cloud top height? Please comment!

We use CloudSat-lidar GEOPROF data, which detect a cloud layer when either CALIPSO or CloudSat detect a cloud layer (footprint 2.5 km x 1.5 km), and to add a different sampling (and because we needed a few other variables like COD) we use the CALIPSO 5km cloud data. In the latter we exclude subvisible cirrus (admitting only clouds detected with horizontal averaging < =5 km) for the evaluation, as we know that IR sounders are not sensitive to those. This corresponds to clouds with COD > 0.05 to 0.1, according to Winker *et al.* (2008).

Then, we require that both samplings detect a cloud, just to be sure that the sampling is coherent. These data are then used for all studies in this paper. We have tried to explain it better in the new section 2.4 :

é .The CALIPSO cloud data also indicate at which horizontal averaging along the track the cloud was detected (1 km, 5 km or 20 km), which is a measure of the COD. As in Stubenrauch et al. (2010), for a direct comparison with AIRS cloud data, we use clouds detected at **horizontal averaging over 5 km or less**. **This corresponds to clouds with visible COD larger than about 0.05 to 0.1** (Winker *et al.*, 2008). The scene type of an AIRS footprint is estimated as cloudy when the CALIPSO sample as well as the GEOPROF sample include at least one cloud layer. Clear sky is defined by cloud-free CALIPSO and GEOPROF samples within the AIRS footprint.

17. Page 13, Section 3.1, line 23, ñunderestimated CODò:

Just for your information: The latest version of the CALIPSO-CALIOP dataset (version 4.1) gives indeed higher CODs. This change can possibly be connected to what you write here (currently I do not know the details behind this change).

Thanks for this information!

18. Page 14, Section 3.2, lines 2-3, ñagreementò:

I have to ask you to specify better what you mean by ñagreementò. There are so many skill scores around so youôd better be strict in describing exactly the measure you use. I guess you refer to what is normally called ñHit Rateò which is the number of correct cloudy AND clear cases divided by the total number of cases.

Indeed, it is the hit rate which we have calculated. We have changed this in the text :

The hit rates between the óa posterioriô cloud detection and the CALIPSO-CloudSat cloud detection are 85% (84%) over ocean, 82% (79%) over land and 70% (73%) over ice / snow.

19. Page 14, Section 3.3, generally on results in Figure 4 (Page 40):

First, please revise the wording of the caption of this figure. The first sentence here is too complicated and the description should possibly be made more clear (the same is actually true for Figure 5). Also make clear (in all figures) what you mean by ñ1:30 LTò (AM or PM??). The question raised in the previous comment 16 remains: Are thin cirrus detected by CALIPSO but not by CloudSat part of this study or not?

If not, what can be said about the quality of these retrieved cloud heights (as compared to CALIPSO data alone)?

1 :30 is 1 :30AM, as defined in section 2.1 (1 :30 and 13 :30) ; however, as this leads to confusion with American readers, we will change this in the whole paper to 1 :30AM and 1 :30PM etcé

As explained before, for this comparison CALIPSO cloud data with COD > 0.05 to 0.1 are used.

The other referee suggested to take out the right panels of Figure 4 (which look very similar to the results published in Subenrauch et al. 2010). We have worked on all figure captions ;

Compared to the publication of Kahn et al. 2008 about the NASA AIRS Science team results of cloud height from Version 5, we show that in both cases, high-level clouds as well as mid- and low-level clouds the height is determined without bias, if one consideres the cloud height given by AIRS as the height of maximum lidar backscatter (Stubenrauch *et al*., 2010), by the mean layer height (for optically thin clouds) or the mean between cloud top and the height at which the cloud reaches opacity, as shown in Figure S2 (considering mid-p_{cld}), or by $z_{COD0.5}$ (Figure 3).

21. Page 16, Section 3.3, lines 5-24, Figure 7:

Very interesting and impressive results shown here! Results for medium and high clouds are probably quite superior to those being presented from passive imagery in other CDRs. Only for low-level clouds we still see quite some discrepancies which is understandable for several reasons. This indicates that the best representation of the true vertical distribution of cloudiness in a climate sense could be a combination of sounding and passive imagery data. Do you agree? Maybe you should mention this. Interesting is that problems for low clouds for sounding applications is not showing up very clearly later in Figure 9, except possibly during night for the land-ocean difference. Maybe you should explain why?

Indeed, a combination of IR sounder and passive imagery would increase the quality during day. During night, sounding provides better results, though the large footprints are a handicap for the identification of low-level cloud fields (as shown in the analysis of new Fig. 5). The concept of the CIRS retrieval was guided by the goal to create a cloud climatology with small biases, also for low-level clouds. Indeed, the noise is much larger for low-level clouds than for high-level clouds, but the biases are small compared to other IR sounder cloud climatologies. The comparison with CALIPSO-CloudSat comes to its limit in the analysis of new Fig 5, as the size of the footprints is very different.

20. Page 15, Section 3.3, line 9, ñcoincidesò:

See previous comment 2.

22. Page 16, Section 3.3, line 32, ñcoincidesò:

See previous comment 2.

26. Page 26, Section 6, line 1, ñcoincidesò:

See previous comment 2.

Replaced by ócan be approximatedô

23. Page 18, Section 4, lines 15-16, ñsensitivity of lidarsò:

You write that ñactive lidar is the most sensitiveò. Quite true but you havenât explained whether CALIPSO results in Figure 9 are already ñfilteredò (so that the thinnest clouds as given by the original CALIOP CLAY product are removed) or not. Has there been any filtering of ósub-visible cloudsô (I assume there has)? This is a relevant question to ask also for the statement in the Conclusions section on page 25, line 25. We need to know exactly what is the used CALIPSO dataset used as reference!

In section 4, the CALIPSO L3 data of the GEWEX Cloud Assessment data base are used ; two teams have provided their data, with the main difference by vertical (CALIPSO-GOCCP) or horizontal averaging (CALIPSO-ST), as mentioned in the text. The details of the GEWEX Cloud Assessment data base are found in (Stubenrauch et al. 2013) and especially in the WCRP report (Stubenrauch et al. 2012), where each team gave details how they created the L3 data. As I remember, CALIPSO-ST includes subvisible cirrus, which explains the larger CA, compared to all other datasets.

In section 3, L2 products have been used, as descibed in the new section 2.4.

24. Page 21, Section 4, line 4, Figure 14, ñSeasonal cycle of cloud temperaturesò:

How come there is a rather large consensus between different methods when studying cloud temperatures for the polar areas (leftmost and rightmost columns) when the spread is very large when it comes to cloud amount (top row of the same columns)? I suspect it is an indication of that cloud temperatures and surface temperatures are very similar here. This implies (in my opinion) that the separation of cloudy and cloud-free areas is indeed not very accurate. So, where is really the truth as regards polar cloudiness? Apart from this reflection, I consider Figure 14 as a very nice compilation of global cloudiness and its variation.

This actually shows that cloud amount, depending on thesholds, might be different by 10%, while the averages of retrieved cloud properties, which only can be given when a cloud is detected, are more similar. (Missing 10% does not mean that the average properties of the clouds are completely different). In addition the polar regions are to be considered with care, as written in the discussions : the CALIPSO data does not conform with the other data sets in the GEWEX Cloud Assessment data base, because they exclude measurements from 1:30PM during polar night (polar winter) and from 1:30AM during polar day (polar summer).

As a similar figure was already published in Stubenrauch *et al.* (2013) (though not CT), we moved this Fig. to the supplement, in order to shorten the paper, and as suggested by referee#1.

25. Pages 21-24, Section 5, ñbeyond scope??ò

In my opinion, Section 5 feels like out of scope of this study. Although introducing highly interesting topics (especially section 5.2), this work would benefit from being presented as a separate (or companion) publication. This manuscript is very, very long and it will put the readers (as it truly has for reviewers!) to a real test when digesting it. I would say that especially section 5.2 on the ENSO effects and its coupling to cloud/radiation feedbacks also requires a different category of expertize for reviewing it with more focus on modelling and studies of climate change and climate feedback effects. Consequently, I have not provided specific comments on this section and I suggest that it is removed for the shortening of this paper.

We do not agree with the suggestion of a complete removal of section 5 óApplicationsô, as the presented method is not new and one of the goals of this article was to present scientific applications (as indicated in the title).

However, we have considerably shortened the section by removing the introduction on ENSO and the discussion about Fig. 16 as well as Fig. 16 itself.

Since the results similar to those presented in new Fig. 12 have recently been published using other data sets, it would be difficult to use the presented material in a separate publication. We plan to work on a more complex analysis to pursue this subject further, but we think itõs important to present these results in the current publication.

27. Page 24-27, Section 6, general comment:

A very comprehensive and good summary of the content of the paper. However, it could be shortened (page 26, lines 14-32) as a consequence of comment 25 above.

Thank you ! We have revised the part considering section 5.

Technical corrections

1. Page 1, Abstract, line 11-14:

The current introductory sentences assumes that the reader already knows about the LMD cloud retrieval scheme. I suggest a slight reformulation to make it less unclear, e.g. like the following

ñ*The Laboratoire de Météorologie Dynamique (LMD) cloud retrieval scheme CIRS (Clouds from IR Sounders) has been adapted to cope with any Infrared (IR) sounding instrument. This has been accomplished by applying improved radiative transfer calculations as well as by introducing an original method accounting for atmospheric spectral transmissivity changes associated with varying CO2 concentrations***ò**.

This is not fully correct, as the cloud retrieval developed in the 1990ôs did not have the name óCIRSô; this name corresponds to the adapted version.

We have rewritten the beginning as:

Global cloud climatologies have been built from 13 years of Atmospheric IR Sounder (AIRS) and 8 years of IR Atmospheric Interferometer (IASI) observations, using an updated Clouds from IR Sounders (CIRS) retrieval. The CIRS software can handle any Infrared (IR) sounder data. Compared to the original retrieval, it uses improved radiative transfer modelling, accounts for atmospheric spectral transmissivity changes associated with CO_2 concentration and incorporates the latest ancillary data (atmospheric profiles, surface temperature and emissivities).

2. Page 2, Abstract, line 3, ***ñ****5 % asymmetry***ò***:*

Please clarify better what you mean with asymmetry. Does it mean that there is generally 5 % more high clouds in the Northern Hemisphere? I assume this is what you mean (supported also by Figure 10) but you should make it crystal clear for the reader in the Abstract!

Rewritten as :

The 5% annual mean excess in upper tropospheric cloud amount in the Northern compared to the Southern hemisphere has a pronounced seasonal cycle with a maximum of 25% in boreal summer, in accordance with the moving of the ITCZ peak latitude to a maximum of 10°N.

3. Page 2, Section 1, line 17, ***ñ****properties***ò***:*

Do you really mean ***ñ****properties***ò** *? I would rather say* ***ñ****cloud detection***ò***.*

Yes : we meant here that in addition to identification (which means detection), also their properties (height and emissivity) are well determined (even better than those for low-level clouds)

4. Page 2, Section 1, line 32, ***ñ****determine***ò***:*

Like the previous comment, I am not sure about the correct wording here. The word ***ñ****determine***ò** *is very strong and almost indicates that the CALIPSO and CloudSat satellites together are creating/defining the clouds. Rather, you should express that they* ***ñ****are capable of observing the cloud vertical structure***ò**.

Changed according to suggestion

5. Page 3, Section 1, line 5, ñthe cloud retrieval methodò:

Be a bit more specific, e.g. write ñthe evolution of the original cloud retrieval methodò.

changed

6. Page 3, Section 1, line 9, ñradiative transferò:

I think you should write ñradiative transfer calculationsò or ñradiative transfer modellingò. To only write ñradiative transferò is too general and (I guess) just a shortening of more correct terms.

changed

7. Page 3, Section 1, line 11, ñinitialò: See 5 above (consider using same notation).

Changed to original

8. Page 3, Section 1, line 11, ñradiative transferò: See 6 above (consider using same notation).

changed

9. Page 4, Section 2.1, line 11, ñThe NASA Science teamé .ò:

I would recommend to start a new paragraph here to increase the readability.

done

10. Page 4, Section 2.1, line 15, ñSusskind et al, 2003ò:

I see inconsequent reference formulations on several places in the manuscript. When you make a direct reference to other publications directly in the text (like here) you should (according to my experience) preferably write: ñThe methodology is essentially unchanged from that described in Susskind et al. (2003).ò You have done this correctly in other places (e.g., Page 5, line 27). I think you should be consistent here. Use the formulation above when specifically discussing a publication and use reference in parenthesis when not making a direct statement of the referred publication (a ñsofterò reference). Check also the following references for the same reason:

- Page 4, line 27

- Page 6, line 5

Thanks, all changed

11. Page 4, Section 2.1, line 20, ñshortwave window channelsò:

Please write ñshortwave infrared window channelsò since ñshortwaveò most often is reserved to define visible channels.

changed

12. Page 4, Section 2.1, line 22, ñpartial cloud coverò:

A better formulation is probably ñunder partially cloudy conditionsò.

changed

*13. Page 4, Section 2.1, line 24, **ñ**snow or ice**ò**:*

*Maybe a better formulation is **ñé** snow or ice covered surfaces also provided by NASA L2 data**ò**.*

changed

*14. Page 4, Section 2.1, line 26, **ñ**ideology**ò**:*

*I would suggest using the term **ñ**concept**ò** rather than **ñ**ideology**ò**.*

changed

*15. Page 4, Section 2.1, line 27, **ñ**and allow**ò**:*

*I suggest replacing this with **ñ**which allows**ò**.*

Rewritten to : The CIRS cloud retrieval allows cloud levels up to 30 hPa above the tropopause.

*16. Page 5, Section 2.2, line 1, **ñ**12 km**ò**:*

Is the 12 km valid for each individual footprint or the 2x2 array?

For each individual footprint, clarified in text

*17. Page 5, Section 2.2, line 9, **ñ**the cloud retrieval**ò**:*

*You should write **ñ**the CIRS cloud retrieval**ò**.*

changed

*18. Page 5, Section 2.2, lines 9-10, **ñ**retrieved atmospheric profiles**ò**:*

*Be more specific. You should write **ñ**IASI-retrieved atmospheric profiles**ò**.*

changed

*19. Page 5, Section 2.2, line 15, **ñ**Therefore**ò**:*

You should not start a new paragraph here if you refer directly to what was written in the previous sentences. Make it also very clear that you never (well, not in time for your development) got access to EUMETSAT Version 6 data otherwise this statement appears rather strange.

We could have gotten access after the development and evaluation of the cloud climatologies were nearly at the end. Since it would have taken another year to build the ancillary data from this data set and evaluate again the IASI cloud climatology (also in combination with AIRS), we opted for ERA-Interim ancillary data to build the combined AIRS-IASI cloud climatologies.

As the sentence about V6 EUMETSAT retrievals seems to cut the flow, we took it out.

*20. Page 5, Section 2.2, line 21, **ñ**same source**ò**:*

I guess you rather mean a ***ñ****less instrument-dependent source****ò****?*

We think it is more ‘retrieval quality-dependent source’, but this would be difficult to write, as the different Science Teams are doing the best with the fundings they have available. (In the case of NOAA for example, the team had to move working on CrIS).

21. Page 6, Section 2.3, line 1, ***ñ****proxy****ò****:*

I donʼt like the word ***ñ****proxy****ò*** *in this context. It indicates that it is a kind of simulation or approximation of the real vertical velocity. The vertical pressure velocity* ***ɤ*** *is just another formulation of the vertical velocity which arises when you use pressure as your vertical coordinate instead of the standard geometrical height in meters. So, to my knowledge, itʼs the* ***ñ****real thing****ò*** *and not a* ***ñ****proxy****ò****.*

But I guess you refer to the fact that the direct calculation of ***ɤ*** *is difficult without making approximations. The most common here is the geostrophic assumption leading to the so-called* ***ñɤ****-equation****ò****. In this sense, I guess you may be correct in interpreting it as an approximation. But still, present day NWP models are capable of calculating* ***ɤ*** *so I just wonder what value you are using here? On the other hand, the approximated value at the 500 hPa level is probably quite accurate anyway (conditions here are largely quasi-geostrophic on the large scale) so perhaps this discussion is less important. Anyway, give it a thought.*

We needed the vertical velocity for the interpretation in the ENSO analysis. Since Fig. 16 and its interpretation is taken out according to the referees suggestion, this sentence is also taken out.

22. Page 7, Section 2.4, line 12, ***ñ****arise****ò****:*

Maybe reformulate to ***ñ****these cases occur in about 7 to 15 % of all cases****ò****?*

Changed to : these cases occur in about 7 to 15 % of all cloudy cases

23. Page 8, Section 2.4.1, line 14, ***ñ****less than ..?..****ò****:*

Strange formulation. Youʼd better write ***ñ****0.99 for wavelengths less than 10 µm and 0.98 for wavelengths larger than 10 µm****ò****.*

Changed to : the surface emissivity is set to 0.99 for $\lambda_i < 10$ µm and 0.98 for λ_i Ó10 µm

24. Page 13, Section 3.1, line 6, ***ñ****spatial resolution CALIPSO****ò****:*

Shouldnʼt it be ***ñ****5 km x 0.3 km****ò****? I thought the basic FOV of CALIOP was 300 meter.*

I have understood that the diameter of the spots is 90m, and the sampling along track is 333 m.

For example : https://calipso.cnes.fr/en/CALIPSO/lidar.htm or Winker *et al.* (2009), p. 2312

25. Page 15, Section 3.3, Figure 5 (Page 41):

I suggest that you try to include some additional explanatory features or legends in the figure (e.g., legend with the three coloured dots explained). To look for all explanations in the caption is not very reader-friendly. Try to speed up the correct interpretation of figures with the use of more graphical legends or marks. This remark is probably valid for many other figures in the manuscript.

We have taken into account the refereeʼs suggestion and revised all figures accordingly.

*26. Page 15, Section 3.3, line 27, **ñ**Considering**é ò**:*

I suggest starting a new paragraph here in order to avoid too long chunks of text (unnecessary tiring for the reader).

This whole paragraph has been rewritten (as Fig. 6 has been taken out, and Fig. 5 has been rebuilt with medians and interquartiles to show the width of the distributions within the same figure). We hope that it is now much easier to read.

27. Page 15, Section 3.3, line 28; Figure 6 (Page 42):

*In the caption you describe one of the curves as **ñ**broken line**ò**. I am not sure whether this is the most common way of describing such a curve. More often the term **ñ**dashed line**ò** is used. Consider changing to **ñ**dashed**ò**. This suggestion is valid for many other figures in the manuscript.*

Thanks ; changed everywhere ; though dashed lines seems also to exist, at least according to google ;)

*28. Page 16, Section 3.3, lines 28-29, **ñ**height of COD**ò**:*

*Semantically, it sounds strange (or even incorrect) to express COD as representing a height. Of course, I understand what you mean but it can actually be misinterpreted. Since you have already defined zCOD0.5 why not use this terminology here, e.g. **ñ**the retrieved cloud height exceeds zCOD0.5 for optically thin clouds while it is lower than zCOD0.5 for optically thick clouds**ò**.*

This is obvious from the figure, but we want to stress the following :

In that case, z_{cld} of thin cirrus should be approximated to a height at which COD reaches a value < 0.5 and z_{cld} of opaque high clouds to a height at which COD reaches a value > 0.5.

*29. Page 20, Section 4, line 17, **ñ**three CIRS datasets?**ò***

It is not obvious what three datasets you mean (not explained in text)! Please clarify.

three CIRS climatologies (AIRS, using AIRS-NASA and ERA-Interim ancillary data, as well as IASI, using ERA-Interim ancillary data)

References

Guignard, A., C. J. Stubenrauch, A. J. Baran, and R. Armante, Bulk microphysical properties of semi-transparent cirrus from AIRS: a six year global climatology and statistical analysis in synergy with geometrical profiling data from CloudSat-CALIPSO, *Atmos, Chem. Phys.*, **12**, 503-525 (2012)

Lamquin N., C. J. Stubenrauch, and J. Pelon, Upper tropospheric humidity and cirrus thickness: a statistical analysis using one year of collocated AIRS-CALIPSO data, *J. Geophys. Res.*, 113, D00A08, doi:10.1029/2008JD010012 (2008).

Menzel, W.P., R.A. Frey, E.E. Borbas, B.A. Baum, G. Cureton, and N. Bearson, Reprocessing of HIRS Satellite Measurements from 1980 to 2015: Development toward a Consistent Decadal Cloud Record. *J. Appl. Meteor. Climatol.*, 55, 2397ï 2410, https://doi.org/10.1175/JAMC-D-16-0129.1 (2016)

Stubenrauch, C. J., N. A. Scott, and A. Chédin: Cloud Field Identification for Earth Radiation Budget Studies: I) Cloud Field Classification using HIRS/MSU Sounder Measurements. *J. Appl. Meteor.,* 35, 416-427 (1996).

Stubenrauch, C. J., A. Chédin, R. Armante, and N. A. Scott: Clouds as Seen by Satellite Sounders (3I) and Imagers (ISCCP): II) A New Approach for Cloud Parameter Determination in the 3I Algorithms. *J. Climate*, 12, 2214-2223 (1999).

Stubenrauch C. J., F. Eddounia, and L. Sauvage: Cloud heights from TOVS Path-B: Evaluation using LITE observations and distributions of highest cloud layers. *J. Geophys. Res.*,110, D19203,doi:10.1029/2004JD005447 (2005).

Stubenrauch C. J., A. Chédin, G. Rädel, N. A. Scott, and S. Serrar: Cloud properties and their seasonal and diurnal variability from TOVS Path-B. J. Climate, 19,5531-5553 (2006).

Stubenrauch. C. J.. S. Cros. A. Guignard, and N. Lamquin, A six-year global cloud climatology from the Atmospheric InfraRed Sounder aboard the Aqua Satellite: statistical analysis in synergy with CALIPSO and CloudSat. *Atmos. Chem. Phys.*, 10, 7197ï 7214 (2010).

Winker, D., Getzewitch, B., and Vaughan, M.: Evaluation and Applications of Cloud Climatologies from CALIOP, Proc. Int. Laser Radar Conference (ILRC), 2008.

Winker, D. M., Vaughan, M. A., Omar, A., Hu, Y., and Powell, K. A.: Overview of the CALIPSO mission and CALIOP data processing algorithms, J. Atmos. Oceanic. Technol., 26, 2310-2323 (2009).

Cloud climatologies from the InfraRed Sounders AIRS and IASI: Strengths~~, Weaknesses~~ and Applications

Claudia J. Stubenrauch[1,2], Artem G. Feofilov[1,2], Sofia E. Protopapadaki[1,2], Raymond Armante[1,2]

[1]Laboratoire de Météorologie Dynamique / Institute Pierre-Simon Laplace, (LMD/IPSL), CNRS, Sorbonne Universities, University Pierre and Marie Curie (UPMC) Paris, University of Paris 06, Paris, France

[2]Laboratoire de Météorologie Dynamique / Institute Pierre-Simon Laplace, (LMD/IPSL), CNRS, Ecole Polytechnique, Université Paris-Saclay, Palaiseau, France

Correspondence to: C. J. Stubenrauch (stubenrauch@lmd.polytechnique.fr)

Abstract

Global cloud climatologies have been built from 13 years of Atmospheric IR Sounder (AIRS) and 8 years of IR Atmospheric Interferometer (IASI) observations, using an updated Clouds from IR Sounders (CIRS) retrieval. Thee CIRS software ~~scheme developed at the Laboratoire de Météorologie Dynamique (LMD) can now be easily been adapted to~~can handle any Infrared (IR) sounder data. ~~The CIRS (Clouds from IR Sounders) retrieval~~Compared to the original retrieval, it uses improved radiative transfer modelling, accounts for atmospheric spectral transmissivity changes associated with CO_2 concentration and incorporates the latest ancillary data (atmospheric profiles, surface temperature and emissivities). ~~applies improved radiative transfer, as well as an original method accounting for atmospheric spectral transmissivity changes associated with CO_2 concentration. The latter is essential when considering long-term time series of cloud properties. For the 13-year and 8-year global~~ cloud ~~climatologies of cloud properties from observations of the Atmospheric IR Sounder (AIRS) and of the IR Atmospheric Interferometer (IASI), respectively., we used the~~ The global cloud amount is estimated to 0.67 ï 0.70, for clouds with IR optical depth larger than about 0.1. The spread of 0.03 is associated with ancillary data. Cloud amount is partitioned into about 40% high-level clouds, 40% low-level clouds and 20% mid-level clouds.~~,~~ ~~T~~the latter two categories ~~only~~are only detectedable ~~onlyed when not hidden by~~in the absence of upper clouds. ~~latest ancillary data (atmospheric profiles, surface emissivities and atmospheric spectral transmissivities).~~ The A-Train active instruments, lidar and radar of the CALIPSO and CloudSat missions, provide a unique opportunity to evaluate the retrieved AIRS cloud properties ~~such as cloud amount and height as well as to explore the vertical structure of different cloud types~~.

~~CIRS cloud detection agreementsment with CALIPSO-CloudSat is byis about 85% over ocean, 80% over land and 70% over ice / snow84% - 85% over ocean, 79% - 82% over land and 70% - 73% over ice / snow, depending on atmospheric ancillary data. Global cloud amount has beenis estimated to 67% - 70%.~~ CIRS cloud height ~~coincides~~ can be approximated either by ~~with~~ the mean layer height (for optically thin clouds) or by the mean ~~middle~~ between ~~the~~ cloud top and the ~~the “apparent” cloud base (real base for optically thin clouds or~~ height at which the cloud reaches opacity~~,~~) ~~independent of cloud emissivity.~~, This is valid for high-level as well as for low-level clouds identified by CIRS. ~~For high-level clouds, especially in the tropics, which tThis height is lies on average about 1 km and 1.5 km to 32.5 km below cloud top for low-level clouds and about 1.5 km to 2.5 km below cloud top for high-level clouds, respectively. For the latter the slight increase relates positively slightly increaswith cloud emissivity,ing because as the apparent vertical cloud extent to reach opacity seems to increase with cloud emissivity is slightly larger for large cloud emissivity.~~ IR sounders are ~~in~~ particularly advantageous ~~for the~~to retrieve~~al of~~ upper tropospheric cloud properties, with a reliable cirrus identification ~~down to an IR optical depth of about 0.1~~, day and night. ~~Total cloud amount consists of about 40% high-level clouds and about 40% low-level clouds and 20% mid-level clouds, the latter two only detected when not hidden by upper clouds. Upper tropospheric~~These clouds are most abundant in the tropics, where high opaque clouds make out 7.5%, thick cirrus 27.5% and thin cirrus about 21.5% of all clouds. The ~~asymmetry~~ 5% annual mean excess in ~~upper tropospheric~~high-level cloud amount ~~between~~ in the Northern ~~and~~ compared to the Southern hemisphere ~~with annual mean of 5%~~ has a pronounced seasonal cycle with a maximum of 25% in boreal summer, in accordance with the moving of the ~~a maximum~~ ITCZ peak latitude, with annual mean of 4°N, to a maximum of ~~shift to~~ 120°N~~, which can be linked to the shift of the ITCZ peak latitude~~. This suggests that this excess is mainly determined by the position of the ITCZ. ~~Comparing~~ Considering interannual variability, ~~tropical geographical change patterns~~ tropical ~~of high opaque clouds with that of thin~~ cirrus ~~and thin cirrus~~ are more frequent ~~among~~relative to all clouds when the global (or tropical) mean surface ~~temperature~~ gets warmer. Changes in relative amount of tropical high opaque and thin cirrus with respect to mean surface temperature show different geographical patterns, suggesti~~as a function of changing tropical mean surface temperature indicat~~nges that their response to climate change might~~ay be quite~~ differ~~ent, with potential consequences on the atmospheric circulation~~.

1 Introduction

Clouds cover about 70% of the Earth’s surface and play a key role in the energy and water cycle of our planet. The Global Energy and Water Exchanges (GEWEX) Cloud Assessment (Stubenrauch *et al.*, 2013) has highlighted the value of cloud properties derived from space observations for climate studies and model evaluation and has identified reasons for discrepancies in the retrieval of specific scenes, ~~(especially~~in particular thin cirrus, alone or with underlying low-level clouds~~)~~. Compared to other passive remote sensing instruments, the high spectral resolution of IR vertical sounders leads to especially reliable properties of cirrus, with IR optical depth as low as 0.1, day and night. ~~CO_2 sensitive~~ C~~c~~hannels varying in CO_2 absorption ~~of IR vertical sounders allow~~ are used ~~the~~ to ~~determination~~ determine ~~of~~ height and emissivity of a single cloud layer, which corresponds to the uppermost cloud layer in the case of multiple cloud layers. While measured radiances near the center of the CO_2 absorption band are only sensitive to the upper atmosphere, radiances from the wing of the band are emitted from successively lower levels in the atmosphere.

Spaceborne ~~instruments~~ IR sounders have been observing our planet since the 1980ôs: the High Resolution Infrared Radiation Sounders (HIRS) aboard the National Oceanic and Atmospheric Administration (NOAA) polar satellites provide data since 1979, the Atmospheric InfraRed Sounder (AIRS) aboard the National Aeronautics and Space Administration (NASA) Earth Observation Satellite Aqua since 2002, the IR Atmospheric Sounding Interferometers (IASI) aboard the European Organisation for the Exploitation of Meteorological Satellites (EUMETSAT) Meteorological Operation (MetOp) since 2006 and the Cross-track Infrared Sounder (CrIS) aboard the Suomi National Polar-orbiting Partnership (NPP) satellite since 2011.~~;~~ ~~while a~~A next generation of IR sounders (IASI-NG) is foreseen as part of the EUMETSAT Polar System ï Second Generation (EPS-SG) program for 2021 (Crevoisier *et al.*, 2014).

Active sensors are part of the A-Train satellite formation (Stephens *et al.*, 2002), synchronous with Aqua, since 2006: The CALIPSO lidar and CloudSat radar, together, ~~determine~~ are capable of observing the cloud vertical structure (~~Stephens *et al.*, 2008~~e.g. Henderson *et al.*, 2013; Mace and Zhang, 2014). Whereas the lidar ~~is highly sensitive and~~ can detect sub-visible cirrus, its beam can only penetrate the cloud down to optical depth of about 3 to 5 (in visible range)~~only reaches the cloud base of clouds which are not opaque with an optical depth less than 3 to 5~~. For ~~larger optical depth (COD) larger than about 5~~optically thicker clouds, the radar ~~is~~ provides~~ing~~ ~~a~~ the cloud base ~~location~~.

Our goal to establish a coherent long-term cloud climatology from different IR sounders has led to the evolution of the original LMD cloud retrieval method ~~developed at the Laboratoire de Météorologie Dynamique~~ (Stubenrauch *et al.*, 1999, 2006, 2008, 2010) towards an operational and modular cloud retrieval algorithm suite (CIRS, Feofilov and Stubenrauch, 2017). The CIRS retrieval ~~which~~ has so far been applied to AIRS and IASI data as well as to HIRS data (Hanschmann *et al.*, 2017). The cloud property retrieval employs radiative transfer modelling and atmospheric and surface ancillary data (atmospheric temperature and water vapour profiles, surface temperature and surface emissivity, identification of snow and ice). Compared to the ~~initial~~ original ~~method~~retrieval, the CIRS retrieval applies ~~an~~ improved radiative transfer calculations and a~~n~~ ~~original~~ novel calibration method, accounting for latitudinal, seasonal and interannual atmospheric CO_2 variations, which ~~to~~ adjusts the atmospheric spectral transmissivity look-up tables~~ies from look-up tables, computed once for a fixed atmospheric gaseous composition, according to latitudinal, seasonal and interannual atmospheric CO_2 variations~~.

~~Compared to the~~AThe 6-year AIRS-LMD cloud climatology (Stubenrauch *et al.*, 2010)~~, which~~ participated in the GEWEX Cloud Assessment. In this article, we present~~,~~ the results of i) an updated and extended 13-year AIRS cloud climatology (2003 – 2015), using two different sets of the latest ancillary data (originating from retrievals and from meteorological reanalyses), and ii) a new 8-year IASI cloud climatology (2008 – 2015)~~ are presented in this article~~. After the description of data and methods in section 2, section 3 is dedicated to the evaluation of cloud detection and cloud height using the unique A-Train synergy of synchronous passive and active measurements. Section 4 presents average cloud properties and their regional, seasonal, inter-annual and long-term variability, in comparison with other datasets, as well as uncertainty estimates with respect to the used ancillary data. Section 5 concentrates on the variability of the upper tropospheric clouds with respect to changes in atmospheric conditions in order to illustrate how these data may be used for climate studies. Conclusions and an outlook are given in section 6.

2 Data and methods

2.1 AIRS Data

The AIRS instrument (Chahine *et al.*, 2006) provides very high spectral resolution measurements of Earth emitted radiation in 2378 spectral bands in the thermal infrared (3.74-15.40 μm). The spatial resolution of these measurements varies from 13.5 km x 13.5 km at nadir to 41 km x 21 km at the scan extremes. The polar orbiting Aqua satellite provides observations at 1:30AM and 1~~3~~:30PM local time (LT). Nine AIRS measurements (3 x 3) correspond to one footprint of the Advanced Microwave Sounder Unit (AMSU), ~~and are~~ grouped as a "golf ball".

The CIRS cloud retrieval uses measured radiances ~~around~~ along the ~~the~~ wing of the 15 μm CO_2 absorption band. We have chosen AIRS channels closely corresponding to the five channels used in the TIROS-N Operational Vertical Sounder (TOVS) Path-B cloud retrieval, at wavelengths of 14.19, 14.00, 13.93, 13.28 and 10.90 μm, and three additional channels at 14.30, 14.09 and 13.24 μm (with peaks in the weighting function at 235, 255, 375, 565, 415, 755, 885 hPa and surface, respectively). ~~The cloud property retrieval (section 2.54) is applied to all data.~~ In a second step~~,~~, ~~after which an "a posteriori"~~The multi-spectral cloud detection, based on the spectral coherence of retrieved cloud emissivities~~, obtained~~

~~by using the retrieved cloud pressure~~, decides whether the AIRS footprint is cloudy (section 2.54.3) ~~or mostly clear (section 2.5)~~. For the latter, radiances in the atmospheric window between 9 and 12 μm are used, at six wavelengths of 11.85, 10.90, 10.69, 10.40, 10.16, 9.12 μm.

Ancillary data necessary for the cloud retrieval, which include atmospheric temperature and water vapour profiles as well as surface skin temperature, are provided by t~~T~~he NASA Science Team ~~provides~~ L2 standard products (Version 6 (V6); Olsen *et al.*, 2017~~6~~)~~, which include atmospheric temperature and water vapour profiles as well as surface skin temperature~~. ~~These are necessary ancillary data for the CIRS cloud retrieval.~~ They were retrieved from cloud-cleared AIRS radiances within each AMSU footprint. The methodology ~~is~~ remains essentially ~~unchanged from that~~the same as described in ~~(~~Susskind *et al.*~~,~~ (2003). Compared to Version 5 (V5), the most significant changes are: i) V6 uses an IRï microwave neural network solution (Blackwell *et al.*, 2014) as a first guess for the retrieval of atmospheric temperature and water vapour profiles as well as for surface skin temperature, instead of the previously used regression approach (Susskind *et al.*, 2014). This leads to physical solutions for many more cases than in ~~Version 5 (~~V5~~)~~. ii) The retrieval of surface skin temperature only uses shortwave IR window channels (Susskind *et al.*, 2014). These modifications ~~have~~ resulted in significant improvement of accurate temperature profiles and surface skin temperatures under partially cloudy ~~cover~~ conditions (Van T. Dang *et al.*, 2012)~~;~~. Compared to V5, the surface skin temperature is larger over land in the afternoon (especially over desert) and over maritime stratocumulus regions.

In addition, w~~W~~e ~~also~~ use the microwave identification of snow or ice covered surfaces, also provided ~~from~~ by the NASA L2 data.

Since the retrieved cloud pressure should be within the troposphere ~~to~~ / lower stratosphere, we have determined the tropopause pressure from the atmospheric profiles, using the ~~ideology~~ concept described in ~~(~~Reichler *et al.*~~,~~ (2003) and in ~~,~~ Feofilov and Stubenrauch~~,~~ (2017). ~~and~~ The CIRS cloud retrieval allows cloud levels ~~to be~~ up to 30 hPa above the tropopause.

2.2 IASI data

IASI, developed by CNES in collaboration with EUMETSAT, is a Fourier Transform Spectrometer based on a Michelson interferometer, which covers~~ing~~ the IR spectral domain from 3.62 to 15.5 **ε**m. As a cross-track scanner, the swath corresponds to 30 ground fields per scan, each of these measures a 2 × 2 array of footprints. The latter have a ~~(~~12-km diameter at nadir~~)~~. IASI raw measurements are interferograms that are processed to radiometrically calibrated spectra on board the satellite. Two instruments were launched so far onboard the European Platforms Metop-A and Metop-B (in October 2006 and September 2012, respectively), with measurements ~~of~~ at 9:30AM / ~~21~~9:30PM LT and

10:30AM / 10~~22~~:30PM LT (local equator crossing time). IASI has been providing water vapour and temperature sounding profiles for operational meteorology (accuracy requirements respectively of 1 K and 10% in the troposphere), ~~while observing simultaneously~~ as well as ~~whole suite of~~ trace gas concentrations~~es~~, surface and atmospheric properties, including those of aerosols and clouds (Hilton *et al.*, 2012). For the cloud retrieval, we use radiances at the wavelengths 14.30, 14.20, 14.06, 14.00, 13.93, 13.40, 13.24 and 10.90 µm, and for the multi-spectral cloud detection the radiances at 11.85, 10.90, 10.70, 10.41, 10.16, and 9.13 µm.

At the time we started incorporating IASI data to the CIRS cloud retrieval, two data sets of IASI-retrieved atmospheric profiles and surface temperature were available: one provided by EUMETSAT (Version 5) and one by NOAA. EUMETSAT L2 temperature and water vapour Version 5 products were only available for clear and partly cloudy scenes, leaving atmospheric and surface retrievals in only 9% of all cases.~~, while the recent Version 6 has extended the retrieval of thermodynamical parameters (such as temperature and water vapor) to cloudy scenes.~~

Therefore we first used IASI L2 ancillary data provided by NOAA. The comparison with collocated temperature profiles of the Analyzed RadioSoundings Archive (ARSA, available at the French data centre AERIS) has shown that, while AIRS-NASA and ERA-Interim (section 2.3) temperature profiles do agree in general with the ARSA profiles within 1 K, differences between IASI-NOAA and ARSA profiles were often larger than 1 K in the lower troposphere (not shown). In addition~~However~~, a study of the influence of the different ancillary data on the CIRS ~~a~~ cloud amount has demonstrated that the ~~comparison with cloud~~ amount~~s d~~ of low-level clouds over ocean was underestimated, when using those deduced from IASI-NOAA (Feofilov *et al.*, 2015a). This might be ~~most probably~~ explained~~deduced from AIRS via CIRS has demonstrated that the amount of low-level clouds over ocean was underestimated (Feofilov *et al.*, 2015a), probably due to~~by an underestimation of the~~ed~~ sea surface temperature (SST) linked to cloud contamination. ~~In addition, the comparison with collocated temperature profiles of the Analyzed RadioSoundings Archive (ARSA, available at the French data centre AERIS) has revealed that the AIRS-NASA and IASI-NOAA L2 atmospheric profiles were quite different. This brought us to the conclusion~~From this we concluded, that the AIRS ï IASI synergy to explore cloud diurnal variability in a coherent way needs ~~one needs~~ ancillary data from similar retrievals or from the same source ~~are necessary, if one wants to make use of the AIRS ï IASI synergy to for exploring e the cloud diurnal cyclevariability in a coherent way~~. ~~Therefore,~~Thus we also implemented ancillary data from the European Centre for Medium-Range Weather Forecasts (ECMWF) meteorological reanalyses into the CIRS cloud retrieval.

2.3 ERA-Interim meteorological reanalyses

ECMWF provides the meteorological reanalyses ERA-Interim, covering the period from 1989 until now. Dee *et al.* (2011) give a detailed description of the model approach and the assimilation of data. The data assimilation scheme is sequential: at each time step, it assimilates available observations to constrain the model, which then provides a short-range ~~built with forecast information obtained in the previous step. The analyses are then used to make a short-range model~~ forecast for the next assimilation time step. Gridded data products (at a spatial resolution of 0.75° latitude x 0.75° longitude) include 6-hourly surface temperature, atmospheric temperature and water vapour profiles, as well as dynamical parameters such as horizontal and vertical large-scale winds. These data are given at universal time of 0:00, 6:00, 12:00 and 18:00. ~~A common proxy for the intensity of the vertical motions in the atmosphere is the vertical pressure velocity at 500 hPa level, ω500 (e.g. Bony and Dufresne, 2005; Martins *et al.*, 2011).~~ To match these data~~, given at universal time of 0:00, 6:00, 12:00 and 18:00,~~ ~~to~~ with the AIRS and IASI observations, we interpolate them to the corresponding local time, using a cubic spline function, as in ~~(~~Aires *et al.*~~,~~ (2004).

2.4 Collocated AIRS – CALIPSO – CloudSat data

All satellites of the A-Train follow each other within a few minutes. We use the same collocation procedure as in Feofilov *et al.* (2015b): First, each AIRS footprint is collocated with NASA CALIPSO L2 cloud data averaged over 5 km (version 3, Winker *et al.*, 2009) in such a way that for each AIRS golf ball, three CALIPSO samples are matched to the centres of three AIRS footprints. These data are then collocated with the NASA L2 CloudSat-lidar geometrical profiling (GEOPROF) data (version R04, Mace and Zhang, 2014). Each of these AIRS footprints thus includes cloud top and cloud base for each of the cloud layers, detected by lidar or radar, at the spatial resolution of the radar footprints (1.4 km x 2.3 km)~~,~~ from the GEOPROF data. ~~and c~~Cloud optical depth (COD), cloud top, z_{top}, and apparent cloud base (corresponding to the real cloud base or to the height at which the cloud reaches opacity), $z_{app\ base}$, are given at the spatial resolution of the CALIPSO cloud data (5 km x 0.09 km). A cloud feature flag indicates whether the cloud is opaque. The CALIPSO ~~L2~~ cloud data also indicate at which horizontal averaging along the track the cloud was detected (1 km, 5 km or 20 km), which is a measure of the ~~optical thickness of the cloud~~COD. As in Stubenrauch *et al.* (2010), for a direct comparison with AIRS cloud data, we use clouds detected at horizontal averaging over 5 km or less. This corresponds to clouds with ~~VIS~~visible ~~optical depth~~COD larger than about 0.05 to 0.1 (Winker *et al.*, 2008).

The scene type ~~over~~of an AIRS footprint is estimated as cloudy when the CALIPSO sample as well as the GEOPROF sample include at least one cloud layer. Clear sky is defined by ~~a~~ cloud-free ~~by using the cloud detection of all three~~ CALIPSO and GEOPROF samples~~s~~ ~~per~~within the AIRS footprint~~ golf ball~~. ~~as: clear sky (all three samples clear sky), overcast (all three samples cloudy) and partly cloudy.~~

For the evaluation of cloud height, we identify the GEOPROF cloud layer which is closest to z_{cld} from AIRS and estimate the height at which the cloud reaches a COD of 0.5, $z_{COD0.5}$, from CALIPSO. $z_{COD0.5}$ is required to be located within the corresponding GEOPROF cloud layer.

$z_{COD0.5}$ is deduced from the CALIPSO L2 COD, assuming a constant increase of COD from cloud top towards cloud base, except for high-level clouds, for which the shape of the ice water content profile as a function of cloud emissivity is taken into account (Feofilov *et al.*, 2015b). As the COD of CALIPSO might be slightly underestimated (Lamquin *et al.*, 2008), especially for larger COD, we reduce the ratio 0.5/COD to 0.4/COD, used in the estimation of $z_{COD0.5}$.

~~To avoid uncertainties in atmospheric and surface ancillary data in the analysis of the diurnal cycle of upper tropospheric clouds from AIRS and IASI retrievals, we use ERA-Interim as ancillary data (Feofilov *et al.*, 2015a). By using different sets of ancillary data in the cloud retrieval we are also able to estimate uncertainties in cloud amounts (sections 3 and 4).~~

2.5~~4~~ CIRS cloud property retrieval

The cloud property retrieval is based on a weighted χ^2 method using channels ~~around~~ along the wing of the 15 μm CO_2 absorption band (Stubenrauch *et al.*, 1999). Cloud pressure and effective emissivity are determined by minimizing $\chi^2(p_k)$, computed at different atmospheric pressure levels by summation over N wavelengths λ_i ~~within the CO_2 absorption band and atmospheric window~~:

$$\chi^2(p_k) = \sum_{i=1}^{N} \left[(I_{cld}(p_k,\lambda_i) - I_{clr}(\lambda_i)) \cdot \varepsilon_{cld}(p_k) - (I_m(\lambda_i) - I_{clr}(\lambda_i)) \right]^2 * W^2(p_k,\lambda_i) \qquad (1)$$

~~where~~ I_m corresponds to the measured radiance. I_{clr} is the simulated radiance the IR Sounder would measure in the case of clear sky, and $I_{cld}(p_k)$ is the radiance emitted by a homogeneous opaque single cloud layer at pressure level p_k. I_{cld} is~~,~~ calculated for 42 p_k levels ~~p_k above surface~~ (from 984 hPa to 86 hPa), ~~and~~ for the ~~corresponding~~ viewing zenith angle of the observation. A sensitivity study has shown that ~~In general,~~ five (for HIRS) to eight channels (AIRS and IASI) ~~around the 15μm CO_2 band (regularly spaced)~~ are sufficient, as ~~a sensitivity study has shown.~~ d~~D~~oubling the number of channels in the retrieval did not change the results.

By introducing empirical weights $W(p_k, \lambda_i)$, the method takes into account i) the vertical ~~weighting~~ contribution of the different channels, ii) the growing uncertainty in the computation of ε_{cld} with increasing p_k and iii) uncertainties in atmospheric profiles. These weights are determined for each of five typical air mass classes (tropical, midlatitude summer and winter, polar summer and winter) as in ~~(~~Stubenrauch *et al.*~~,~~ (1999) and in Feofilov and Stubenrauch (2017)~~; Feofilov and Stubenrauch, 2017)~~, using~~,~~ ~~using~~ the spread of clear sky radiances within these air mass classes. The clear sky radiances have been simulated for each of the atmospheric profiles of these five air mass classes, using the 4A radiative transfer model (Scott and Chédin, 1981), and stored in ~~within these air mass classes obtained from~~ the Thermodynamic Initial Guess Retrieval (TIGR) data base (Chédin *et al.*, 1985; Chevallier *et al.*, 1998; Chédin *et al.*, 2003). Minimizing χ^2 in Eq. 1 is equivalent to $d\chi^2/d\varepsilon_{cld} = 0$, from which one can extract ε_{cld} as:

$$\varepsilon_{cld}(p_k) = \frac{\sum_{i=1}^{N}\left[I_m(\lambda_i) - I_{clr}(\lambda_i)\right]\cdot\left[I_{cld}(p_k,\lambda_i) - I_{clr}(\lambda_i)\right]\cdot W^2(p_k,\lambda_i)}{\sum_{i=1}^{N}\left[I_{cld}(p_k,\lambda_i) - I_{clr}(\lambda_i)\right]^2\cdot W^2(p_k,\lambda_i)} \qquad (2)$$

In general, the $\chi^2(p)$ profiles have a more pronounced minimum for high-level clouds than for low-level clouds. We stress here that for the identification of low-level clouds it is important to allow values larger than 1 for ε_{cld}, because at larger pressure I_{clr} and I_{cld} become very similar and their uncertainties may lead to values larger than 1 (Stubenrauch *et al.*, ~~1996,~~ 1999). ~~Therefore,~~Thus only pressure levels leading to ε_{cld} >1.5 are excluded from the solution. Typical p_{cld} uncertainties have been estimated from a statistical analysis of the $\chi^2(p)$ profiles: they range from 30 hPa for high-level clouds to 120 hPa for low-level clouds, corresponding to about 1.2 km in altitude, z_{cld}.

In the case of atmospheric temperature inversions in the lower troposphere, ~~for which temperature first increases with height before decreasing, with $T(z_{inv}) > T_{surf}$,~~ the cloud height is moved to the inversion ~~layer~~ level, z_{inv}, defined as the highest level with $T(z_{inv})>T_{surf}$. To detect these cases, the inversion strength, defined by $T(z_{inv})$ - T_{surf}, has to be larger than 2 K. Depending on the ancillary data, these cases ~~arise~~ occur in about 7 to 15 % of all ~~the time~~cloudy cases~~.~~ ε_{cld} as defined in Eq. (2) does not have a physical meaning in the case of an inversion, since $I_{cld}(p_{cld})$ will be greater than I_{clr}. Therefore, we scale ε_{cld} and the spectral emissivities in accordance with the ratio p_{inv} / p_{cld}.

Cloud temperature, T_{cld}, is determined from p_{cld}, using the ancillary temperature profile similar to the observed situation (see section 2.~~5~~4.1). Cloud types are distinguished according to p_{cld} and ε_{cld}. High-level clouds are defined by p_{cld} < 440 hPa, midlevel clouds by 440 hPa < p_{cld} < 680 hPa and low-level clouds by p_{cld} > 680 hPa. High-level clouds may be further distinguished into opaque (ε_{cld} > 0.95), cirrus (0.95 > ε_{cld} > 0.50) and thin cirrus (ε_{cld} < 0.50). p_{cld} is transformed to cloud altitude, z_{cld}, using a standard hydrostatic conversion~~, with the virtual temperature profile accounting for humidity, again from ancillary data similar to the observed situation~~.

~~The retrieval is applied to all footprints. In a second step, an óa posterioriô cloud detection is applied (section 2.5). When sufficient channels are available in the atmospheric window, as for the high spectral resolution IR sounders like AIRS, CrIS and IASI, a test based on the spectral coherence of retrieved cloud emissivities decides whether the footprint is cloudy (overcast or mostly cloudy) or clear (or not cloudy enough to determine reliable cloud properties). Thresholds have been established using the A-Train synergy (section 3). In the case of HIRS, other methods have been developed to decide if the scene is cloudy (e. g. Stubenrauch *et al.*, 2006; Hanschmann *et al.*, 2017).~~

For the computation of I_{clr} and I_{cld} in Eq. (1), we need i) surface type (ocean, land, ice / snow), ~~skin~~ surface temperature and spectral ~~surface~~ emissivities, ii) ~~as well as~~ atmospheric temperature and water vapour profiles as well as ~~and~~ spectral transmissivity profiles for the atmospheric situation of the measurements. The ~~atmospheric spectral transmissivity profiles~~latter ~~were~~ have been calculated using the 4A radiative transfer model ~~(Scott and Chédin, 1981)~~, separately for each satellite viewing zenith angle (up to 50°) and for about 2300 representative clear sky atmospheric temperature and humidity profiles of the TIGR data base.

In the cloud retrieval, the TIGR data base is searched for the atmospheric profile corresponding best to the observational conditions by applying a proximity recognition which compares the atmospheric temperature and water vapour profiles from the ancillary data with those from TIGR as in ~~(~~Stubenrauch *et al.*~~,~~ (2008). The preparation and evaluation of these ancillary data is presented in 2.5~~4~~.1.

2.5~~4~~.1 Preparation and comparison of atmospheric / surface ancillary data

Spectral surface emissivities: Over land, we use monthly mean spectral surface emissivity climatological values at a spatial resolution of 0.25° x 0.25°, retrieved from IASI measurements (Paul *et al.*, 2012). For AIRS, these spectral surface emissivities have been ~~and spectrally~~ interpolated to the AIRS ~~channels~~wavelengths. Over ocean, the surface emissivity is set to 0.99 for ~~ωαϖελενγτησ λεσσ τηαν~~$\lambda_i \leq 10$ μm and 0.98 for λ_i Ó~~wavelengths larger than~~ 10 μm (Wu and Smith, 1997). Over snow and ice, the spectral surface emissivities are taken from (Hori *et al.*, 2006), and ~~since~~ as the~~y~~se depend ~~in this case~~ on the viewing zenith angle, they ~~are~~ had to be corrected ~~as~~ like in ~~(~~Smith *et al.*~~,~~ (1996).

Atmospheric profiles and surface temperature: ~~Since~~ ~~As~~Since IR sounders, in combination with microwave sounders, were originally designed for the retrieval of atmospheric temperature and humidity profiles, the atmospheric clear sky situation can then be directly described by simultaneous L2 atmospheric profiles of good quality ~~(when the situation is not too cloudy)~~. ~~When these are~~In the case

~~that ancillary data of~~ If good quality data are not ~~not~~ available for a given measurement, we use ~~we use atmospheric profiles, surface skin temperature and tropopause~~ those ~~of good quality~~ are averaged within, ~~averaged over~~ 1° latitude x 1° longitude averages of good quality data.~~,~~ ~~and i~~If ~~there are~~ still no data are available, we interpolate these averages in time (inversely proportional to distance within maximal ±15 days) and then in space (inversely proportional to distance within maximal 3° longitude, considering the same surface type).

To define atmospheric temperature and humidity profiles as well as surface temperature of good quality, one has to find a compromise between an acceptable quality and enough statistics.

This led to the following quality criteria in the case of ancillary data from AIRS-NASA (V6)~~ ~~:

- Surface temperature is of good quality, if the provided retrieval error is smaller than 3 K / 6 K / 7 K for ocean / land / ice or snow, respectively. It should also be larger than 180 K and smaller than 400 K.
- Atmospheric temperature profiles are of bad quality, when three consecutive layers have ~~large~~ retrieval errors larger than~~,~~ 2 K / 2K / 2K over ocean, 2.5 K / 2.5 K / 3 K over land and 2.5 K / 2.5 K / 5 K over ice or snow, ~~with thresholds in the upper part (~~between 70 hPa ~~to~~ and 500 hPa~~)~~ / ~~lower part of the troposphere (~~between 500 hPa ~~to~~ and surface~~)~~ / near surface ~~of 2 K / 2K / 2K over ocean, 2.5 K / 2.5 K / 3 K over land and 2.5 K / 2.5 K / 5 K over ice or snow~~, respectively.
- For atmospheric water vapour profiles the NASA L2 quality criteria ~~of NASA~~ were kept (Olsen *et al.*, 2013).

Nevertheless, the ~~when comparing~~ SSTs of good quality from AIRS-NASA ~~with a~~were still slightly colder than those ~~SST from~~of ERA-Interim~~, AIRS values were slightly colder~~. ~~Since~~ As this effect is most probably ~~due to a slight underestimation of the AIRS SST~~ linked to AIRS-NASA residual cloud contamination, we ~~applied a small~~added to the AIRS-NASA SSTs the minimum between the retrieval error and 0.5 K ~~correction to SST by adding the minimum between 0.5 K and the retrieval error~~. Since differences~~the behaviour~~ over land ~~is~~ might be positive or negative (Figure 2)~~more complex~~, we left the AIRS-NASA surface temperature (T_{surf}) values ~~as they are~~unchanged.

For ERA-Interim, the ~~When we use t~~tTime-interpolated ~~ERA-Interim~~ atmospheric profiles and surface temperatures are always available ~~as ancillary data in the cloud retrieval, these data are always available~~. However, ~~However, since the~~An analysis revealed,~~W~~we ~~observed~~found that the ~~time~~ time-interpolated ERA-Interim SSTs dido ~~did~~ not show a diurnal cycle, with ~~(~~most ~~of the~~ amplitudes ~~are~~ less than 0.2 K~~)~~.~~,~~ ~~which~~ As this is not consistent with observations (e.~~g~~g. Webster *et al.*, 1996), we applied a simple parameterized correction,~~,~~ ~~which~~ linking~~s~~ the SST diurnal cycle to peak insolation (~~based on Fig. 11 of (~~Webster *et al.*~~,~~, 1996). ~~This parameterization links the SST diurnal cycle to peak insolation.~~ The coefficient between the SST diurnal amplitude and the maximal solar flux at given latitude, longitude, solar zenith angle and local time ~~and the SST diurnal amplitude~~ was adjusted to 0.005 K/Wm^{-2}, ~~to~~ so that the SST diurnal amplitude is ~~make the latter~~ consistent with ~~that of~~ recent observations (e.g. Seo *et al.*, 2014). Without this correction, the cloud amount (CA) ~~difference between~~at ~~over ocean was larger during~~ night ~~(78%) than in the~~and/ early afternoon was 78% -/ ~~(~~71%~~)~~, ~~while~~ compared to 71% -/ 71% when using AIRS ancillary data. The correction led to ~~now cloud amount is more similar (~~76% ~~/~~ -/ 73%~~)~~, ~~in better agreement with~~closer to the results using AIRS ancillary data ~~(71% / 71%)~~. ~~The behaviour~~ O~~o~~ver land, ~~is more complex, so we left the~~without changes in T_{surf} ~~values as they are~~, ~~leading to~~ CA ~~of during~~at night / ~~day~~early afternoon is 62% / 56%, with ERA-Interim, and 56% / 58%, with AIRS-NASA, ~~at 1:30AM / 1:30PM~~respectively.

Figure 1 presents comparisons ~~of~~ between T_{surf}, as used in the cloud retrieval, deduced from ~~NASA~~ AIRS-NASA ~~retrievals~~ and from ERA-Interim, ~~with~~ and collocated surface air temperature, T_{surf}^{air}, from the ARSA data base. One would expect that over land T_{surf} is colder than T_{surf}^{air} during night and warmer than T_{surf}^{air} in the afternoon; this effect should be stronger for ~~temperate and~~ warmer temperatures, especially if the climate is dry. SST should be similar to T_{surf}^{air} in the tropics, slightly warmer in midlatitudes and colder in polar regions. ~~Considering Figure 1, t~~The distributions in Figure 1 reflect the expectations, with similar peak positions for AIRS-NASA and ERA-Interim ~~corresponding to similar differences with ARSA~~. ~~When looking more in detail,~~Though ~~the land~~ distributions over land are slightly ~~larger~~ broader for AIRS-NASA than for ERA-Interim.~~, and~~ T~~t~~hey are also shifted towards colder values ~~for colder T_{surf} and~~ at night ~~for warmer T_{surf}~~. In the afternoon, ~~For warmer T_{surf} in the afternoon,~~ T_{surf} of AIRS-NASA ~~T_{surf}~~ is slightly larger than T_{surf} of ERA-Interim ~~T_{surf}. C~~for situations with warm T_{surf}. Colder AIRS-NASA values might still indicate some cloud contamination, whereas the colder values of ERA-Interim over warm land in the afternoon might indicate an underestimation, especially over desert, as has already been pointed out by Trigo *et al.* (2015). The effect of T_{surf} on cloud amount will be further investigated in section 3.1~~2~~.

2.5~~4~~.2 ~~Calibration~~ Accounting for changes in atmospheric CO_2 concentration

The TIGR data base of atmospheric spectral transmissivities was created for an atmosphere with a fixed CO_2 volume mixing ratio of 372 ppmv. However, the atmospheric CO_2 concentration varies latitudinally, seasonally and with time. ~~While b~~Both the increase during the last ten years and the seasonal variability in the Northern hemisphere (NH) are of the order of ~20 ppmv.~~,~~ ~~the latitudinal gradient in the NH varies from ‑0.1 ppmv / ° to +0.1 ppmv / °. Seasonal variability in the NH~~The latter is related to the vegetation and fossil fuel burning seasonality. The difference between an averaged value and actual CO_2 volume mixing ratio can easily reach 10%.~~,~~ ~~which~~ This is a noticeable change, ~~since~~ as the concentration enters the power of the exponent in the calculation of~~ing~~ the transmissivity, τ. To avoid errors associated with CO_2 changes in the radiative transfer computations~~associated with CO_2 changes~~, we rescale the transmissivity ~~according to the following rule~~as:

$$\tau = \exp(-\beta - \alpha \cdot CO_2^{current})$$ ~~τ = exp(-β ï α $CO_2^{current}$)~~ (3)

with $\alpha = -k \cdot \log(\tau^{ref}) / CO_2^{ref}$ ~~α = -k log (τ^{ref})/ CO_2^{ref}~~ and $\beta = \alpha \cdot CO_2^{ref} \cdot \log(1-k)/k$ ~~β = α CO_2^{ref} (1-k)/k~~, where k is the relative CO_2 contribution to the opacity of the channel. Details are described in ~~(~~Feofilov and Stubenrauch~~,~~ (2017). The CO_2 concentrations are taken from (GLOBALVIEW-CO2, 2013).

This correction also removes long-term biases due to increasing CO_2 in the atmosphere from anthropogenic CO_2 emissions, which introduced an artificial increase~~efact~~ in the cloud amount time series~~ of cloud amount~~. Applying the correction of equation (3) has eliminated this bias (see section 4).

2.5.3 Multi-spectral ‘a posteriori’ cloud detection

Once the cloud properties are retrieved, to constrain cloud definition, we use the spectral standard deviation (ů(ε(λ$_i$)) of retrieved cloud emissivities between 9 and 12 µm, wavelengths in the IR atmospheric window, as described in Stubenrauch *et al.* (2010). For each footprint, cloud emissivities ε_{cld} are determined at six wavelengths, λ$_i$, (section 2.1), as:

$$\varepsilon_{cld}(\lambda_i) = \frac{I_m(\lambda_i) - I_{clr}(\lambda_i)}{I_{cld}(p_{cld}, \lambda_i) - I_{clr}(\lambda_i)} \qquad (4)$$

I_{cld} is now determined for p_{cld}, retrieved by the χ^2 method (see above).

The relative standard deviation of these cloud emissivities, ů(ε(λ$_i$))~~ů(ε$_{cld}$)~~/ε_{cld}, is much larger when the footprint is partly cloudy or clear and hence p_{cld} is biased, than for cloudy cases, when p_{cld} and ε_{cld} are well determined. This behaviour is illustrated in Figure 2 of Stubenrauch *et al.* (2010) and in Figure S1 of the supplement, contrasting distributions of the relative standard deviation of these cloud emissivities, ů(ε(λ$_i$))/ε_{cld}, of cloudy and clear sky scenes from CALIPSO samples. Guided by these figures and experimenting with thresholds to obtain a good agreement in cloud amount compared to CALIPSO-CloudSat (section 3) and to other datasets (section 4), we define the AIRS footprint ~~is identified~~ as cloudy if the following conditions are fulfilled: ů(ε(λ$_i$))/ε_{cld}, < 0.17 for ocean (both ancillary data), ů(ε(λ$_i$))/ε_{cld}, < 0.20 for land (both ancillary data) and ů(ε(λ$_i$))/ε_{cld}, < 0.30 / 0.20 for ice and snow (AIRS-NASA / ERA-Interim ancillary data).

For IASI we do not have the possibility to distinguish $\mathring{u}(\varepsilon(\lambda_i))/\varepsilon_{cld}$ distributions according to CALIPSO-CloudSat cloudy and clear sky scenes. However, the overall distributions of $\mathring{u}(\varepsilon(\lambda_i))/\varepsilon_{cld}$ are similar for AIRS and IASI, comparing retrievals based on ERA-Interim ancillary data. Therefore we use the same thresholds for the IASI cloud detection.

To reduce misidentification of clear sky as high-level clouds, only clouds with ε_{cld}Ó0.10 are considered.

2.~~5~~4.~~4~~3 Summary of changes compared to the previous version of the AIRS-LMD cloud ~~climatology~~retrieval

Compared to the retrieval used to produce the six-year AIRS-LMD cloud climatology (Stubenrauch *et al.*, 2010), the following changes have been implemented into the CIRS algorithm:

- extension of m~~M~~inimum cloud pressure ~~has been extended~~ from 106 hPa to 86 hPa,~~.~~
- update of a~~Ancillary A~~atmospheric and surface ancillary data ~~have been updated~~ from NASA V5 to NASA V6,~~.~~
- improved ~~To fill gaps~~interpolation ~~in~~ of atmospheric and surface ancillary data ~~of good quality, the interpolation method has slightly changed~~,~~.~~
- moving ~~In the case of atmospheric temperature inversions,~~ the cloud ~~is moved~~ to the inversion layer level and scaling ε_{cld} ~~is scaled accordingly~~in the case of atmospheric temperature inversions,~~.~~
- ~~The~~ improved radiative transfer computations ~~to determine~~of the TIGR atmospheric spectral transmissivities,
- ~~haves been improved.~~
- ~~The~~adjusting the TIGR ~~atmospheric near-surface~~ spectral transmissivit~~y~~ies~~y~~ for the lowermost layer ~~of the TIGR data base near the surface wereas adjusted~~in accordance with the observed ~~to the~~ surface pressure ~~of the observed situation~~,~~.~~
- decreased cloud detection t~~Thresholds in the cloud detection are decreased, thanks~~due to ~~The~~ improved radiative transfer computations ~~of clear sky radiances led to a decreased thresholds on the variability of the cloud spectral emissivities between 9 and 12 μm, used in the cloud detection, (see section 2.5.35)~~,~~.~~
- ~~Only~~ reducing the number of ~~one~~ cloud detection tests to one, which is based on the coherence of cloud spectral emissivity,~~ is applied.~~
- ~~C~~considering ~~Only~~ clouds with ε_{cld}Ó0.10, ~~are considered (~~instead of ε_{cld}Ó0.05,~~)~~

- ~~T~~taking into account variable CO_2 concentration in ~~Simulated clear sky atmospheric~~ spectral transmissivityies estimates~~have been corrected for variability in atmospheric CO_2 concentration~~.

As we will see in section 4, t~~T~~he impact of these changes ~~, however,~~ is in general small, but taking into account variable CO_2 concentration is important for addressing the long-term variability of clouds.~~, as can be seen in the latitudinal averages of total, high, midlevel and low-level cloud amounts presented in section 4.~~

~~A posteriori cloud detection~~

~~Once the cloud properties are retrieved, we use the same cloud detection strategy as in (Stubenrauch *et al.*, 2010), based on the spectral coherence of retrieved cloud emissivities between 9 and 12 µm, wavelengths in the IR atmospheric window. For each footprint, cloud emissivities ε_{cld} are determined at six wavelengths, λ_i, as:~~

$$\varepsilon_{cld}(\lambda_i) = \frac{I_m(\lambda_i) - I_{clr}(\lambda_i)}{I_{cld}(p_{cld}, \lambda_i) - I_{clr}(\lambda_i)} \qquad (4)$$

~~where I_{cld} is now determined for p_{cld} which has been retrieved by the χ^2 method (see above). When p_{cld} is well determined, these spectral cloud emissivities should only slightly differ. The variability should be larger, when the footprint is partly cloudy or clear and hence p_{cld} is not well determined. In that case, the footprint is declared as not cloudy.~~

~~To determine thresholds, we make use of the A-Train synergy: by comparing distributions of the standard deviation ů(ε_a) over these wavelengths divided by the retrieved ε_{cld}, separately for cloudy scenes and for clear sky scenes as determined by CALIPSO (see section 3.1). Overcast / clear sky scenes are situations for which all three CALIPSO samples within the AIRS golf ball are cloudy / clear, respectively, and partly cloudy scenes include a mix of cloudy and clear sky within the three samples. Figure 2 presents these distributions, separately over ocean, land and ice / snow, when AIRS ancillary data and when ERA-Interim ancillary data are used in the AIRS cloud retrieval. First of all, we observe that the distributions are in general narrower for cloudy scenes than for clear sky, as expected. The large tails of the clear sky distributions are presented as a large peak at ů(ε_a)/ε_{cld}, = 0.59, the maximum value to which ů(ε_a)/ε_{cld}, was set. The separation between cloudy and clear is best over ocean, followed by land and then ice / snow. Distributions are similar over ocean and land between both ancillary data, whereas the distinction between cloudy and clear sky over ice / snow is slightly better when ERA-Interim is used. This might be explainable by the fact that the retrieval of atmospheric profiles with good quality is challenging over ice / snow. According to these figures and by experimenting with thresholds to obtain a~~

~~good agreement in the identification of cloudy and clear sky scenes with CALIPSO-CloudSat (see section 3.2), we perform the following tests for the AIRS-CIRS cloud detection.~~

~~The footprint is identified as cloudy if the following conditions are fulfilled:~~

~~ů(ε_a) / ε_{cld} < 0.17 / 0.20 / 0.30 for ocean / land / snow or ice and AIRS ancillary data~~

~~ů(ε_a) / ε_{cld} < 0.17 / 0.20 / 0.20 for ocean / land / snow or ice and ERA-Interim ancillary data~~

~~For IASI we do not have the possibility to test these distributions with CALIPSO-CloudSat. However, the overall distributions of ů(ε_a)/ε_{cld} are similar for AIRS and IASI, comparing retrievals both based on ERA-Interim ancillary data. Therefore we use the same thresholds for the IASI cloud detection.~~

~~To reduce noise, we declare footprints with a cloud of ε_{cld} < 0.10, corresponding to a visible (VIS) optical depth of about 0.2, as not cloudy.~~

3 Evaluation of cloud properties using the A-Train synergy

The ~~A-Train active instruments,~~ lidar and radar of the CALIPSO and CloudSat missions, provide a unique opportunity to evaluate the retrieved AIRS cloud properties such as cloud amount and cloud height, as well as to explore the vertical structure of the AIRS cloud types (Stubenrauch *et al.*, 2010). These results can then be transposed to cloud types determined by the CIRS retrieval ~~method~~ using other IR sounders.

In the following, we analyse three years (2007-2009) of collocated AIRS-CALIPSO-CloudSat data, separately for three latitude bands: tropical / subtropical latitudes (30°N-30°S), midlatitudes (30°N-60°N and 30°S-60°S) and polar latitudes (60°N-90°N and 60°S-90°S).

~~3.1 Collocated AIRS ï CALIPSO ï CloudSat data~~

~~We use the same colocation procedure as in (Feofilov *et al.*, 2015b): all satellites of the A-Train follow each other within a few minutes. First, each AIRS footprint is collocated with NASA CALIPSO L2 cloud data averaged over 5 km (version 3, Winker *et al.*, 2009) in such a way that for each AIRS golf ball, three CALIPSO samples closest to the centres of each AIRS footprint are kept. These data are then collocated with the vertical profiling of the NASA L2 Lidar CloudSat geometrical profiling (GEOPROF) data (version P1_R04; Mace and Zhang, 2014). Each AIRS footprint includes thus information on the vertical structure (cloud top and cloud base for each of the cloud layers) at the spatial resolution of the radar footprints (1.4 km x 2.3 km) and in addition to cloud detection, cloud optical depth, cloud top and apparent cloud base (corresponding to the real cloud base or to the height at which the cloud reaches opacity) at the spatial resolution of the CALIPSO cloud data (5 km x 0.09 km). A cloud feature flag indicates whether the cloud is opaque. The CALIPSO L2 cloud data also indicate at~~

~~which horizontal averaging the cloud was detected (1 km, 5 km or 20 km), which is a measure of the optical thickness of the cloud. For a direct comparison with AIRS cloud data, we use clouds detected at horizontal averaging over 5 km or less, corresponding to minimum particle backscatter coefficient of about 0.0008 $km^{-1}sr^{-1}$ at night and about 0.0015 $km^{-1}sr^{-1}$ during day, for a cirrus with an altitude of about 12 km (Fig. 4 of Winker *et al.*, 2009). This corresponds to clouds with VIS optical depth larger than about 0.05 to 0.1 (Winker *et al.*, 2008). The scene over each AIRS footprint is estimated by using the cloud detection of all three CALIPSO samples per AIRS golf ball as: clear sky, partly cloudy and overcast.~~

~~For the evaluation of cloud height we determine the lidar CloudSat GEOPROF cloud layer which is closest to z_{cld} from AIRS. From the 5 km averaged CALIPSO data we also determine the height at which the cloud reaches a certain optical depth, in particular 0.5, $z_{COD0.5}$. We then require that this height is located within the corresponding cloud layer of the lidar CloudSat GEOPROF data.~~

~~Cloud optical depth (COD) determined from lidar backscatter depends on a correction for multiple scattering which itself depends on COD and microphysics (e. g. Comstock and Sassen, 2001; Chen *et al.*, 2002; Lamquin *et al.*, 2008). As CALIPSO assumes a constant multiple scattering coefficient of 0.6 in the retrieval (Winker, 2003), COD might be slightly underestimated, especially for larger COD. We therefore estimate from Figure 3 in (Lamquin *et al.*, 2008) a correction factor and deduce that a COD of 0.50 should correspond to a COD given by CALIPSO of about 0.37. To determine the height within the cloud at which COD reaches 0.5 we also use an assumption on the shape of the ice water content vertical profile between cloud top and cloud base (Feofilov *et al.*, 2015b).~~

~~In the following, we analyze three years (2007-2009) of collocated AIRS-CALIPSO-CloudSat data, separately for three latitude bands: tropical / subtropical latitudes (30°N-30°S), midlatitudes (30°N-60°N and 30°S-60°S) and polar latitudes (60°N-90°N and 60°S-90°S).~~

3.1~~2~~ Cloud detection

The hit rates (fraction of agreeing cloudy and clear cases) between the ~~«a posteriori»~~AIRS-CIRS cloud detection ~~leads to an agreesment with~~and the lidar-radar ~~CALIPSO-CloudSat~~ cloud detection (section 2.4) ~~from GEOPROF and CALIPSO in about~~are 85% (84%) over ocean, 82% (79%) over land and 70% (73%) over ice / snow~~,~~. Values in parantheses correspond to ~~using atmospheric and surface ancillary data, deduced from AIRS-NASA (~~ERA-Interim~~)~~ ancillary data. Table 1 presents separate ~~these agreements~~comparisons ~~separately~~ for the three latitude bands. ~~CALIPSO-CloudSat cloud detection is defined by at least one cloud layer from GEOPROF and from CALIPSO and clear sky is defined by three CALIPSO clear sky samples within one golf ball (section 2.4).~~ In general, these ~~agreements~~ hit rates are quite high, considering that CALIPSO and GEOPROF data only sample a small area of the AIRS footprints. They are slightly higher over ocean than over land. Compared to the AIRS-LMD cloud retrieval presented in ~~(~~Stubenrauch *et al.*~~,~~ (2010), the agreement with CALIPSO-CloudSat has improved both over ocean and land, but slightly decreased over sea ice. The latter can be explained by applying now only one test over all surface types. In the earlier version we used an additional brightness temperature difference test related to temperature inversions. A detailed analysis (not shown) indicated that it also introduced noise.

To further illustrate ~~cloud amount (~~CA~~)~~ uncertainties ~~due~~ linked to ancillary data, we investigate, in Figure 2, ~~presents~~ geographical maps of differences in CA ~~differences~~ and T_{surf} ~~between~~ , using~~AIRS-CIRS based on~~ ancillary data from AIRS-NASA and from ERA-Interim~~, together with~~ ~~T_{surf}~~ ~~differences, are shown in Figure 3~~. ~~When using~~With AIRS-NASA ancillary data, CA over land is ~~mostly~~ often smaller ~~over land~~ during night and larger ~~over land~~ in the afternoon, with~~. One might observe a positive correlation with differences in~~ ~~T_{surf}:~~ T_{surf} ~~of the ancillary data deduced from AIRS-NASA is slightly~~ also smaller during night and larger in the afternoon ~~during daytime~~ over large parts of the continents. ~~From t~~~~T~~Considering the T_{surf} comparison with ARSA ~~in (~~section 2.5),~~4~~ ~~leads then to the conclusion,~~this means ~~we deduced~~ that over land ~~AIRS-CIRS~~ CA is slightly underestimated during night ~~when using~~with AIRS-NASA ancillary data, while slightly underestimated in the afternoon ~~when using~~with ERA-Interim ancillary data. Patterns of differences in atmospheric water vapour are less reflected in those of CA (not shown), but slightly more atmospheric water vapour in the ancillary data (as in the tropics for AIRS-NASA compared to ARSA and ERA-Interim) might lead to a slight underestimation of CA.

3.2~~3~~ Cloud height

~~For the evaluation of cloud height we determine the lidar CloudSat GEOPROF cloud layer which is closest to~~ ~~z_{cld}~~ ~~from AIRS. From the 5 km averaged CALIPSO data we also determine the height at which the cloud reaches a certain optical depth, in particular 0.5,~~ ~~$z_{COD0.5}$~~~~. We then require that this height is located within the corresponding cloud layer of the lidar CloudSat GEOPROF data.~~

~~Cloud optical depth (COD) determined from lidar backscatter depends on a correction for multiple scattering which itself depends on COD and microphysics (e. g. Comstock and Sassen, 2001; Chen~~ ~~*et al.*~~~~, 2002; Lamquin~~ ~~*et al.*~~~~, 2008). As CALIPSO assumes a constant multiple scattering coefficient of 0.6 in the retrieval (Winker, 2003), COD might be slightly underestimated, especially for larger COD. We therefore estimate from Figure 3 in (Lamquin~~ ~~*et al.*~~~~, 2008) a correction factor and deduce that a COD of 0.50 should correspond to a COD given by CALIPSO of about 0.37. To determine the height within the cloud at which COD reaches 0.5 we also use an assumption on the shape of the ice water content vertical profile between cloud top and cloud base (Feofilov~~ ~~*et al.*~~~~, 2015b).~~

Figure 3~~4~~ presents normalized distributions of the difference between ~~the height at which COD reaches a value of about 0.5,~~ $z_{COD0.5}$~~,~~ from CALIPSO (section 2.4) ~~determined from CALIPSO,~~ and ~~the retrieved cloud height from AIRS,~~ z_{cld}, from AIRS for the three latitude bands ~~as well as normalized distributions of the difference between the cloud top height from CALIPSO, z_{top}, and z_{cld}~~. We compare results for p_{cld} < 440 hPa and p_{cld} Ó440 hPa, ~~of the CIRS cloud retrieval, using ancillary data from AIRS-NASA and ERA-Interim,~~ separately for AIRS-NASA and ERA-Interim ancillary data ~~for high-level clouds (p_{cld} < 440 hPa) and lower-lever clouds (p_{cld} Ó440 hPa)~~. ~~The AIRS cloud height is compared to the CALIPSO-CloudSat cloud layer, which is the closest to z_{cld}. This is justified, because CALIPSO and CloudSat sample only sparsely the AIRS footprint, and AIRS could observe a mixture of several clouds.~~ In general, all distributions ~~of differences between $z_{COD0.5}$ and z_{cld}~~ peak around 0 km and are slightly narrower for lower -level clouds than for high-level clouds. Results are similar for both ancillary data, with a slight cloud height overestimation ~~for~~ of lower level clouds ~~in the~~ over tropicals ~~over~~ ocean ~~(not shown), when using~~for ERA-Interim (not shown),~~,~~ and a height overestimation of some clouds ~~in~~ over polar ~~regions over~~ ocean ~~(not shown), when using~~for AIRS-NASA ancillary data (not shown). The latter ~~might~~ can be explained by the fact that in some of these regions ~~*surface temperature*~~T_{surf} and atmospheric profiles of good quality are only available in 10% of the ~~situations~~time. When comparing distributions of z_{top} - z_{cld}, the peaks for lower clouds are still around 0 km, whereas for high-level clouds z_{cld} lies on average 1.5 km below the cloud top (not shown), ~~as~~ very similar to results in Stubenrauch *et al.* (2010)~~)~~. This~~,~~ mean~~sing~~ that T_{cld} is about 10 K warmer than the cloud top (Figure S2 of the supplement~~1~~). The broader distributions for high-level clouds compared to low-level clouds may be explained by the fact that high-level clouds often have diffuse cloud tops (e. g. Liao *et al*., 1995), especially in the tropics (z_{top} - z_{cld} is slightly larger for the same ε_{cld}, as shown in Figure 5). To summarize, z_{cld}~~;~~ ~~The CIRS retrieved cloud height coincides~~can be approximated ~~with~~ by i) the height of maximum lidar backscatter (Stubenrauch *et al.*, 2010), ~~with by~~ii) $z_{COD0.5}$ (Figure 3), or iii) ~~mid-height~~the mean ~~between of cloud top and «apparent» cloud base~~layer height (~~real cloud base~~ for optically thin clouds) or the mean between cloud top and ~~cloud~~ the height at which the cloud reaches opacity), as shown in Figure S2 (considering mid-p_{cld})~~1, or with by $z_{COD0.5}$, as shown in(Figure 3)4~~.

~~To~~ For a more detailed investigation of the different height approximations~~e more in detail how the CIRS retrieved cloud height~~, ~~relates to the height of COD of about 0.5 and to cloud top (z_{top}), we analyze in~~ Figure 4~~5~~ compares median values of z_{cld} - $z_{COD0.5}$, z_{top} - z_{cld} and (z_{top} - z_{cld})/(z_{top} ~~z_{top}~~ - $z_{app\ base}$)~~their average difference~~ as a function of ~~*ΑΙΡΣ χλουδ εμισσιϖιτψ*~~ε_{cld}~~, separately~~ for high-level clouds ~~and lower level clouds~~. For this analysis we have selected cases for which z_{cld} ~~AIRS cloud height~~ lies ~~within the cloud borders~~between top and base ~~from~~ of the closest ~~CALIPSO-CloudSat~~ GEOPROF cloud layer.

This~~,~~ leaves~~ing~~ about 82% / 73% / 57% ~~and about 55% / 59% / 58%~~ of the statistics ~~of high-level and lower level clouds over the~~in tropics / midlatitudes / polar regions, respectively. ~~In general, for low-level clouds, the AIRS cloud height lies about 250 m – 500 m below the height at which the cloud reaches an optical depth of about 0.5, independently of ε_{cld}, while z_{cld} lies about 1 km below the cloud top. For high-level clouds the~~ z_{cld} varies from 1 km above for ε_{cld} = 0.1 to 1 km below $z_{COD0.5}$ ~~the height corresponding to COD of 0.5~~ for ε_{cld} = 1, assuming that $z_{COD0.5}$ ~~COD~~ is accurately ~~determined~~ estimated for all ε_{cld} (section 2.4)~~.~~. In that case, ~~This means that for thin cirrus~~ z_{cld} ~~from AIRS~~of thin cirrus should be approximated~~corresponds to~~ by a height ~~of at which~~with COD ~~reaches a value~~ < 0.5~~, while for~~and z_{cld} of opaque high clouds ~~to~~ by a height ~~at which~~with ~~of~~ COD ~~reaches a value~~ > 0.5. On the other hand, z_{cld} lies about 1~~.5~~ km to 2~~.5~~ km below z_{top}~~zt_{op}~~~~the cloud top~~, the difference to cloud top increasing with ε_{cld} ~~.~~(except for ε_{cld} close to 1). Since z_{top} ~~zt_{op}~~ - $z_{app\ base}$ ~~the apparent vertical extent~~ also increases with ε_{cld}, (not shown), ~~the~~ $(z_{top} - z_{cld})/(z_{top}$ ~~zt_{op}~~ $- z_{app\ base})$ ~~difference between z_{top} and z_{cld} scaled by apparent vertical extent~~ does not depend on ε_{cld}, and ~~it~~ is about 0.5 ~~for high-level and for low-level clouds~~. ~~Considering the normalized frequency distributions of z_{top} – $z_{COD0.5}$ and z_{top} – z_{cld}, as well as these differences scaled by apparent cloud vertical extent, presented in Figure 6, W~~We deduce that it probably needs less ~~geometrical thickness~~vertical extent for opaque clouds than for semi-transparent ~~clouds~~ cirrus to reach a COD of 0.5, while the χ^2 method determines a height within the cloud, which corresponds well to the ~~middle~~ mean between cloud top and ~~apparent cloud~~ base or the height at which the cloud reaches opacity, in dependent of ε_{cld}. This is important to take into account for the determination of radiative fluxes and heating rates of upper tropospheric clouds, when using ~~the~~ CIRS cloud height~~s retrieved from IR sounder measurements~~. We want to stress that also for low-level clouds $(z_{top} - z_{cld})/(z_{top}$ ~~zt_{op}~~ $- z_{app\ base})$ is about 0.5 (0.4 to 0.6), while ~~The broader distributions for high-level clouds compared to low-level clouds in Figures 4 and 6 may be explained by the fact that high-level clouds often have diffuse cloud tops (e. g. Liao *et al.*, 1995), especially in the tropics (z_{top} – z_{cld} is slightly larger for the same ε_{cld}).~~ z_{cld} of low-level ~~clouds~~ lies only about 0.1~~400~~ to~~m –~~ ~~100~~0.4 km below $z_{COD0.5}$~~, while z_{cld} lies~~and about ~~500~~ 0.5 km below z_{top}~~zt_{op}~~ ~~and (z_{top} – z_{cld})/(zt_{op} – $z_{app\ base}$) varies between 0.4 and 0.6~~ (Figure S3 of the supplement).

Finally,~~In order to see how well the distribution of clouds is represented within the atmosphere, we compare in~~ Figure 5 presents~~7 the~~ normalized frequency distributions of z_{cld} ~~from AIRS~~, using both sets of ancillary data, and of $z_{COD0.5}$ ~~from CALIPSO~~, whenever clouds are detected (excluding subvisible cirrus, see section ~~3.1~~2.4). The CALIPSO $z_{COD0.5}$ distributions have a slightly larger part of high-level clouds, especially in the tropics, and the AIRS z_{cld} distributions show a slightly larger part of low-level clouds over land. ~~, separately over land and over ocean in the three latitude bands. AIRS z_{cld} distributions are very similar, with slightly more low-level clouds over land using ERA-Interim and slightly more~~

~~higher clouds over polar ocean (which are mostly misidentifications as pointed out earlier). The $z_{COD0.5}$ distributions from CALIPSO have a slightly larger part of high-level clouds in the tropics and AIRS z_{cld} distributions show a slightly larger part of low-level clouds in the tropics.~~ The latter disappear if one considers only cases with all three CALIPSO samples cloudy within an AIRS golf ball.~~,~~ ~~so~~ Thus these low-level clouds are part of partly cloudy fields for which it is difficult to compare results from samples of very different spatial resolution. ~~Thus t~~The distributions ~~look more similar~~compare better when only mostly covered cloud fields are considered (three CALIPSO samples cloudy within an AIRS golf ball). In the tropics, the peak of the AIRS z_{cld} distributions for high-level clouds is still slightly broader towards lower heights than for CALIPSO (not shown). Additional filtering, ~~out of~~excluding multi-layer clouds, ultimately leads to very similar distributions, ~~as~~ also presented in Figure 5~~7~~. A plausible interpretation is, that in cases of multiple cloud layers ~~and if~~with the upper cloud layer ~~does~~ not fully covering the large AIRS footprint, instrument ~~the 15 km footprints~~received ~~of AIRS often mix~~ radiation is mixed from different cloud layers, ~~when the upper cloud layer does not fully cover the footprint,~~ and thus ~~*determines a cloud height*~~z_{cld} ~~which might be~~is slightly lower than the one of the uppermost cloud layer. The distributions in the midlatitudes still peak at slightly lower heights, ~~due to the fact that~~because high-level clouds in these latitudes are on average optically thicker (storm tracks) than in the tropics.~~,~~ In these cases z_{cld} lies below $z_{COD0.5}$, ~~and~~ as we have seen in Figure 4~~5~~.~~,~~ ~~in these cases z_{cld} lies below $z_{COD0.5}$.~~ The choice of ancillary data influences only mildly the z_{cld} distributions, with a slightly larger contribution of low-level clouds over land for ERA-Interim. This difference disappears ~~when considering~~if we consider only mostly covered cloud fields, as the contribution of low-level clouds~~ in all data sets,~~ strongly decreasees over land.~~,~~ ~~while o~~Over ocean, the effect is much smaller. This indicates that low-level clouds over ocean appear more often as stratus decks whereas those over land appear more frequently as cumulus, as expected.

~~To summarize, the evaluation of cloud height has shown that IR sounders capture quite well the vertical distribution of uppermost clouds in the atmosphere. The retrieval provides a cloud height of about 1 km below cloud top in the case of low-level clouds and of about 1.5 km to 2.5 km below cloud top height in the case of high-level clouds. In the latter case, the retrieved cloud height corresponds to a height of COD < 0.5 for optically thin clouds and to a height of COD > 0.5 for optically thick clouds. On the other hand, multiple scattering within optically thicker clouds is in general larger so that the correction we have applied above, which was meant for clouds with a total COD of 0.5, was probably not enough. As already shown by Stubenrauch *et al.* (2010), the CIRS retrieved cloud height coincides with the middle between cloud top and apparent cloud base, and this for all cloud heights. Even though the spatial~~

~~resolution of 15 km may mix clear sky and cumulus clouds, or thin cirrus with optical thicker high clouds, the cloud height is in general well determined within 1.5 km.~~

4 Average ~~Cloud~~ cloud properties and variability

In this section we give a short overview of cloud properties ~~obtained from~~of the AIRS-CIRS and IASI-CIRS cloud climatologies. Monthly L3 data, gridded at a spatial resolution of 1° latitude x 1° longitude, have been produced in the same manner as for the GEWEX Cloud Assessment data base (Stubenrauch *et al.*, 2013): in a first step, ~~averages were determined~~cloud properties and their uncertainties, deduced from the χ^2 method, were averaged per observation time over 1° latitude x 1° longitude, and in a second step, these ~~cloud properties were~~were averaged per month. In addition to the monthly averages, ~~,~~ the data base also includes ~~time variability and~~ histograms of the cloud properties~~. In addition, We~~ we ~~have also added~~provide p_{cld} and ε_{cld} ~~uncertainties on p_{cld} and ε_{cld} deduced from the χ^2 method~~.

Figure 6~~8~~ compares normalized frequency distributions of p_{cld} (CP) over 30° wide latitude bands during boreal winter and boreal summer, separately over land and over ocean. As one can see, t~~T~~he AIRS and IASI CP distributions are very similar. Their relative contribution of high-level clouds is slightly larger over land than over ocean, especially in the tropics, ~~and~~ while the contribution of low-level clouds is larger over ocean. Considering seasonality, the strongest signature is the shift of the Intertropical Convergence Zone (ITCZ) towards the summer hemisphere, ~~linked to~~manifested by a large amount of high-level clouds (from cirrus anvils), especially over land.

Figure 7~~9~~ presents global averages of total cloud amount (CA) and relative contributions of high-level, mid-level and low-level clouds, determined by dividing these cloud amounts (CAH, CAM, CAL) by CA. The sum of the relative contributions, CAHR, CAMR and CALR is equal to 1. ~~Pressure limits for high-level/mid-level and mid-level/low-level cloud classification are 440 hPa and 680 hPa, corresponding to altitudes of about 6 km and 3 km, respectively.~~ Relative cloud amount values give an indication of how the detected clouds are vertically distributed in the atmosphere, when observed from above. ~~Compared to the absolute values, they are less influenced by differences in cloud detection sensitivity and should be more useful for comparison with climate models (Stubenrauch *et al.*, 2013).~~ Global averages of AIRS-CIRS and IASI-CIRS are compared with those from selected cloud climatologies of the GEWEX Cloud Assessment data base: the International Satellite Cloud Climatology Project (ISCCP; Rossow and Schiffer, 1999), two cloud climatologies derived from observations of the Moderate Resolution Imaging Spectroradiometer (MODIS) aboard the Aqua satellite, by the MODIS Science Team (MODIS-ST; Frey *et al.*, 2008) and by the MODIS CERES Science Team (MODIS-CE; Minnis *et al.*, 2011), and two cloud climatologies derived from CALIPSO observations, the one ~~by~~ of the CALIPSO Science Team (CALIPSO-ST; Winker *et al.*, 2009) and the GCM-Oriented CALIPSO Cloud Products (CALIPSO-GOCCP; Chepfer *et al.*, 2010). The latter two use vertical averaging (CALIPSO-GOCCP) and horizontal averaging (CALIPSO-ST) to reduce the noise of the relatively small samples. The latter is more sensitive to thin layers of subvisible cirrus. ISCCP is essentially using two atmospheric window channels (IR and VIS, the latter only during daytime). Considering passive remote sensing, ~~For the GEWEX Cloud Assessment data base the eight-times-daily ISCCP results have been averaged to four specific local observation times: 3:00 AM, 9:00 AM, 3:00 PM and 9:00 PM, and a day-night adjustment on CA, which is included in the original data, has not been included to better illustrate the differences between VIS-IR and IR-only results. We separately examine daytime and nighttime observations mostly during day, corresponding to 1:30PM (3:00PM for ISCCP, 9:30AM for IASI), and mostly during night, corresponding to 1:30AM (3:00AM for ISCCP and 9:30PM for IASI) LT, respectively.~~ t~~T~~otal cloud amount from the GEWEX Cloud Assessment data base is about 0.68±0.03 (Stubenrauch *et al.*, 2013), while CALIPSO-ST provides a cloud amount of 0.73, because it includes subvisible cirrus.

We separately examine daytime and nighttime observations. While all data sets agree quite well on ~~the total cloud amount~~CA, with ISCCP and MODIS-CE providing smaller CA during night (both including VIS information for cloud detection during daytime), CAHR exhibits a large spread, ~~essentially~~ due to different sensitivity to thin cirrus : active lidar is the most sensitive, followed by IR sounders~~, as confirmed in Figure 9~~. The CIRS results are very similar to the results from the AIRS-LMD cloud climatology (Stubenrauch *et al.*, 2010). The choice of ancillary data only slightly affects CA at night. ~~AIRS-CIRS results based on different ancillary data are also very similar as well as~~ IASI-CIRS and AIRS-CIRS results are also very similar, day and night. They present global averages of CA around 0.67 ï 0.70, formed by 40% high-level ~~clouds~~, 20% midlevel ~~clouds~~ and 40% low-level uppermost clouds ~~as seen from above~~. This is in excellent agreement with the results from CALIPSO. ~~A~~ The slightly ~~higher~~ smaller value in CALIPSO CAMR (~~20~~14% instead of ~~14~~20%) ~~can be explained~~is due ~~by the fact~~to ~~that~~ the different distinction between high-level and mid-level clouds: ~~of~~ CALIPSO ~~is according to~~uses cloud top height, whereas AIRS and IASI ~~provide~~ use a cloud height which is about 1~~.5~~ km lower than the top (~~see~~ section 3.2~~3~~). When combining VIS and IR information, thin cirrus above low-level clouds tend to be misidentified as mid-level clouds (ISCCP) or as low-level clouds (MODIS), leading to a not negligible underestimation of CAHR (30% instead of 40%). ~~During~~ At night~~time~~, ~~for which~~when only ~~one~~ the IR channel is available, ISCCP underestimates the height of all semi-transparent high-level clouds, so that CAHR drops to 15%. When IR spectral information is available, as for IR sounders and MODIS, results are similar to those during daytime.

Differences between ocean and land, also presented in Figure 9~~7~~, correspond to about ~~15% for~~0.15 in total CA, with about 20% more low-level clouds over ocean and about 10% more high-level and mid-level clouds over land. The CIRS retrievals provide similar values during day and night. It is interesting to note that during daytime the difference in CA shows a larger spread between the datasets, while ~~during nighttime~~at night the spread is larger for CALR. ~~During nighttime~~At night, low-level clouds are more difficult to detect, especially over land.

Table 2 summarizes averages of these cloud amounts over the whole globe, over ocean and over land, also contrasting NH and Southern hemisphere (SH) midlatitudes (30°-60°) and tropics (15°N-15°S). The largest fraction of high-level clouds is situated in the tropics, ~~and~~ while the largest fraction of single layer low-level clouds in the SH midlatitudes. Only about 10% of all clouds in the tropics are single layer midlevel clouds, compared to about 22% in the midlatitudes. As already discussed in sections 2.5~~4~~ and 3.1~~2~~, the uncertainty due to ancillary data in CA, as well as in CALR, ~~due to ancillary data~~ is largest over land (about 5% and 10%, respectively), because~~linked to underestimation of~~ low-level clouds are underestimated ~~during night~~ with AIRS-NASA~~,~~ during night and ~~in the afternoon~~ with ERA-Interim in the afternoon. Uncertainties ~~due to ancillary data~~ are much smaller for high-level clouds. ~~C. When separating them into C~~Considering further three distinct high-level cloud classes, ~~of~~ opaque, thick cirrus and thin cirrus ~~according to ε_{cld}~~ (~~see~~ section 2.5~~4~~)~~, uncertainties due to ancillary data are less than 5% at low latitudes. In the midlatitudes,, increasing touncertainties for opaque clouds increase to 10% at midlatitudes for opaque clouds, while those for cirrus do not exceed 5%. This can be explained by the fact thatmight be due to interpolation of ancillary data in the case of opaque clouds the ancillary data often have to be interpolated in time, with and atmospheric profiles and T_{surf} have having a larger variability in the midlatitudes than in the tropics. While~~ high-level opaque clouds only ~~make out~~represent about 5.2% of all clouds, while relative cloud amounts of thick cirrus and thin cirrus are about 21.5% and 13%~~.,~~ Maximum values are observed in the tropics, ~~respectively, with maximum appearance in the tropics,~~ of 7.5%, 27.5% and 21.5%, respectively (Table 3). ~~Their relative amounts are summarized in Table 3. TheAn~~The independent use of p_{cld} and ε_{cld} ~~made it possible~~enabled us to ~~construct~~ build a climatology of upper tropospheric cloud systems, ~~by i) applying a spatial composite technique on adjacent p_{cld} and ii)~~ using ε_{cld} to distinguish convective core, cirrus anvil and thin cirrus of these systems. These data have revealed for the first time that the ε_{cld} structure ~~within~~ of tropical anvils is related to the convective depth (Protopapadaki *et al.*, 2017)~~, which might have important consequences on radiative feedbacks~~.

Figure ~~10~~ 8 presents zonal averages of CA, CAH and CAL as well as effective cloud amount for total (CAE) high-level (CAEH) and low-level (CAEL) clouds, ~~. The annual zonal averages are presented~~

~~from~~for the three CIRS climatologies (AIRS, using ~~AIRS-NASA and ERA-Interim~~two sets of ancillary data, ~~as well as~~and IASI~~, using ERA-Interim ancillary data~~) and the prior AIRS-LMD cloud climatology. ~~In addition, boreal winter and boreal summer zonal averages are shown for AIRS-CIRS alone, but separately for each of the thirteen years to illustrate the inter-annual spread.~~ Effective cloud amount corresponds to the cloud amount weighted by cloud emissivity. ~~and~~ It therefore includes the IR radiative effect of the detected clouds. In general, CAE is about 0.2 smaller than CA. Maximum CAH and CAEH appear in the ITCZ, while maximum CAL and CAEL is found in the SH midlatitudes. ~~All~~The results of all CIRS climatologies are very similar, ~~Interannual variability is largest in CA and CAL (CAE and CAEL) in the NH polar region. One also observes that the midlatitude interannual variability of CAH is larger in winter than in summer, most probably linked to storm track variability. When comparing the different CIRS retrievals, all agree in general very well, with AIRS-CIRS and IASI-CIRS with ERA-Interim being very close, while~~with AIRS-CIRS ~~with~~ using AIRS-NASA ancillary data presentings slightly more high-level clouds and less low-level clouds~~-~~ around 60S and slightly less CA and CAL in the NH polar region.

Figure~~s~~ ~~11 and 12~~9 presents geographical maps of annual CAH and CAL~~, respectively~~.~~,~~ We ~~as well as seasonal differences.~~ c~~C~~ompare~~d~~ ~~are~~ AIRS-CIRS, ISCCP and CALIPSO-GOCCP, the latter two from the GEWEX Cloud Assessment data base. In all datasets the most prominent feature in CAH is the ITCZ~~ and its shift towards the summer hemisphere~~. However, due to the better sensitivity to cirrus, the absolute values ~~and seasonal variations~~ are more pronounced for AIRS-CIRS (IASI-CIRS, not shown) and CALIPSO-GOCCP than for ISCCP. Due to the narrow nadir track of CALIPSO and the reduced statistics of CALIPSO-GOCCP in the present GEWEX Cloud Assessment data base, these data look noisier than AIRS-CIRS and ISCCP. ~~In addition, jet streams and midlatitude storm tracks in winter, as well as continental cirrus in summer can be distinguished.~~ Considering CAL, AIRS-CIRS ~~well~~ captures well the stratocumulus regions off the West coasts of the continents and stratus decks in the subtropical subsidence regions in winter, even if this type of cloud is easier to detect by using instruments including VIS channels (during daytime, ISCCP) or active instruments (CALIPSO-GOCCP).

Time series of deseasonalized anomalies in global monthly mean CA, CAEH and CAEL of the three CIRS data sets are shown in Figure ~~13~~ 10 over the time period of 2004 ï 2016 for AIRS and 2008 ï 2016 for IASI. To illustrate the effect of the calibration accounting for changes in atmospheric CO_2 concentration (section 2.5~~4~~.2), ~~a~~ the time series of the AIRS-CIRS ~~deseasonalized~~ CA anomalies, without ~~having applied~~ this correction, is added. Whereas the uncorrected CA anomalies increase by about 0.040 within a decade, the magnitude of the calibrated CA and CAEL variations lie within 0.010

and of CAEH within 0.005, being mostly stable with~~with~~in the uncertainty range.~~ Indeed, g~~G~~lobal surface temperature did not increase much over this period (not shown).~~

~~The ~~Latitudinal seasonal cycles of ~~different cloud properties~~CA, CAH, CAL and T_{cld} (CT) from the different data sets agree in general quite well (~~, is presented in ~~Figure ~~11~~S4 of the supplement)~~,4 agree in general quite well for six 30° wide latitude bands ranging from SH polar to NH polar, comparing results from CIRS data and those from the GEWEX Cloud Assessment data base. As already acknowledged during the GEWEX Cloud Assessment (Stubenrauch *et al.*, 2013), the seasonal cycles agree quite well between the different data sets, with exception of the polar regions where passive remote sensing does not perform well and the CALIPSO data are not conform with the other data sets in the GEWEX Cloud Assessment data base, because they exclude measurements from 1:30PM during polar night (polar winter) and from 1:30AM during polar day (polar summer)~~. The most prominent features of the latitudinal seasonal cycles are i) the shift of the ITCZ towards the summer hemisphere, seen as an amplitudinal signal of 0.1 in CA, 0.3 in CAH and 16 K in CT in the SH and NH tropical bands (mostly over land, not shown) and ii) less clouds in late summer in the midlatitudes (mostly over ocean and stronger in NH, not shown). The seasonal cycle of ~~cloud temperature~~CT is largest in the polar regions (coherent for all data sets)~~, followed by SH sub-tropical band, NH midlatitudes, NH sub-tropical band~~ and smallest in SH midlatitudes, with amplitudes ranging from 20 K to 10 K. However, while the CT amplitude is linked to change in cloud height ~~in the~~at low latitudes, it is more related to change in atmospheric temperature (and corresponding ~~cloud temperature~~CT) at higher latitudes.

5 Applications

After ~~the comparisons to other datasets~~having demonstrated the reliability of the CIRS cloud climatologies~~y~~ in sections 3 and 4, ~~which have proven the reliability of the CIRS upper tropospheric clouds, ~~we present ~~in the following two ~~analyses on upper tropospheric (UT) cloud variability with respect to changes in atmospheric conditions. ~~to ~~These illustrate the ~~usefulness ~~added value of the CIRS cloud data for climate studies.

5.1 ~~Studying h~~Hemispheric differences in UT clouds

While the NH and the SH reflect the same amount of sunlight within 0.2 Wm^{-2} (Stephens *et al.*, 2015), there is a small energy imbalance between both hemispheres of our planet, with slightly more energy absorbed by the SH (0.9 Wm^{-2}). This~~,~~ yields~~ing~~ more frequent precipitation in the SH ~~and ~~while more intense precipitation in the NH (Stephens *et al.*, 2016). The latter might be linked to the characteristics of the ITCZ, a zone of strong convection, which itself produces large cirrus anvils. As the size of these anvils is on average positively related to convective strength (e. g. Protopapadaki *et al.*, 2017), we explore ~~.~~the annual mean and seasonal hemispheric difference of high cloud amount and try to relate it to the characteristics of the ITCZ, such as its peak strength, the latitudinal position of the peak and its width.

T~~For this analysis, t~~hese ITCZ characteristics have been determined by fitting a Gaussian around the tropical peak of the latitudinal CAH distributions (Figure 8), per month and year. This yields the latitude of the peak position, the value of the peak itself, and the width of the tropical CAH distribution. ~~The peak height might give an indication of the strength of the ITCZ.~~

~~The more intense precipitation in the NH is probably linked to the fact that on annual average the ITCZ peak latitude is about 5°N, shown in Figure 115. On average, total CA is about 10% (0.06) smaller in the NH than in the SH (excluding the polar regions), without a pronounced seasonal cycle (not shown). This is linked to more clouds over ocean than over land, producing the increased reflection in the SH midlatitudes as discussed in (Stephens *et al.*, 2015).~~ From Figure ~~15~~ 11 we deduce that the annual NH-SH difference in CAH ~~between NH and SH~~ is 0.05, with a pronounced seasonal cycle of about 0.3 in amplitude. Results from the three ~~three~~ CIRS cloud climatologies (AIRS with two ancillary data sets and IASI), AIRS-LMD, CALIPSO-GOCCP, ISCCP and MODIS-CE are ~~very~~ similar. This seasonal cycle ~~corresponds~~ is well related to the one of the ITCZ peak latitude, which moves up to 12°N in July. It is ~~also~~ interesting to note that the width of the ITCZ is smaller in July / August (10.5° ï 12.5°) than in January (17°) and the CAH peak is about 10% larger in August than in January.~~,~~ ~~which~~ This ~~would~~ might suggest a more ~~even more~~ intense ~~precipitation in the~~ ITCZ (and hence more intense precipitation) when it is located in the NH ~~in boreal summer~~than when it is located in the SH.

All datasets agree well on the ITCZ peak latitude. The smaller maximum CAH values of MODIS-CE and ISCCP are due to smaller sensitivity to thin cirrus, and the reduced seasonal cycle of maximum CAH and of ITCZ width for CALIPSO-GOCCP is due to the inclusion of ubiquitous thinner cirrus, leading to less well pronounced CAH minima in the subtropics. The CIRS climatologies reveal the seasonal behaviour of the ITCZ characteristics clearly. ~~For this analysis, the properties of the ITCZ have been determined by fitting the tropical peak of the latitudinal CAH distributions per month and year (as in Figure 10). While all datasets agree on the ITCZ peak latitude and mostly on the ITCZ width (with the Gaussian fit on the ITCZ maximum producing falsely a smaller width for CALIPSO-GOCCP, because due to ubiquitous thin cirrus, the minima in the subtropics are not as well pronounced as in the other data sets), MODIS-CE and ISCCP produce smaller absolute values of maximum CAH because of smaller sensitivity to thin cirrus. The seasonal cycle of maximum CAH is reduced for CALIPSO-GOCCP and AIRS-LMD due to the inclusion of thinner cirrus (for AIRS-LMD clouds down to~~ ~~$\varepsilon_{cld} > 0.05$~~~~, compared to a threshold for CIRS clouds of 0.10).~~ Figure 115 confirms and extends the interpretation of the results of (Stephens *et al.*, 2016), by displaying a ~~linking~~ relation between the hemispheric difference ~~in hemispheric~~of CAH ~~to the~~and ~~shifting~~ characteristics of the ITCZ, which seems to be more intense when its peak is situated in the NH ~~and its stronger intensity in the NH during boreal summer~~ (smaller width and larger maximum).

5.2 ~~Studying El Niño-Southern Oscillation (ENSO) effects~~Relating surface temperature anomalies to changes in UT clouds

~~ENSO is the most dominant mode of interannual variability in the Earthôs climate system (e.g. Bjerknes, 1969). The trade winds, blowing from east to west, warm the water as they push it, which leaves warm water in the West Pacific Maritime Continent (WPMC) and cool water in the tropical East Pacific. While warm air is rising, building up convection and upper tropospheric clouds, air dries over the cooler water in the east, thus this SST gradient is responsible for the Walker circulation. ENSO events, El Niño (warm phase) and La Niña (cold phase), are characterized by large-scale SST anomalies in the tropical Pacific, compared to the normal situation described above. El Niño events are initiated by a positive SST anomaly in the equatorial eastern and central Pacific which reduces the east-west SST gradient and hence the strength of the Walker circulation (Gill, 1980), resulting in weaker trade winds. The weaker trade winds in turn drive the ocean circulation changes that further reinforce the SST anomaly. The positive ocean-atmosphere feedback leads to the warm phase of ENSO, which is characterized by strong rising motion in the central Pacific and a descending branch over the initially strong convective area over the WPMC. After an El Niño reaches its mature phase, negative feedbacks are required to terminate growth. According to Lloyd *et al.* (2012), the major source of this negative feedback stems from the reduction in solar energy at the ocean surface by increased cloud cover over the warm water. Depending on the location of maximum SST anomalies and associated atmospheric heating, El Niño events may be distinguished as eastern and central Pacific warming events. A review is given by Wang *et al.* (2016). The cold phase of ENSO (El Niña) starts with a cold SST anomaly in the tropical Pacific, increasing the SST gradient and amplifying the Walker circulation, leading to stronger convection and more upper tropospheric clouds over the WPMC.~~

~~To illustrate maximum climate variability patterns in the tropics, we contrast the strongest El Niño and La Niña events during the AIRS observation period, with multivariate ENSO index of 2.1 in Dec. 2015 and -1.6 in Dec. 2010, respectively. Figure 16 presents geographical difference patterns between these two ENSO modes in surface temperature and resulting atmospheric parameters, using AIRS-CIRS cloud data, collocated ERA-Interim data and outgoing longwave radiation (OLR) from NASA-AIRS (Susskind *et al.*, 2012). As described in the literature, and summarized in the paragraph above, Figure 16 confirms that during an El Niño event East and central Pacific strongly warm, while temperatures are~~

~~slightly cooler over the WPMC. The latter is warmer during La Niña. Higher SSTôs lead to more water vapour in the atmosphere, while the WPMC with its lower SSTôs is drier. The vertical updraft (negative difference in vertical wind) intensifies in a narrow band just north of the equator over the Pacific west of the WPMC and a short branch to the South-East, in a typical pattern. The pattern differences in fraction of opaque high clouds represents the ones of convection, very similar to the updraft pattern, while high-level clouds increase over a wider part as outflowing anvils, in coherence with increasing water vapour, while they decrease over the drier WPMC. Thin cirrus increase as parts of anvils in the two branches, but also in the drier WPMC and North-west of the convective band. The OLR pattern is very similar to the one of CAH, increasing over WPMC and decreasing where CAH increases over the Pacific. The pattern of changes in high-level cloud temperature (CTH) shows some differences from the patterns of the other variables. In general, CTH warms where there are also less high-level clouds and it is lower where the updraft increases.~~

~~So far, th~~Since thee observational period of AIRS and IASI is too short to directly ~~obtain~~ study long-term cloud ~~feedbacks~~variability related to climate warming,~~.~~ ~~An~~ an alternative approach is to ~~assess~~ analyse cloud ~~feedback~~ variability in response to interannual climate variability ~~like ENSO~~. ~~Dessler (2010) demonstrated that as the surface warms, cloud changes lead to trapping additional energy, i.e. the longwave cloud feedback is positive. Zelinka and Hartmann (2011) investigated the response of tropical mean cloud parameters to the ENSO cycle and their effect on top of atmosphere radiative fluxes. They found during El Niño periods a decrease of high-level cloud amount as well as an increase in their height which would have opposite effects on the OLR, with a dominating effect coming from the first. Susskind *et al.* (2012) have shown that global mean and tropical mean OLR anomaly time series are strongly correlated with ENSO variability, with OLR change resulting primarily from changes in mid-tropospheric water vapour and cloud amount over the WPMC and the East Pacific. Observed variability in cloud, atmospheric and surface patterns due to ENSO variability can be used to constrain climate modelling and to understand the processes behind these changes (e. g. Stephens *et al.*, 2017).~~ Though interannual global ~~tropical~~ mean ~~the ENSO related SST~~surface temperature anomalies might not ~~correspond~~ directly relate to patterns of anthropogenic climate warming, Zhou *et al.* (2015) have shown that interannual cloud feedback may be used to directly constrain the long-term cloud feedback. Changes in ~~the geographical pattern and amount of~~ tropical ~~high-level~~UT ~~tropical~~ clouds ~~s~~ leads to variations in ~~cloud radiative~~atmospheric heating and cooling which then may influence the large-scale circulation, as has already been shown by ~~(e.g.~~ Slingo and Slingo (1991~~, Tian and Ramanathan, 2003~~).

Since the radiative effects of high opaque clouds and thin cirrus are quite different, we investigate the geographical patterns of UT cloud amount ~~changes~~ anomalies ~~(p_{cld} < 330 hPa)~~ with respect to tropical and ~~tropical~~ global mean surface temperature ~~changes~~anomalies, ~~separately~~ by separating them into ~~for high~~ opaque, ~~thick~~ cirrus and thin cirrus (~~p_{cld} < 330 hPa,~~ ε_{cld} > 0.95, ~~ε_{cld} between~~ 0.45 ~~and~~ - 0.95 and ~~ε_{cld}~~ < 0.45, corresponding to visible COD > 6, 1 - 6 and < 1, respectively). By making use of the whole period between 2003 and 2015 (covering 156 months), we ~~determine~~ estimate a change in ~~upper tropospheric~~UT cloud amount as a function of change in ~~tropical~~ mean surface temperature by a linear regression of their deseasonalized monthly ~~time~~ anomalies, at a spatial resolution of 1° latitude x 1° longitude. Similar techniques were already utilissed in other studies related to El Niño ï Southern Oscillation (ENSO) and cloud feedback (e.g. Lloyd *et al.*, 2012; Zhou *et al.*, 2013, ~~Zhou *et al.*, 2014, Yue *et al.*, 2017~~Liu *et al.*, 2017). Figure ~~17~~ 12 presents the change in amount of high opaque cloud (mostly of convective origin), in thick cirrus (often formed from convective outflow as anvils) and in thin cirrus (which might be formed as anvil or via in situ freezing) per *K*~~°C~~ of global surface warming ~~in the tropics (20°N ï 20°S),~~, obtained as the linear slopes of these deseasonalized monthly ~~time~~ anomaly relationships. The cloud amounts are from AIRS-CIRS, while the surface temperatures are from the ERA-Interim ancillary data. Results are very similar when using T_{surf} anomalies ~~surface temperatures~~ from AIRS-NASA (not shown~~Figure S5 of the supplement2~~). Zhou *et al.* (2013) have shown that ERA-Interim T_{surf} anomalies give similar results in their short-term cloud feedback analysis, compared to other T_{surf} data sets. In our study, we concentrate on the change of UT clouds of different height (p_{cld} < 440 hPa and p_{cld} < 330 hPa), and we compare changes in absolute UT cloud amounts and in UT cloud amounts relative to total cloud amount. ~~Figure 127 also presents~~The geographical patterns of the relative slope uncertainty are shown in Figure S5 in the supplement~~y~~. In general, large changes in cloud amount per ~~°C~~*K* of warming have smaller uncertainty than small ones, indicating robust patterns.

During this period, global mean T_{surf} anomalies and tropical mean T_{surf} anomalies are strongly correlated (not shown), and the spatial patterns in Figure 12 are compatible with ENSO-like patterns. The left panels of Figure 12 agree quite well with Figure ~~9~~8 of Liu *et al.* (2017), based on MODIS cloud amount and HadCRUT4 T_{surf} anomalies, even though our cloud types categories differ slightly. In particular, we have separated thin cirrus. Therefore the analyses suggest that the change patterns address ENSO variability rather than long-term trends. When considering relative cloud type changes (middle panels in Figure 12), the signals are stronger. An interesting feature appears when considering changes in the relative amounts of higher clouds (p_{cld} < 330 hPa, left panels of Figure 12): ~~Even though the change in tropical mean temperature is mostly linked to ENSO variability over the studied period and it is still uncertain how to relate these to long-term patterns due to anthropogenic climate warming, it is very interesting to note that high opaque clouds and thin cirrus show very different change patterns.~~ While the high opaque clouds, linked to strong precipitation (Protopapadaki *et al.*, 2017), relative to all clouds, increase in a narrow band in the tropics, there is a large increase in relative thin cirrus amount around these regions, the latter might~~hypothesized to~~ directly affect ~~directly~~ the atmospheric circulation through their radiative heating (e.g. Sohn, 1999; Lebsock *et al.*, 2010).

As in Liu *et al.* (2017), we ~~We~~ have also examined linear regression slopes from anomaly averages over the tropics and other latitudinal bands~~, as in Liu *et al.* (2017)~~. Although in general the relationships are very noisy, on the interannual scale tropical cirrus amount slightly decreases with warming (-0.76 ± 0.21 %/K), while thin cirrus amount seems not affected (-0.09 ± 0.20 %/K),~~-~~ in agreement with Liu *et al.* (2017). However, when considering changes in tropical cirrus and thin cirrus amount relative to total cloud amount, at higher altitude (p_{cld} < 330 hPa), both increase with warming (1.87 ± 0.52 %/K and 1.70 ± 0.54 %/K), which means that these clouds are more frequent among all clouds when T_{surf} gets warmer.

Even though the changes in mean T_{surf} are mostly linked to interannual variability over the studied period and it is still uncertain how to relate these to long-term patterns due to anthropogenic climate warming, it is very interesting to note that changes in amounts of high opaque clouds and thin cirrus, relative to all clouds, show very different geographical patterns. To get a better understanding on the ~~these~~ underlying feedback processes one has to consider the heating rates of these ~~upper tropospheric~~UT cloud systems and link them to the dynamics, which is foreseen in future work.

6 Conclusions

We have presented t~~T~~wo global climatologies of cloud properties ~~have been presented~~, ~~obtained~~ built from AIRS and IASI observations by the CIRS cloud retrieval. This retrieval software package, developed at LMD, can be easily adapted to any IR sounder. The retrieval method itself, based on a weighted χ^2 method on radiances ~~around~~ along the wing of the 15 μm CO_2 absorption band, and ~~the óa posterioriô~~a multi-spectral óa posterioriô cloud detection, based on the spectral coherence of retrieved cloud emissivities, have ~~already~~ been evaluated in previous publications.~~, and~~In this study, we have further demonstrated the reliability of these updated cloud climatologies ~~in this study~~. IR sounders are especially advantageous ~~for the~~to retriev~~eal of~~ upper tropospheric cloud properties,~~. Their good spectral resolutions~~as they ~~allows a~~ reliably determine~~e~~ cirrus ~~identification~~ properties down to an IR optical depth of 0.1, day and night. The CIRS retrieval uses~~applies~~ improved radiative transfer modelling, employs the latest ancillary data (surface temperature, atmospheric profiles), and ~~an original calibration method to adjust~~accounts ~~simulated~~ for atmospheric spectral transmissivity ~~profiles~~ changes ~~according~~ associated ~~to~~ with latitudinal, seasonal and interannual atmospheric CO_2 concentration variations. ~~This Taking into account CO_2 calibration method has removedvariability~~The latter eliminates an artificial CA trend of about 4% over the observation period 2004 to 2016~~;, which was directly related to not having taken into~~

~~account the anthropogenic CO_2 increase in the spectral transmissivities simulated for a specific atmospheric CO_2 concentration.~~ The magnitude of ~~calibrated~~ cloud amount and effective low-level cloud amount deseasonalized variations lie within 1% and of effective high-level cloud amount within 0.5% over this period.

~~Common a~~Ancillary data ~~(surface temperature, atmospheric profiles) come~~ from the meteorological reanalyses ERA-Interim~~, which~~ have been interpolated to the observation times of AIRS and IASI. Additional ancillary data, established ~~application of~~from NASA AIRS retrievals, ~~retrieved AIRS-NASA ancillary data allowed~~permitted to iteratively make adjustments to both sets of ancillary data for optimal results in cloud properties and ~~also~~ to estimate uncertainties in cloud amounts. Since the cloud detection depends on the coherence of spectral cloud emissivity, the surface temperature influences only slightly the cloud amount (in particular the one of low-level clouds). AIRS total cloud amount is ~~67~~70% ~~/~~ (~~70~~67%), high-level cloud amount 27% ~~/~~ (27%) and low-level cloud amount 2~~9~~7% ~~/~~ (2~~7~~9%), using ERA-Interim (AIRS-NASA) ~~/ ERA-Interim~~ancillary data. ~~,~~This ~~giving an~~corresponds to uncertainty estimates of 5% ~~/~~ and 10% ~~uncertainty~~ on global averages ~~for~~ of CA ~~/~~ and CAL, respectively. Uncertainties are larger over land and ice ~~/~~ or snow than over ocean, in particular because T_{surf} of ERA-Interim is underestimated in the afternoon and T_{surf} of AIRS-NASA is underestimated during night due to cloud contamination. In the future, the CIRS cloud retrieval might use ancillary data from ~~ECMWF meteorological analyses or from~~ the new ECMWF meteorological reanalysis ERA5, ~~both also having~~with a better temporal and spatial resolution.

~~Cloud / clear sky~~Cloud detection hit rates between AIRS-CIRS and ~~detection agrees with the one of~~ CALIPSO-CloudSat are ~~in~~ 8~~5~~4% ~~/~~ (~~84~~85%) over ocean, ~~79~~82% ~~/~~ (~~82~~79%) over land and ~~73~~70% ~~/~~ (~~70~~73%) over ice and snow, for ERA-Interim (AIRS-NASA) ~~/ ERA-Interim~~ ancillary data~~, respectively~~. Typical p_{cld} uncertainties ~~in *cloud pressure*~~ range from 30 hPa for high-level clouds to 120 hPa for low-level clouds, ~~coinciding with~~which corresponds to about 1.2 km ~~in altitude~~. A comparison with CALIPSO-CloudSat ~~has~~ show~~n~~s, that on average the CIRS retrieved cloud height ~~lies only about 1 km below~~is close to cloud top in the case of low-level clouds and lies about 1~~.5~~ km ~~to 2.5 km~~ below cloud top in the case of high-level clouds. The latter leads to retrieved cloud temperatures which are about 10 K warmer than the cloud top. This has to be considered when determining radiative effects or when evaluating climate models. The CIRS retrieved cloud height ~~coincides~~ can be approximated ~~with~~ by the ~~middle~~ mean layer height (for optically thin clouds) or the mean between cloud top and ~~apparent cloud base (real cloud base for optically thin clouds or~~the ~~cloud~~ height at which the cloud reaches opacity, for both high-level and low-level clouds)~~, independently of ε_{cld}~~. ~~When comparing to the height at which the cloud reaches a VIS optical depth of about 0.5, the CIRS retrieved cloud height, in the case of high-level~~

~~clouds, lies about 1 km above for optically thin clouds and about 1 km below for optically thick clouds.~~ While for low-level clouds thise ~~apparent cloud~~ vertical ~~extent~~ distance is about ~~1~~ 0.5 km, for high-level clouds it slightly increases with ε_{cld}, from ~~3~~ 0.7 km to 1.5~~4~~ km, with slightly ~~higher~~ larger values in the tropics than in the midlatitudes, linked to diffusive cloud tops.

Total cloud amount ~~consists of~~is partitioned into about 40% high-level clouds, ~~and about~~ 40% low-level clouds and 20% mid-level clouds.~~,~~ T~~t~~he latter two categories ~~only~~ are only detected ~~ed when not hidden by~~in the absence of upper clouds. Upper tropospheric clouds are most abundant in the tropics, where high opaque clouds make out 7.5%, thick cirrus 27.5% and thin cirrus 21.5% of all clouds. IASI values are very similar. The most prominent features of latitudinal seasonal cycles ~~are~~ is the shift of the ITCZ towards the summer hemisphere, ~~with~~ seen as an ~~an~~ amplitudinal signal~~e~~ of 0.1 in CA, 0.3 in CAH and 16 K in CT in the SH and NH tropical bands~~,~~ (and even stronger over land).

The 5% annual mean excess in upper tropospheric cloud amount in the Northern compared to the Southern hemisphere has a pronounced seasonal cycle with a maximum of 25% in boreal summer have been related to the characteristics of the ITCZ. The annual mean ITCZ peak latitude lies about 5°N with a maximum of 10°N in boreal summer. At that time the ITCZ width is also narrower and the peak slightly larger. This suggests that the NH-SH excess in CAH is mostly determined by the position ~~and moving~~ of the ITCZ.

~~The asymmetry in CAH between Northern and Southern hemisphere with annual mean of 5% has a pronounced seasonal cycle with a maximum of 25% in boreal summer, which can be linked to the shift of the ITCZ peak latitude. The latter has an annual mean of 5°N, moving to 12°N with a slightly more intense ITCZ (smaller width and larger maximum) in boreal summer.~~

To illustrate ~~further~~ the ~~usefulness~~ added value of the CIRS cloud data for climate studies, we have finally presented ~~ENSO effects and tropical~~ geographical ~~change~~ patterns in changes of amount of high opaque, cirrus and ~~clouds and~~ thin cirrus with respect to ~~tropical~~ global mean T_{surf} ~~surface temperature~~ changes. These are in agreement with earlier studies, while an examination of changes in tropical high cirrus and thin cirrus amounts relative to total cloud amount revealed that these are more frequent among all clouds when T_{surf} gets warmer.~~.~~ Even though the change in ~~tropical~~ mean T_{surf} ~~temperature~~ is mostly linked to ENSO variability over the studied period and it is still uncertain how to relate these to long-term patterns due to anthropogenic climate warming, the large difference in geographical ~~change~~ patterns in changes of amounts of high opaque clouds and thin cirrus, realtive to total cloud amount, indicates that their response to climate change may be different. ~~which~~ This might then ~~has~~ have consequences on the atmospheric circulation. To get a better understanding on ~~these~~ the underlying feedback processes, one has to consider the heating rates of these upper tropospheric cloud systems and link them to the dynamics. Therefore the AIRS-CIRS and IASI-CIRS cloud data have been further used to build upper tropospheric cloud systems (based on p_{cld}) and then to distinguish convective cores, cirrus anvil and thin cirrus according to ε_{cld} (Protopapadaki *et al.*, 2017). These data are being further exploited, together with other data and modelling at different scales, within the framework of the GEWEX PROcess Evaluation Study on Upper Tropospheric Clouds and Convection (UTCC PROES, Stubenrauch and Stephens, 2017) to advance our understanding on ~~upper tropospheric~~UT cloud feedbacks.

The AIRS-CIRS and IASI-CIRS cloud climatologies will be made available at the French data centre AERIS, which also will continue their production.

7 Data availability

AIRS L1 data are available at https://mirador.gsfc.nasa.gov/. The NASA Science Team L2 standard products (Version 6; Olsen *et al.*, 2017~~6~~) are available at https://mirador.gsfc.nasa.gov/. IASI L1 data are available at the French Data ~~centre~~ Centre AEROS. IASI L2 data provided by NOAA, are available at the Comprehensive Large Array-data Stewardship System (CLASS) center (https://www. class.ncdc.noaa.gov). The ARSA database is available at : http://climserv.ipsl.polytechnique.fr/fr/les-donnees/arsa-analyzed-radiosoundingsarchive .html. The operational version of the 4A radiative transfer model (Scott and Chédin, 1981) is available at http://www.4aop.noveltis.com. The cloud climatologies of the GEWEX Cloud Assessment data base are available at: http://ipsl.polytechnique.fr/gewexca. ~~THE~~ The AIRS-CIRS and IASI-CIRS cloud climatologies will be made available by the French Data Centre AERIS.

Acknowledgements

This work has been financially supported by CNRS, by the ESA Cloud_cci project (contract No.: 4000109870/13/I-NB) and by CNES. The authors thank the members of the IASI, AIRS, CALIPSO and CloudSat science teams for their efforts and cooperation in providing the data as well as the engineers and space agencies who control the data quality~~ of the data~~. We thank the Aeris data infrastructure for providing access to the data used in this study and for ~~the~~ continuing~~ation~~ ~~of~~ the data production.~~-~~ We also thank Filipe Aires for providing the surface emissivity climatology built from IASI. In addition, we thank two anonymous referees for their thoughtful comments, which improved the quality of the manuscript.

References

Aires, F., Prigent, C., and Rossow, W. B.: Temporal interpolation of global surface skin temperature diurnal cycle over land under clear and cloudy conditions, J. Geophys. Res., 109, D04313, DOI:10.1019/2003JD003527, 2004.

~~Bjerknes, J.: Atmospheric teleconnections from the equatorial Pacific, Mon. Weather Rev., 97, 163-172, 1969.~~

Blackwell, W. J., Milstein, A. B., Zavodsky, B., and Blankenship, C. B.: Neural Network Estimation of Atmospheric Thermodynamic State for Weather Forecasting Applications, Foundations of Augmented Cognition. Advancing Human Performance and Decision-Making through Adaptive Systems: 8th International Conference, AC 2014, Held as Part of HCI International 2014, Heraklion, Crete, Greece, June 22-27, pp. 93-103, Springer International Publishing, DOI :10.1007/978-3-319-07527-3_9, 2014.

~~Bony, S., and Dufresne, J.-L. : Marine boundary layer clouds at the heart of tropical cloud feedback uncertainties in climate models, Geophys. Res. Lett., 32, L20806, doi:10.1029/2005GL023851, 2005.~~

Chahine, M. T., and Coauthors: AIRS: Improving weather forecasting and providing new data on greenhouse gases, Bull. Amer. Meteor. Soc., 87, 911-926, 2006.

Chédin, A., Scott, N. A., Wahiche, C., and Moulinier, P.: The improved initialization inversion method: A high resolution physical method for temperature retrievals from satellites of the TIROS-N series, J. Climate Appl. Meteor., 24, 128-143, 1985.

Chédin, A., Serrar, S., Scott, N. A., Crevoisier, C., and Armante, R.: First global measurement of midtropospheric CO_2 from NOAA polar satellites: Tropical zone, J. Geophys. Res., 108, doi:101029/2003JD003439, 2003.

~~Chen, W.-N., Chiang, C.-W., and Nee, J.-B.: Lidar ratio and depolarization ratio for cirrus clouds, Appl. Opt., 41, 6470ï 6476, 2002.~~

Chepfer H., Bony, S., Winker, D., Cesana, G., Dufresne, J. L., Minnis, P., Stubenrauch, C. J., and Zeng, S.: The GCM Oriented Calipso Cloud Product (CALIPSO-GOCCP), J. Geophys. Res., 115, D00H16, doi:10.1029/2009JD012251, 2010.

Chevallier, F., Cheruy, F., Scott, N. A., and Chédin, A.: A neural network approach for a fast and accurate computation of longwave radiative budget, J. Appl. Meteor., 37, 1385-1397, 1998.

~~Comstock, J. M., and Sassen, K.: Retrieval of cirrus cloud radiative and backscattering properties using combined lidar and infrared radiometer (LIRAD) measurements, J. Atmos. Oceanic Technol., 18, 1658ï 1673, 2001.~~

Crevoisier, C., Clerbaux, C., Guidard, V., Phulpin, T., Armante, R., Barret, B., Camy-Peyret, C., Chaboureau, J.-P., Coheur, P.-F., Crépeau, L., Dufour, G., Labonnote, L., Lavanant, L., Hadji-Lazaro, J., Herbin, H., Jacquinet-Husson, N., Payan, S., Péquignot, E., Pierangelo, C., Sellitto, P., and Stubenrauch, C.: Towards IASI-New Generation (IASI-NG): impact of improved spectral resolution and radiometric noise on the retrieval of thermodynamic, chemistry and climate variables, Atmos. Meas. Tech., 7, 4367-4385, 2014.

Dee, D. P., Uppala, S. M., Simmons, A. J., Berrisford, P., Poli, P., Kobayashi, S., Andrae, U., Balmaseda, M. A., Balsamo, G., Bauer, P., Bechtold, P., Beljaars, A. C. M., van de Berg, L., Bidlot, J., Bormann, N., Delsol, C., Dragani, R., Fuentes, M., Geer, A. J., Haimberger, L., Healy, S. B., Hersbach, H., Holm, E. V., Isaksen, L., Kallberg, P., Kohler, M., Matricardi, M., McNally, A. P., Monge-Sanz, B. M., Morcrette, J.-J., Park, B.-K., Peubey, C., de Rosnay, P., Tavolato, C., Thepaut, J.-N., and Vitart, F.: The ERA-Interim reanalysis: configuration and performance of the data assimilation system, Q. J. R. Meteorol. Soc., 137, 553ï 597, 2011.

~~Dessler, A. E. : A determination of the cloud feedback from climate variations over the past decade, Science, 330, 1523-1527, doi :10.1126/science.1192546, 2010.~~

Feofilov, A., Stubenrauch, C., and Armante, R.: Diurnal variation of cloud properties from the synergy of AIRS and IASI infrared sounders, EUMETSAT 2015 conference oral proceedings, session 5, 8 pp., available at : http://www.eumetsat.int/website/home/News/ConferencesandEvents/DAT_2305526.html, session 5, oral proceedings, or at: https://goo.gl/UCitVZ, 2015a.

Feofilov, A. G., Stubenrauch, C. J., and Delanoë, J.: Ice water content vertical profiles of high-level clouds: classification and impact on radiative fluxes, Atmos. Chem. Phys., 15, 12327-12344, 2015b.

Feofilov, A. and Stubenrauch, C.:~~,~~ LMD Cloud Retrieval using IR sounders. Algorithm Theoretical Basis, CIRS-LMD software package V2, 19 pp., DOI:10.13140/ RG.2.2.15812.63361, 2017.

Frey, R. A., Ackerman, S. A., Liu, Y., Strabala, K. I., Zhang, H., Key, J., and Wang, X.: Cloud Detection with MODIS, Part I: Recent Improvements in the MODIS Cloud Mask, *J. Atmos. Oceanic Tech.*, **25**, 1057-1072., 2008

~~Gill, A. E.: Some simple solutions for heat-induced tropical circulation, Q. J. Roy. Meteor. Soc., 106, 447-462, 1980.~~

GLOBALVIEW-CO2: Cooperative Global Atmospheric Data Integration Project. 2013, updated annually. Multi-laboratory compilation of synchronized and gap-filled atmospheric carbon dioxide records for the period 1979-2012 (obspack_co2_1_GLOBALVIEW-CO2_2013_v1.0.4_2013-12-23).

Compiled by NOAA Global Monitoring Division: Boulder, Colorado, U.S.A. Data product accessed at http://dx.doi.org/10.3334/OBSPACK/1002, 2013.

Henderson, D. S., ~~T.~~ LǒEcuyer, T., ~~G.~~ Stephens, G. L, ~~P.~~ Partain, P., and ~~M.~~ Sekiguchi, M.:~~;~~ A Multisensor Perspective on the Radiative Impacts of Clouds and Aerosols, J. Appl. Meteor. Climatol., 52, 853ï 871, doi: 10.1175/JAMC-D-12-025.1, 2013.

Hilton, F., Armante, R., August, T., Barnet, C., Bouchard, A., Camy-Peyret, C., Capelle, V., Clarisse, L., Clerbaux, C., Coheur, P.-F., Collard, A., Crevoisier, C. , Dufour, G., Edwards, D., Faijan, F., Fourrié, N., Gambacorta, A., Goldberg, M., Guidard, V., Hurtmans, D., Illingworth, S., Jacquinet-Husson, N., Kerzenmacher, T., Klaes, D., Lavanant, L.,. Masiello, G , Matricardi, M., McNally, A., Newman, S., Paveli, E., Payan, S., Péquignot, E., Peyridieu, S., Phulpin, T., Remedios, J., Schlüssel, P., Serio, C., Strow, L., Stubenrauch, C. J., Taylor, J. , Tobin, D., Wolf, W., Zhou, D.: Hyperspectral Earth Observation from IASI, Bull. Amer. Meteor. Soc., 93, 347-370, doi:10.1175/BAMS-D-11-00027.1, 2012.

Hanschmann T., ~~A. G.~~ Feofilov ~~A. G.~~, A. G., ~~S.~~ Kothe, S., ~~M.~~ Stengel ~~M.~~, M., and ~~S. Kothe, C. J.~~ Stubenrauch, C. J.: ~~C. J., Kothe S.: High clouds from space - a new HIRS based climate data record~~ Cloud properties from 35 years of HIRS observations: challenges to build a consistent long term cloud record, to be submitted to Atmos. Meas. Techn., 2017.

~~Henderson, D. S., T. LǒEcuyer, G. Stephens, P. Partain, and M. Sekiguchi, A Multisensor Perspective on the Radiative Impacts of Clouds and Aerosols, *J. Appl. Meteor. Climatol.*, **52**, 853ï 871, doi: 10.1175/JAMC-D-12-025.1, 2013.~~

Hori, M., Aoki, T., Tanikawa, T. , Motoyoshi, H., Hachikubo, A., Sugiura, K., Yasunari, T. J., Eide, H., Storvold, R., Nakajima, Y., Takahashi, F.: In-situ measured spectral directional emissivity of snow and ice in the 8ï 14 µm atmospheric window, Rem. Sens. Environ., 100, 486ī 502, 2006.

Lamquin, N., Stubenrauch, C. J., and Pelon, J.: Upper tropospheric humidity and cirrus geometrical and optical thickness: Relationships inferred from 1 year of collocated AIRS and CALIPSO data, J. Geophys. Res., 113, D00A08, doi:10.1029/2008JD010012, 2008.

Lebsock, M. D., ~~G. L.~~ Stephens, G. L., and ~~C.~~ Kummerow, C.:~~;~~ An observed tropical oceanic radiative-convective cloud feedback, J. Climate, 23, 2065-2078, DOI: 10.1175/2009JCLI3091.1, ~~(~~2010.~~)~~

Liao, X., Rossow, W. B., and Rind, D.: Comparison between SAGE II and ISCCP high-level clouds, Part II: Locating cloud tops, J. Geophys. Res., 100, 1137-1147, 1995.

Liu, R., Liou, K.-N., Su, H., Gu, Y., Zhao, B., Jiang, J. H., and Liu, S. C. : High cloud variations with surface temperature from 2002 to 2015: Contributions to atmospheric radiative cooling rate and precipitation changes, J. Geophys. Res.: Atmospheres, 122, 5457-5471, doi :10.1002/2016JD026303, 2017.

Lloyd, J., Guilyardi, E., and Weller, H.: The Role of Atmosphere Feedbacks during ENSO in the CMIP3 Models. Part III: The Shortwave Flux Feedback, J. Climate, 25, 4275-4293, DOI:10.1175/JCLI-D-11-00178.1, 2012.

Mace, G. G., and Zhang, Q.: The CloudSat radar-lidar geometrical profile product (RL-GeoProf): Updates, improvements, and selected results, J. Geophys. Res. Atmos., 119, doi:10.1002/ 2013JD021374, 2014.

~~Martins, E., Noel, V., and Chepfer, H.: Properties of cirrus and subvisible cirrus from nighttime Cloud-Aerosol Lidar with Orthogonal Polarization (CALIOP), related to atmospheric dynamics and water vapor, J. Geophys. Res., 116, D02208, doi:10.1029/2010JD014519, 2011.~~

Minnis, P., Sun-Mack, S., Young, D. F., Heck, P. W., Garber, D. P., Chen, Y., Spangenberg, D. A., Arduini, R. F., Trepte, Q. Z., Smith Jr., W. L., Ayers, J. K., Gibson, S. C., Miller, W. F., Chakrapani, V., Takano, Y., Liou, K.-N., Xie, Y., and P. Yang, Y.: CERES Edition-2 cloud property retrievals using TRMM VIRS and Terra and Aqua MODIS data, Part I: Algorithms, IEEE Trans. Geosci. Remote Sens., 49, *11*, 4374-4400, 2011.

Olsen, E. T., and authors: AIRS/AMSU/HSB Version 6 Level 2 Quality Control and Error Estimation, Version 1.0, 30 pp., Jet Propulsion Laboratory, Pasadena, CA, available at : https://docserver.gesdisc.eosdis.nasa.gov/repository/Mission/AIRS/3.3_ScienceDataProductDocumentation/3.3.5_ProductQuality/V6_L2_Quality_Control_and_Error_Estimation.pdf, 2013

Olsen, E. T., and ~~Co-~~authors~~-~~: AIRS/AMSU/HSB Version 6 Level 2 Product User Guide, Version 1.6~~1~~, 148~~0~~ pp., Jet Propulsion Laboratory, Pasadena, CA, available at : https://docserver.gesdisc.eosdis.nasa.gov/repository/Mission/AIRS/3.3_ScienceDataProductDocumentation/3.3.4_ProductGenerationAlgorithms/V6_L2_Product_User_Guide.pdf ~~https://disc.sci.gsfc.nasa.gov/AIRS/documentation/v6_docs/v6releasedocs1/V6_L2_Product_User_Guide.pdf~~, 2017~~6~~.

Paul, M., Aires, F., Prigent, C., Trigo, I., and Bernardo, F.: An innovative physical scheme to retrieve simultaneously surface temperature and emissivities using high spectral infrared observations from IASI. JGR, 117, D11302, DOI : 10.1029/2011JD017296, 2012.

Protopapadaki, E.-S., Stubenrauch, C. J., and Feofilov, A. G.: Upper Tropospheric cloud Systems derived from IR Sounders: Properties of Cirrus Anvils in the Tropics, Atmosph. Chem. Phys., 17, 3845-3859, doi:10.5194/acp-17-3845-2017, 2017.

Reichler, T., Dameris, M., and Sausen, R.: Determining the tropopause height from gridded data, Geophys. Res. Lett., 30**,** 2042, doi:10.1029/2003GL018240, 2003.

Rossow, W. B., and Schiffer, R. A.: Advances in understanding clouds from ISCCP, Bull. Amer. Meteor. Soc., 80, 2261-2287, 1999.

Scott, N. A., and Chédin A.: A fast line-by-line method for atmospheric absorption computations: the 4A Automized Atmospheric Absorption Atlas, J. Appl. Meteor., 20, 801-812, 1981.

Seo, H., Subramanian, A. C., Miller, A. J., and Cavanaugh, N. R.: Coupled Impacts of the Diurnal Cycle of Sea Surface Temperature on the Maddenï Julian Oscillation, J. Climate, 27, 8422-8443, ~~DOI~~doi: 10.1175/JCLI-D-14-00141.1, 2014.

Slingo, J. M., and Slingo, A.: The response of a general circulation model to cloud longwave radiative forcing. II: Further studies, Quart. J. Roy. Meteor. Soc., 117, 333ï 364, 1991.

Smith, W. L., Knuteson, R. O., Revercomb, H. E., Feltz, W., Howell, H. B., Menzel, W. P., Nalli, N. R., Brown, O., Brown, J., Minnett, P., McKeown, W.: Observations of the Infrared Radiative Properties of the Ocean-Implications for the Measurement of Sea Surface Temperature via Satellite Remote Sensing, Bull. Amer. Met. Soc., 77, 41ï 52, 1996.

Sohn, B.-J.: Cloud-Induced Infrared Radiative Heating and Its Implications for Large-Scale Tropical Circulations, J. Atmos. Sc., 56, 2657-2672, 1999.

Stephens, G., and Coauthors: The CloudSat mission and the A-train, Bull. Amer. Meteor. Soc., 83, 1771-1790, 2002.

~~Stephens, G. L., and co-authors: CloudSat mission: Performance and early science after the first year of operation, J. Geophys. Res., 113, D00A18, doi:10.1029/2008JD009982, 2008.~~

Stephens, G. L., OôBrien, D., Webster, P. J., Pilewski, P., Kato, S., and Li, J.-l.: The albedo of Earth, Rev. Geophys., 53, 141ï 163, doi:10.1002/2014RG000449, 2015.

Stephens, G. L., Hakuba, M. Z., Hawcroft, M., Haywood, J. M., Behrangi, A., Kay J. E., and Webster P. J.: The Curious Nature of the Hemispheric Symmetry of the Earthôs Water and Energy Balances, Curr Clim Change Rep, 2, 135-147, doi:10.1007/s40641-016-0043-9, 2016.

~~Stubenrauch, C. J., N. A. Scott, and A. Chédin: Cloud Field Identification for Earth Radiation Budget Studies: I) Cloud Field Classification using HIRS/MSU Sounder Measurements. *J. Appl. Meteor.*, 35, 416-427, 1996.~~

~~Stephens, G. L., Hakuba, M. Z., Lebsock, M., Yue, Q., Kahn, B. H., Hristova-Veleva, S., Rapp, A., Stubenrauch, C. J., Elsasser, G. S., and Slingo, J.: Observational evidence of a super Clausius-Clapeyron intensification of the tropical hydrological cycle, in preparation, 2017.~~

Stubenrauch, C. J., Chédin, A., Armante, R. and Scott, N. A.: Clouds as Seen by Satellite Sounders (3I) and Imagers (ISCCP): II) A New Approach for Cloud Parameter Determination in the 3I Algorithms, J. Climate, 12, 2214-2223, 1999.

Stubenrauch C. J., Chédin, A., Rädel, G., Scott, N. A., and Serrar, S.: Cloud properties and their seasonal and diurnal variability from TOVS Path-B, J. Climate, 19, 5531-5553, 2006.

Stubenrauch, C. J., Cros, S., Lamquin, N., Armante, R., Chédin, A., Crevoisier, C., and Scott, N. A.,~~:~~ Cloud properties from AIRS and evaluation with CALIPSO, J. Geophys. Res., 113, D00A10, doi:10.1029/2008JD009928, 2008.

Stubenrauch C. J., Cros, S., Guignard, A., and Lamquin, N.,~~:~~ A six-year global cloud climatology from the Atmospheric InfraRed Sounder aboard the Aqua Satellite: statistical analysis in synergy with CALIPSO and CloudSat, Atmos. Chem. Phys., 10, 7197-7214, 2010.

Stubenrauch, C. J., Rossow, W. B., Kinne, S., Ackerman, S., Cesana, G., Chepfer, H., Di Girolamo, L., Getzewich, B., Guignard, A., Heidinger, A., Maddux, B., Menzel, P., Minnis, P., Pearl, C., Platnick, S., Poulsen, C., Riedi, J., Sun-Mack, S., Walther, A., Winker, D., Zeng, S., Zhao, G.: Assessment of Global Cloud Datasets from Satellites: Project and Database initiated by the GEWEX Radiation Panel, Bull. Amer. Meteor. Soc., DOI:10.1175/BAMS-D-12-00117.1, 2013.

Stubenrauch, C. J., Stephens, G. L., and UTCC PROES Team : Process Evaluation Study on Upper Tropospheric Clouds and Convection (UTCC PROES), GEWEX Newsletter, Mai 2017, available at : : http://www.gewex.org/gewex-content/files_mf/1500657263May2017.pdf , 2017~~http://www.gewex.org/resources/gewex-news/~~.

Susskind, J., Barnet, C., and Blaisdell, J.: Retrieval of atmospheric and surface parameters from AIRS/AMSU/HSB data in the presence of clouds, IEEE Trans. Geosci. Remote Sens., 41, 390-409, 2003.

~~Susskind, J., Molnar, G., Iredell, L, and Loeb, N. G.: Interannual variability of outgoing longwave radiation as observed by AIRS and CERES, J. Geophys. Res., 117, D23107, doi:10.1029/ 2012JD017997, 2012.~~

Susskind, J., Blaisdell, J., and Iredell, L.: Improved methodology for surface and atmospheric soundings, error estimates, and quality control procedures: the atmospheric infrared sounder science team version-6 retrieval algorithm. J. Appl. Remote Sens. 0001;8(1):084994. doi:10.1117/1.JRS.8.084994, 2014.

~~Tian, B., and Ramanathan, V.: A Simple Moist Tropical Atmosphere Model: The Role of Cloud Radiative Forcing, J. Climate, 16, 2086-2092, 2003.~~

Trigo, I. F., Boussetta, S., Viterbo, P., Balsamo, G., Beljaars, A., and Sandu, I. : Comparison of model land skin temperature with remotely sensed estimates and assessment of surface-atmosphere coupling, J. Geophys. Res. Atmos., 120, 12,096ï 12,111, DOI:10.1002/2015JD023812, 2015.

Van T. Dang, H., Lambrigtsen, B., and Manning, E.: AIRS/AMSU/HSB Version 6 Level 2 Performance and Test Report, Version 1.2, 197 pp., Jet Propulsion Laboratory, available at: https:// disc.sci.gsfc.nasa.gov/AIRS/documentation/v6_docs/v6releasedocs1/V6_L2_Performance_and_Test_Report.pdf, 2012.

Webster, P. J., Clayson, C. A., and Curry, J. A.: Clouds, Radiation, and the Diurnal Cycle of Sea Surface Temperature in the Tropical Western Pacific, J. Climate, 9, 1712-1730, 1996.

Winker, D. M.: Accounting for multiple scattering in retrievals from space lidar, Proc. SPIE Int. Soc. Opt. Eng., 5059, 128ï 139, 2003.

Winker, D., Getzewitch, B., and Vaughan, M.: Evaluation and Applications of Cloud Climatologies from CALIOP, Proc. Int. Laser Radar Conference (ILRC), 2008.

Winker, D. M., Vaughan, M. A., Omar, A., Hu, Y., and Powell, K. A.: Overview of the CALIPSO mission and CALIOP data processing algorithms, J. Atmos. Oceanic. Technol., 26, 2310-2323, 2009.

~~Wang, C., Deser, C., Yu, J.-Y., DiNezio, P., and Clement, A.: El Nino-Southern Oscillation (ENSO): A Review, in book Coral Reefs of the Eastern Tropical Pacific, P. Glymn, D. Manzello, and I. Enochs, Eds., Springer Science Publisher, pp.85-106, DOI: 10.1007/978-94-017-7499-4_4, 2017.~~

Wu, X., and Smith, W. L.: Emissivity of rough sea surface for 8 ï 13 μm: modelling and verification, Appl. Optics, 36, 2609-2619, 1997.

~~Yue, Q., Kahn, B. H., Fetzer, E. J., Wong, S., Frey, R., and Meyer, K. G.: On the response of MODIS cloud coverage to global mean surface air temperature, J. Geophys. Res. Atmos., 122, 966ï979, doi:10.1002/2016JD025174, 2017.~~Zhou, C., Zelinka, M. D., Dessler, A. E., and Yang, P.: An analysis of the short-term cloud feedback using MODIS data, J. Climate, 26, 4803-4815, doi:10.1175/jcli-d-12-00547.1, 2013.

~~Zhou, C., Dessler, A. E., Zelinka, M. D., Yang, P., and Wang, T.: Cirrus feedback on interannual climate fluctuations, Geophys. Res. Lett., 41, 9166-9173, doi:10.1002/2014GL062095, 2014.~~

Zhou, C., Zelinka, M. D., Dessler, A. E., and Klein, S. A.: The relationship between interannual and long-term cloud feedbacks, Geophys. Res. Lett., 42, 10463-10469, doi:10.1002/2015GL066698, 2015.

Table 1. ~~Agreement in cloudy and clear sky scenes~~Hit rates between ~~CALIPSO and the~~ AIRS-CIRS and CALIPSO-CloudSat ~~"a posteriori"~~cloud detection. Statistics include three years (2007-2009) collocated observations at 1:30AM LT.

surface \ latitude	tropics		mid- latitudes		polar	
ancillary data	AIRS	ERA	AIRS	ERA	AIRS	ERA
ocean	86.5%	84.2%	90.2%	91.5%	93.0%	95.0%
land	86.4%	83.2%	80.7%	77.6%	77.3%	79.7%
sea ice			71.5%	82.0%	71.2%	81.2%
snow	73.5%	71.9%	74.9%	68.5%	65.5%	66.7%

Table 2. Averages of ~~a)~~ CA, ~~b)~~ CAHR, ~~c)~~ CAMR and ~~d)~~ CALR (in %) from AIRS-LMD (2003-2009) / ~~,~~ AIRS-CIRS (2003-2015, ~~using~~ with AIRS-NASA / ERA-Interim ancillary data) ~~and~~ / IASI-CIRS (2008-2015, ~~using~~ with ERA-Interim ancillary data).

~~a) CA (%)~~

latitude band	~~AIRS-LMD V1~~CA (%)	~~AIRS-CIRS~~CAHR (%)	~~IASI-CIRS~~CAMR (%)	CALR (%)
globe	67 / 67 / 70 / 67	41 / 41 / 40 / 40~~67 / 70~~	~~67~~ 18 / 19 / 19 / 20	41 / 40 / 41 / 40
ocean	72 / 71 / 74 / 72	38 / 38 / 37 / 37~~71 / 74~~	16 / 16 / 17 / 18~~72~~	47 / 45 / 46 / 44
land	56 / 57 / 59 / 56	48 / 49 / 47 / 47~~57 / 59~~	~~56~~ 23 / 25 / 23 / 23	29 / 27 / 30 / 30
60°N ï 30°N	69 / 69 / 72 / 69	40 / 40 / 40 / 40~~69 / 72~~	~~69~~ 22 / 23 / 22 / 22	38 / 37 / 38 / 38
15°N ï 15°S	67 / 63 / 66 / 62	59 / 58 / 57 / 58~~63 / 66~~	~~62~~ 11 / 10 / 10 / 11	30 / 32 / 33 / 31
30°S ï 60°S	80 / 84 / 85 / 85	28 / 30 / 30 / 29~~84 / 85~~	~~85~~ 21 / 23 / 22 / 23	51 / 47 / 48 / 48

Table 3. Averages of relative amount (in %) of opaque ($\varepsilon_{cld} > 0.95$), cirrus ($0.95 > \varepsilon_{cld} > 0.5$) and thin cirrus (0.5 > ε_{cld} ~~<~~> 0.1~~5~~) from AIRS-CIRS (2003-2015, using AIRS-NASA / ERA-Interim ancillary data) / IASI-CIRS (2008-2015, using ERA-Interim ancillary data).

latitude band	opaque / tot CA	cirrus / tot CA	thin Cirrus / tot CA
globe	5.3 / 5.0 / 5.4	21.7 / 21.5 / 20.9	13.4 / 13.0 / 12.9
ocean	5.0 / 4.5 / 4.9	20.0 / 19.9 / 19.2	12.5 / 12.0 / 12.1
land	6.1 / 5.9 / 6.6	25.8 / 25.3 / 24.9	15.6 / 15.2 / 14.7
60°N ï 30°N	5.4 / 4.8 / 5.4	22.9 / 23.5 / 22.8	11.1 / 11.0 / 10.9
15°N ï 15°S	7.3 / 7.0 / 7.7	28.2 / 27.5 / 26.8	21.6 / 21.3 / 22.1
30°S ï 60°S	4.8 / 4.2 / 4.4	17.5 / 18.9 / 18.1	6.9 / 6.6 / 5.9

1

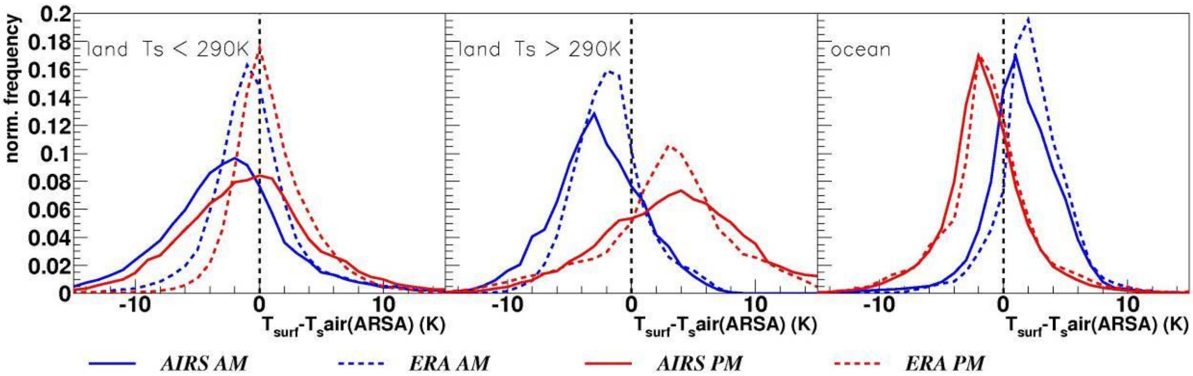

Figure 1. Normalized distributions of the difference between surface skin temperature, as used in the cloud retrieval, deduced from AIRS-NASA of good quality and from ERA-Interim, and collocated surface air temperature of the ARSA data base. Statistics includes January and July from 2003 ï 2015, separately over land for colder temperatures (T_{surf} < 290 K), over land for warmer temperatures (T_{surf} > 290 K) and over ocean.

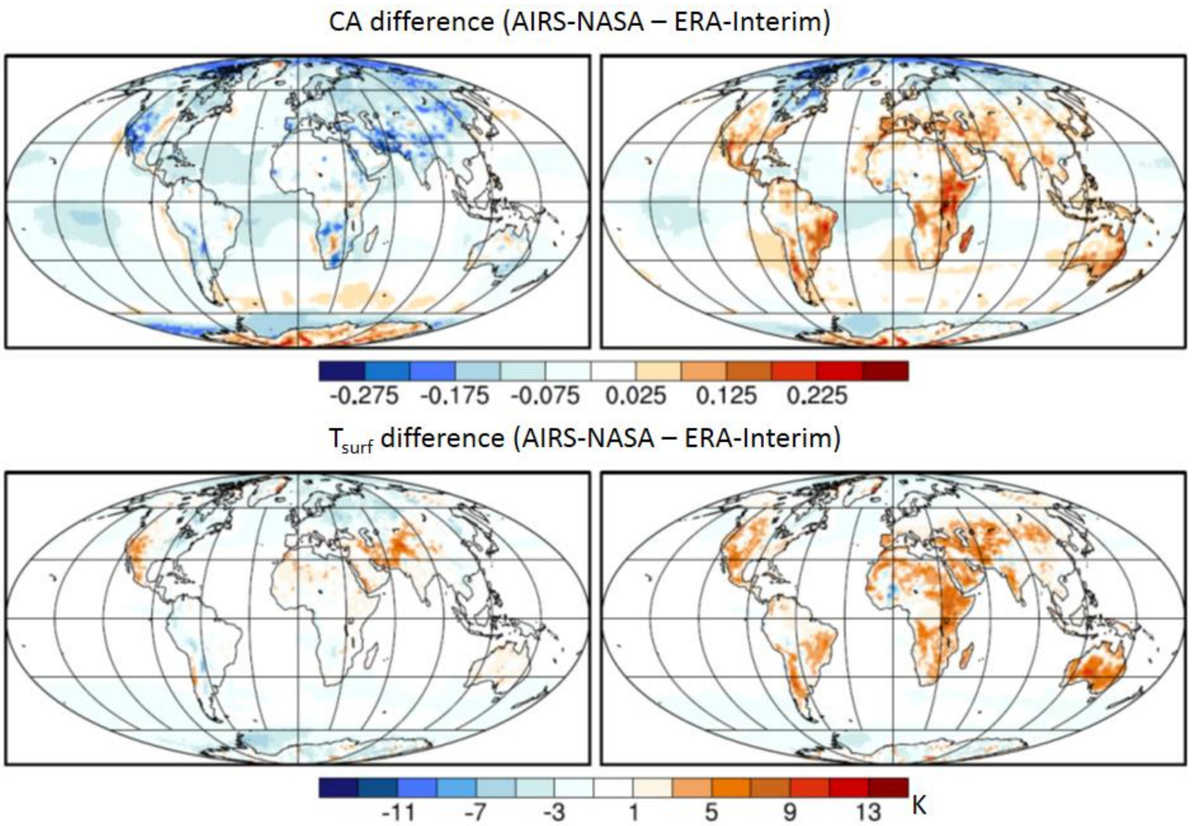

Figure ~~3~~2. Geographical maps of difference in total CA (above) between the two AIRS-CIRS data sets, based on ancillary data from AIRS-NASA and from ERA-Interim, and in T_{surf} (below) between AIRS-NASA and ERA-Interim as used in the retrieval, separately at 1:30AM (left) and at 1:30PM (right)

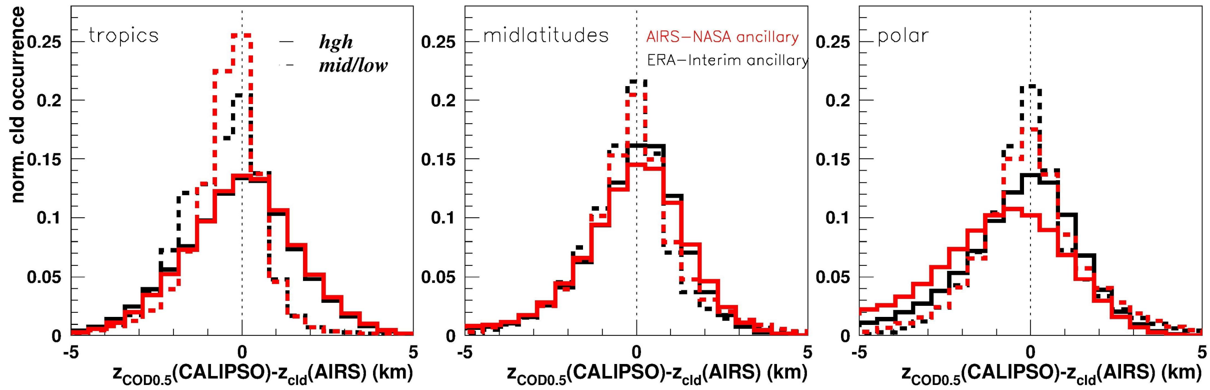

Figure 34. Normalized frequency distributions of the difference between the cloud height at which the optical depth reaches a value of 0.5 from CALIPSO and z_{cld} from AIRS~~ (left) and between the cloud top height from CALIPSO and z_{cld} from AIRS (right)~~;; z_{cld} ~~from AIRS~~ is compared to the cloud ~~cloud~~ layer of CALIPSO, ~~coherent with~~which ~~also~~ corresponds to the one of ~~CALIPSO~~ CloudSat-lidar GEOPROF, and which is the closest to z_{cld}. Analysis over tropics (30°N-30°S), midlatitudes (30°-60°) and polar latitudes (60°-85°), separately for high-level clouds and for clouds with p_{cld} > 440 hPa. ~~Statistics includes three years (2007-2009) of observations at 1:30 LT. AIRS-CIRS cloud retrievals~~The effect of using different ancillary data is also presented~~ from AIRS-NASA in red and from ERA-Interim in black, separately for high-level clouds (full line) and for clouds with p_{cld} > 440 hPa (broken line)~~. ~~Analysis over three latitude bands: 30°N-30°S (upper panel), 30°-60° (middle panel) and 60°-85° (lower panel).~~Statistics includes three years (2007-2009) of observations at 1:30AM LT.

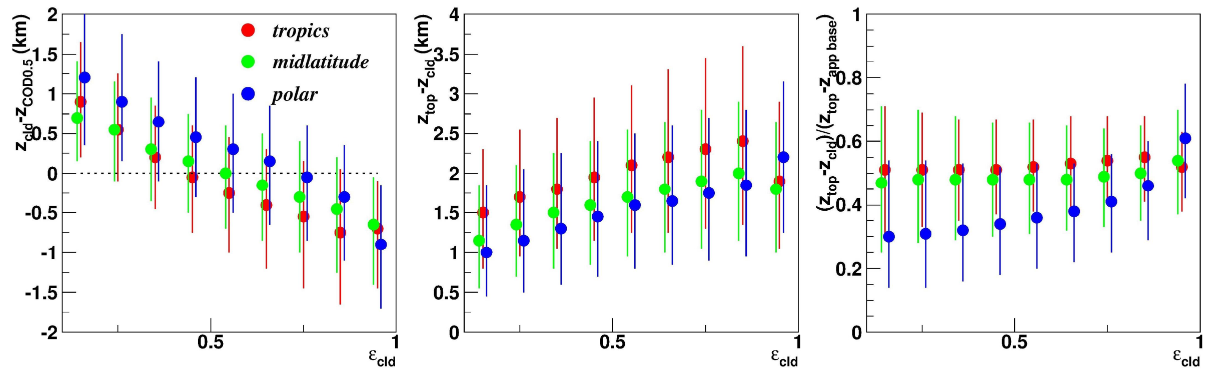

Figure ~~4~~5. ~~Average d~~Difference ~~between~~ a) z_{cld} – $z_{COD0.5}$~~from AIRS-CIRS and CALIPSO height at which the COD reaches about 0.5 (top)~~, ~~between~~ b) z_{top} ~~from CALIPSO and~~ - z_{cld} ~~(middle)~~ and ~~between~~ c) (z_{top} ~~and~~ - z_{cld} ~~)~~, / (z_{top} – $z_{app\ base}$)~~scaled by "apparent" cloud vertical extent~~, ~~(bottom)~~ as function of ~~AIPΣ–XIPΣ χλουδ εμισσιωιτψ~~ε_{cld} for high-level clouds in the tropics ~~(red)~~, midlatitudes ~~(green)~~ and polar latitudes ~~(blue), separately for high-level clouds (left) and for low-level (right) clouds~~. Presented are median values and the interquartile ranges. Three years of statistics, for ~~cases where~~which z_{cld} ~~from AIRS~~ and $z_{COD0.5}$~~CALIPSO height~~ lie within vertical cloud borders ~~determined~~ from ~~CloudSat-CALIPSO lidar~~ GEOPROF. Observations at 1:30AM LT.

~~Statistical errors are negligible and the broken lines indicate a range between single layer clouds and multi-layer clouds.~~

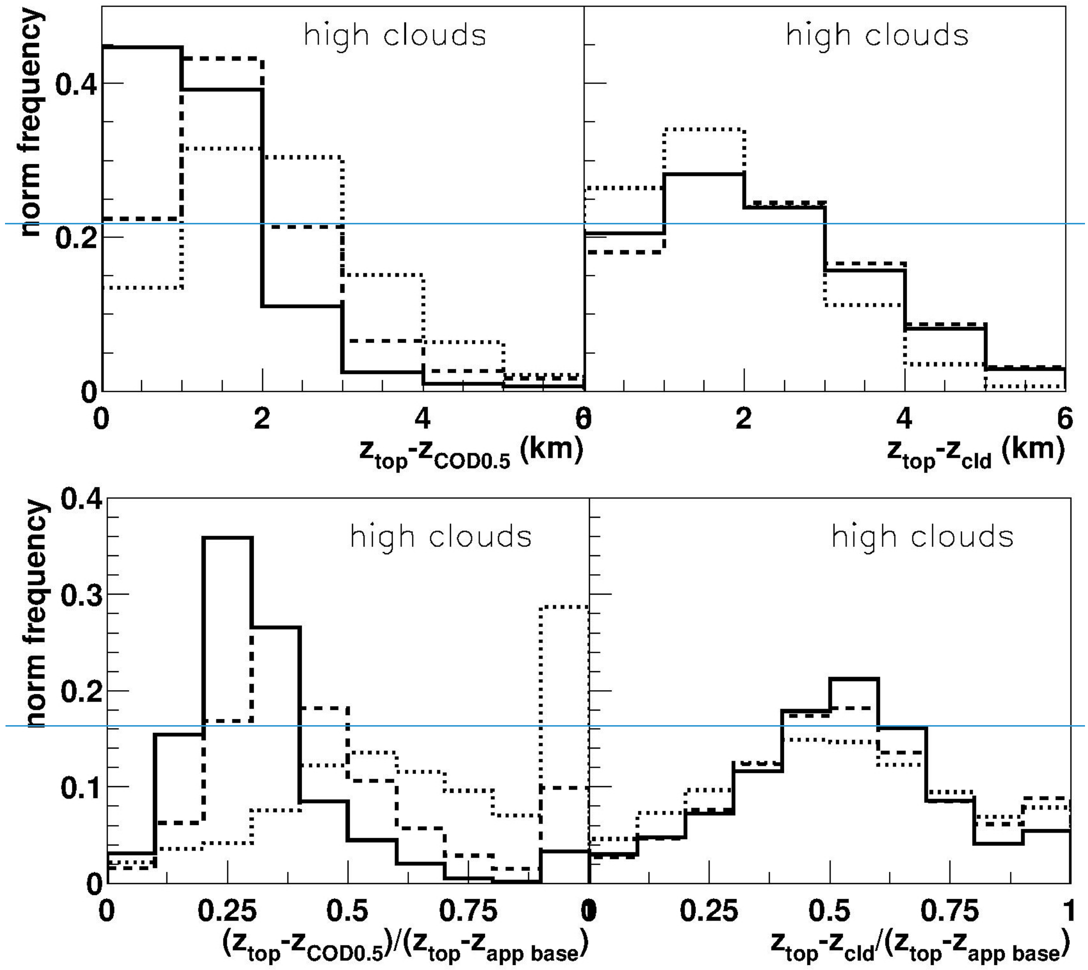

~~Figure 6. Normalized frequency distributions of differences between CALIPSO cloud top and height at which the COD reaches about 0.5 (left) and between CALIPSO cloud top and~~ z_{cld} ~~from AIRS (right) for high-level clouds, in absolute values (top) and scaled by apparent vertical cloud extent (bottom). Distributions are compared for clouds with~~ $\varepsilon_{cld} > 0.8$ ~~(full line),~~ $0.8 > \varepsilon_{cld} > 0.4$ ~~(broken line) and~~ $0.4 > \varepsilon_{cld} > 0.1$ ~~(dotted line). Three years of statistics for cases where~~ z_{cld} ~~from AIRS and CALIPSO height lie within vertical cloud borders determined from CloudSat-CALIPSO GEOPROF. Observations at 1:30 LT.~~

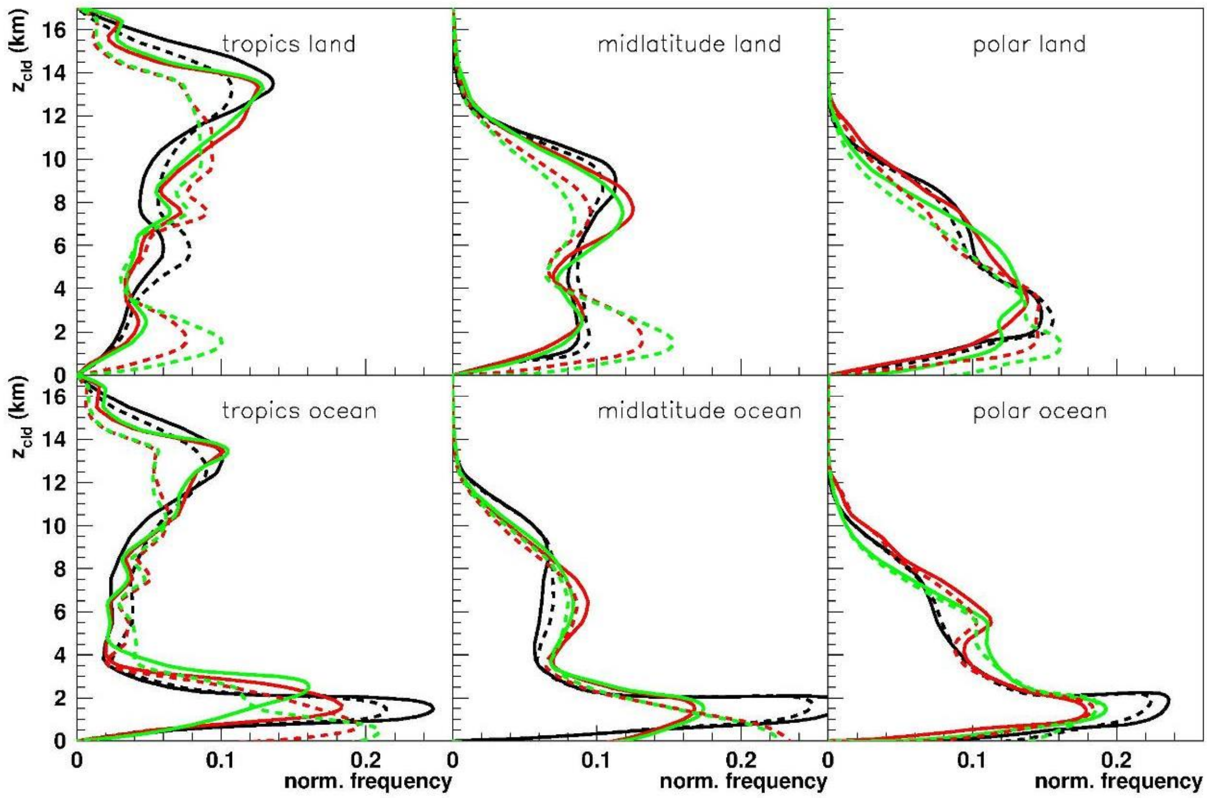

Figure 5~~7~~. Normalized frequency distributions of $z_{COD0.5}$ from CALIPSO (black) and of z_{cld} from AIRS, using ancillary data from AIRS-NASA (red) and from ERA-Interim (green) ~~and $z_{COD0.5}$ from CALIPSO (black)~~, separately over land (top) and over ocean (bottom), in the tropics ~~(left)~~, midlatitudes~~s (middle)~~ and polar latitudes ~~(right)~~. For each data set, two distributions are ~~shown~~compared: ~~for~~ statistics of all detected clouds, except subvisible cirrus, (~~broken~~ dashed line) and ~~for~~ only of single layer clouds with a ~~mostly~~ cloud~~y~~ ~~fields of~~coverage filling the AIRS golf ball ~~single layer clouds~~ (full line).

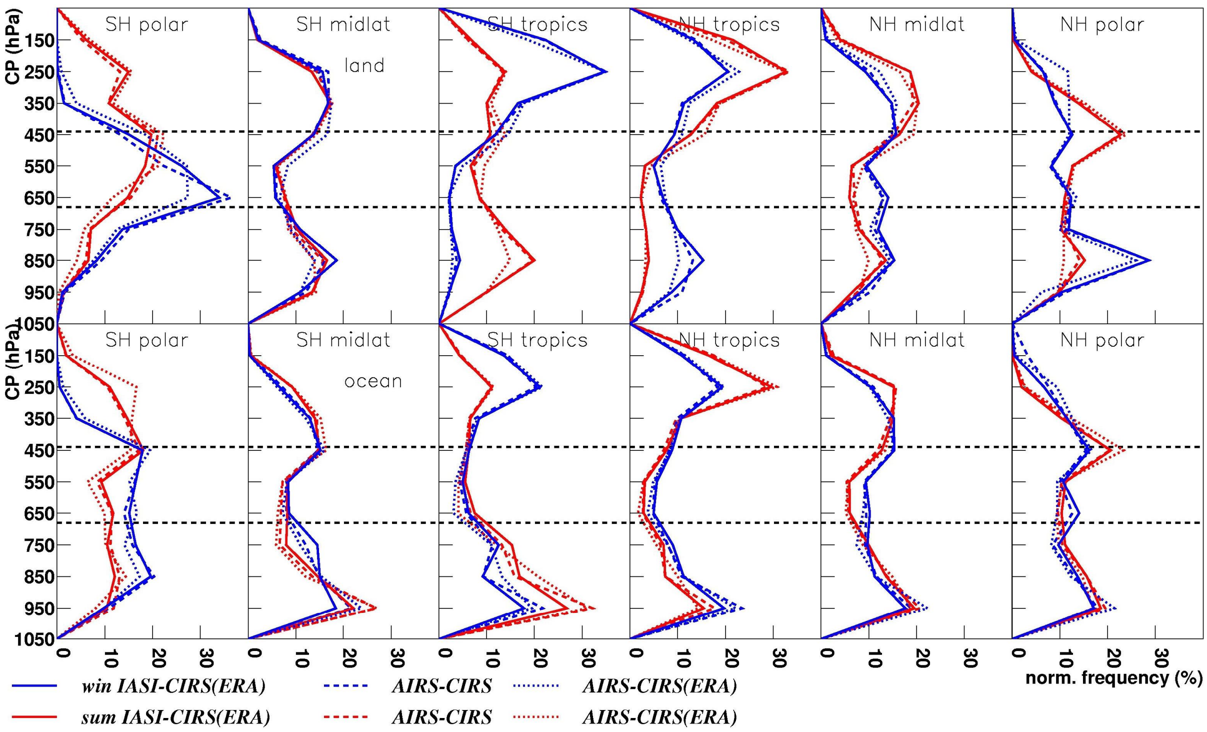

Figure 6~~8~~. Normalized frequency distributions of p_{cld} , separately over land and over ocean in six latitude bands of 30° from SH polar (left) to NH polar latitudes (right), in boreal winter (December, January, February; blue) and in boreal summer (June, July, August; red). Compared are results from AIRS-CIRS using two sets of ancillary data ~~from AIRS-CIRS, using ancillary data from(~~ AIRS-NASA~~, (~~ (dashed line) and ~~from (~~ERA-Interim~~, (~~ (dotted line), as well as from IASI-CIRS (full line), ~~separately over land (top) and over ocean (bottom) in six latitude bands of 30° from Southern hemisphere polar (left) to Northern hemisphere polar latitudes (right), in boreal winter (December, January, February; blue) and in boreal summer (June, July, August; red).~~ Statistics from 2008.

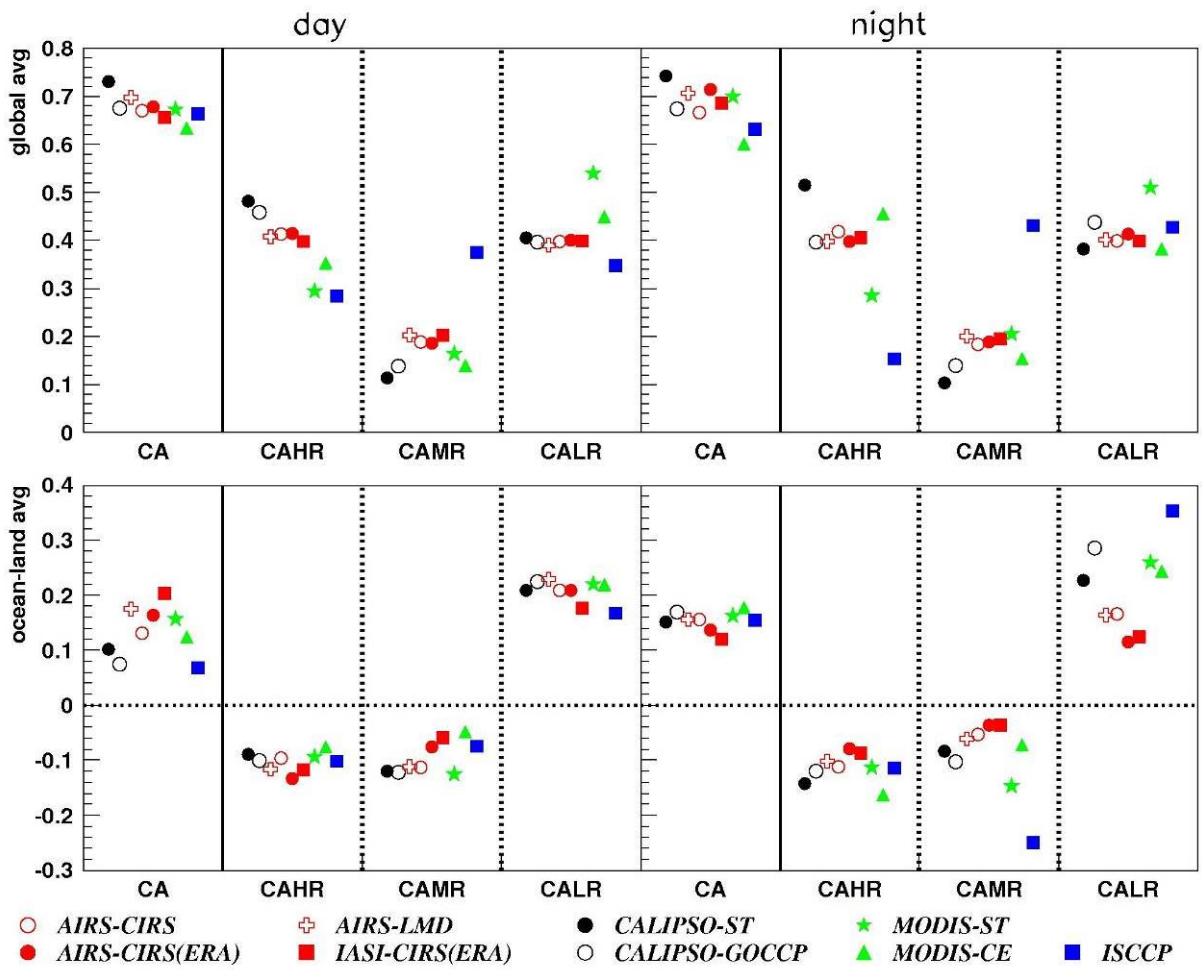

Figure 7~~9~~. Top: Global averages of total cloud amount (CA) ~~, as well as of~~and fraction of high-level, mid-level and low-level cloud amount, relative to total cloud amount, (CAHR + CAMR + CALR = 1). Comparisons of IR sounder cloud data (AIRS, IASI) with L3 data from the GEWEX Cloud Assessment data base, separately for observations mostly during day (~~left), corresponding to~~ 1:30PM; ~~(~~3:00PM for ISCCP and 9:30AM for IASI, left), and mostly during night (~~right), corresponding to~~ 1:30AM; ~~(~~3:00AM for ISCCP and 9:30PM for IASI). Compared to the original ISCCP data, the day-night adjustment on CA has not been included to better illustrate the differences between VIS-IR and IR-only results. Bottom: Averages of ocean-land differences for the same parameters and data sets.

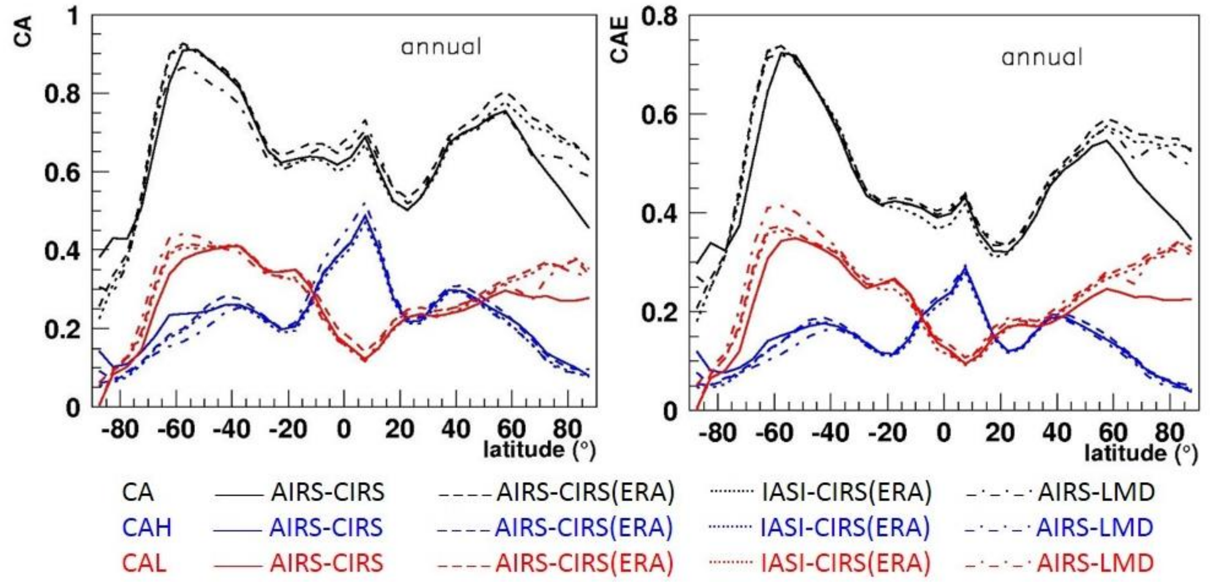
CA
annual
CAE
annual
latitude (°)
latitude (°)
CA AIRS-CIRS AIRS-CIRS(ERA) IASI-CIRS(ERA) AIRS-LMD
CAH AIRS-CIRS AIRS-CIRS(ERA) IASI-CIRS(ERA) AIRS-LMD
CAL AIRS-CIRS AIRS-CIRS(ERA) IASI-CIRS(ERA) AIRS-LMD

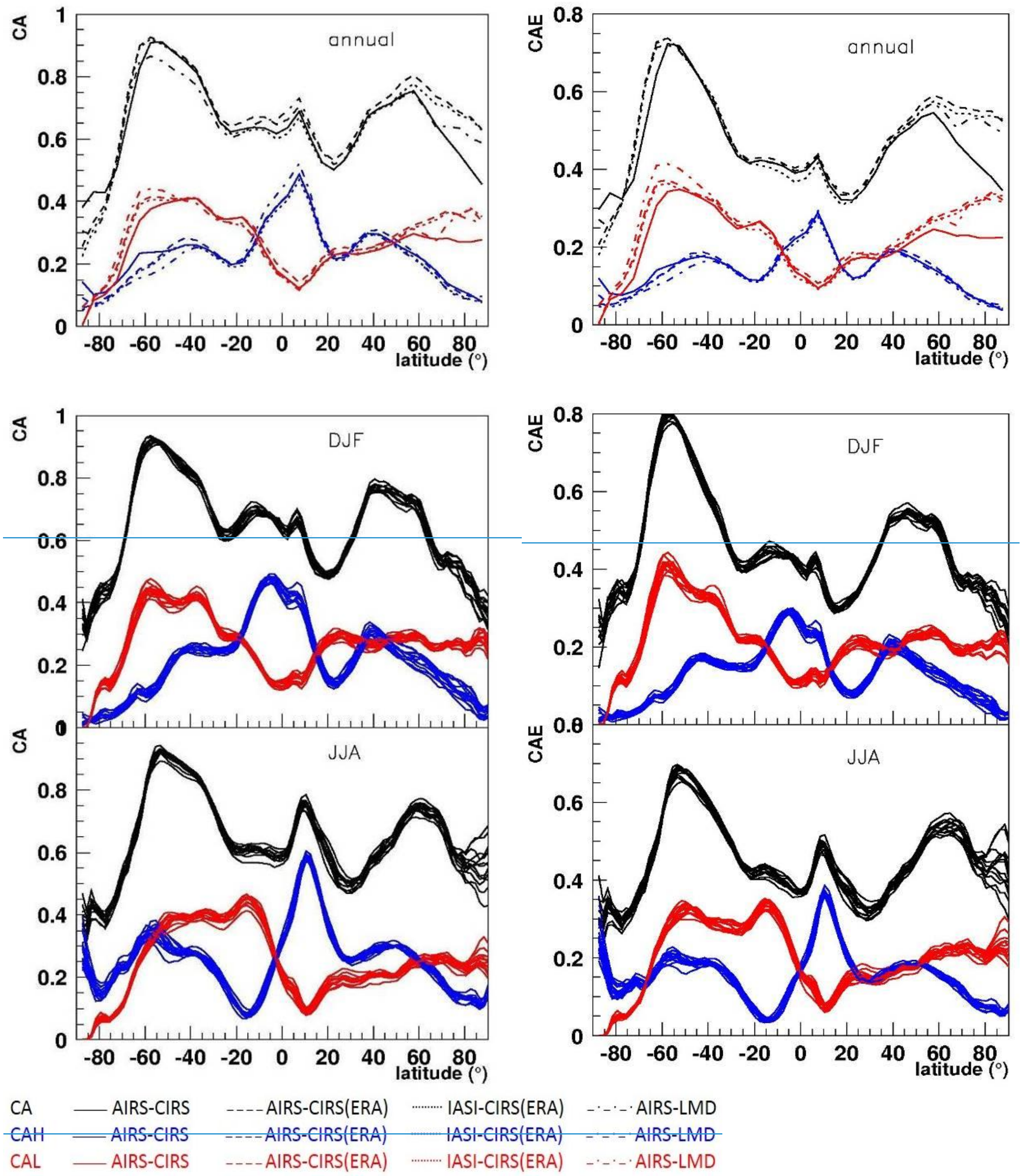

Figure ~~10~~8. Annual mean z~~Z~~onal distributions of CA, CAH and CAL (left) and CAE, CAEH and CAEL (right)~~, separately as annual mean (top), in boreal winter (December, January, February; middle) and in boreal summer (June, July, August; bottom)~~. Results ~~For the annual mean, cloud amounts~~ are compared between AIRS-CIRS, using ancillary data from AIRS-NASA ~~(full line)~~ and from ERA-Interim ~~(broken dashed line)~~, IASI-CIRS ~~(dotted line)~~ and AIRS-LMD ~~(dash-dotted line)~~.

~~For boreal winter and boreal summer, AIRS-CIRS (using AIRS-NASA ancillary data) is shown separately for each year between 2003 to 2015, illustrating inter-annual variability .~~

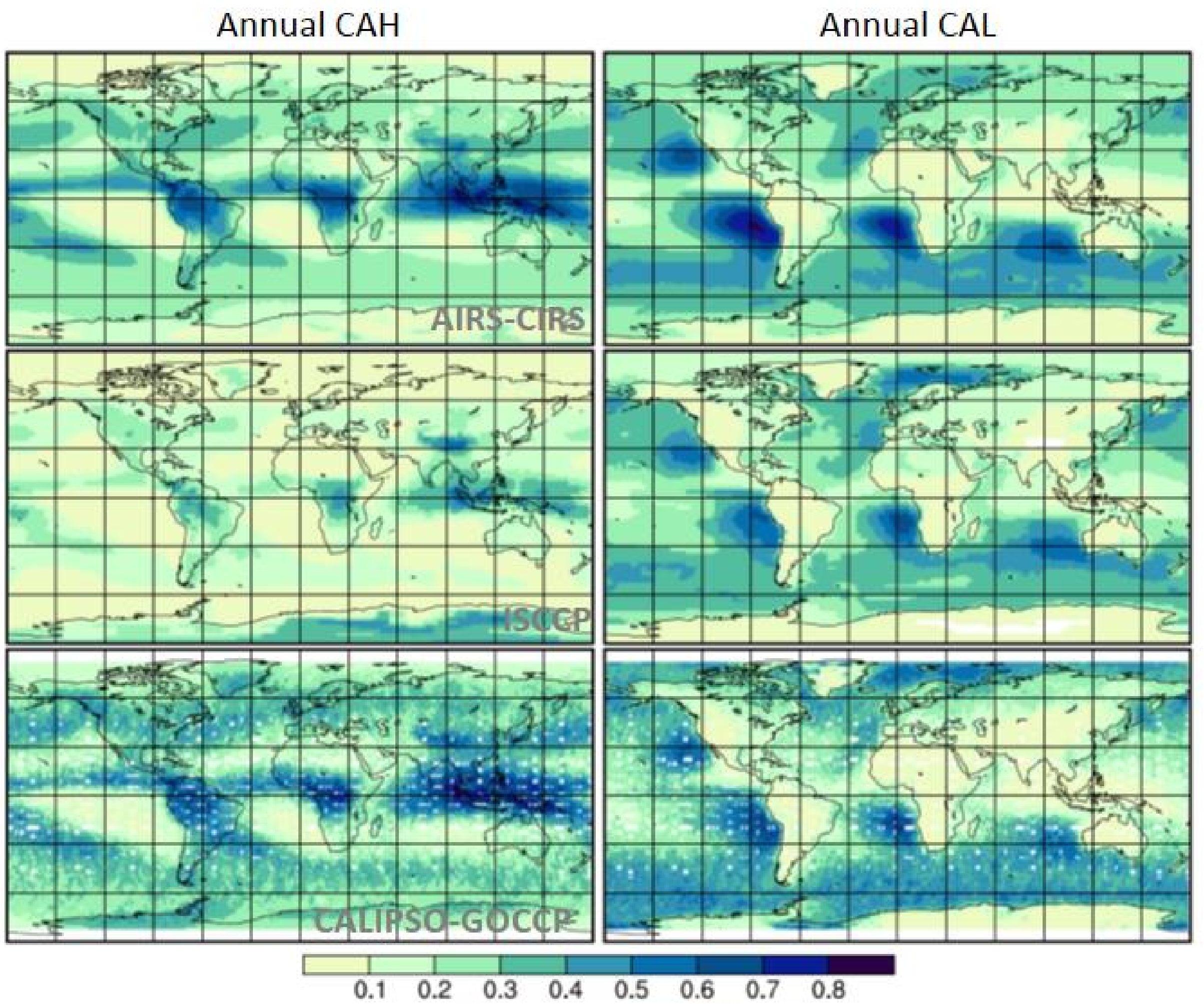

Figure 9~~11~~. Top: Geographical maps of annual CAH (left) and CAL (right), from ~~of~~ AIRS-CIRS (2003-2015, top),~~(2003-2015, top)~~ ~~compared to~~ ISCCP (2003~~1984~~-2007, middle) and CALIPSO-GOCCP (2007-2008, bottom),~~-~~ the latter two from the GEWEX Cloud Assessment data base~~, as well as seasonal anomalies of DJF (middle) and of JJA (right)~~.

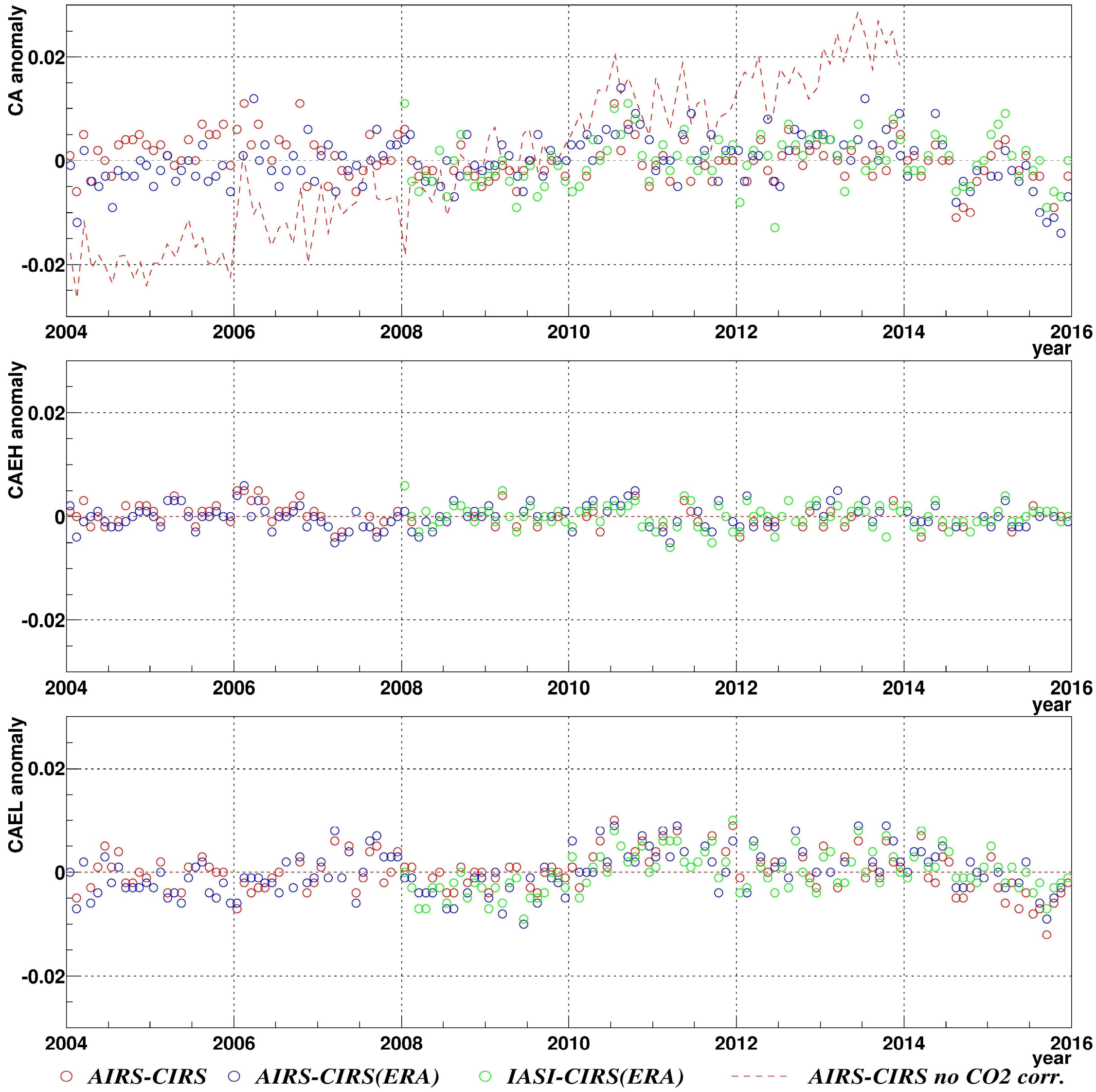

~~Figure 12. Geographical maps of annual CAL (left) of AIRS-CIRS (2003-2015, top) compared to ISCCP (1984-2007, middle) and CALIPSO-GOCCP (2007-2008, bottom) from the GEWEX Cloud Assessment data base, as well as seasonal anomalies of DJF (middle) and of JJA (right).~~

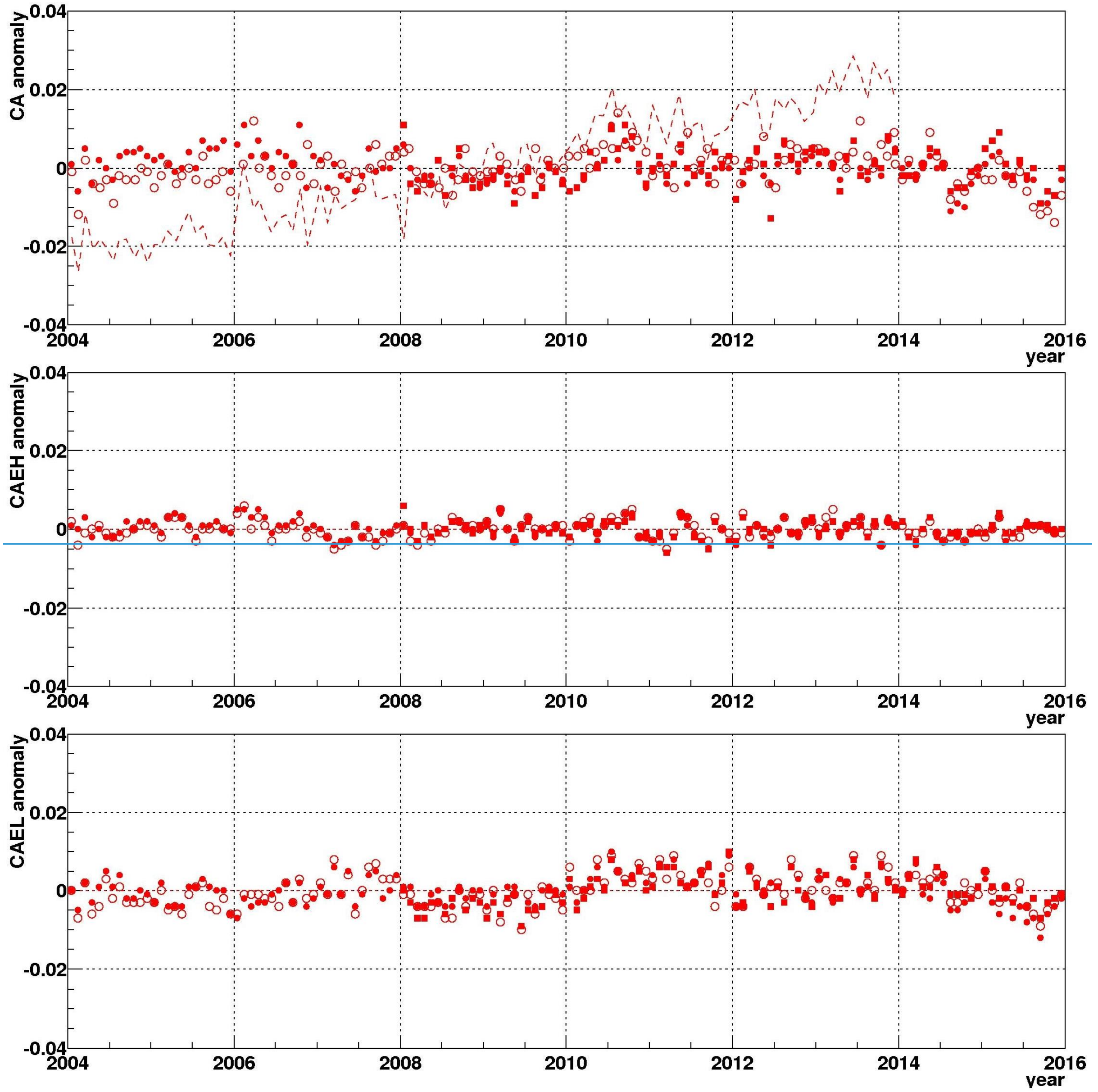

~~AIRS-CIRS~~ ~~AIRS-CIRS(ERA)~~ ~~IASI-CIRS(ERA)~~ ~~AIRS-CIRS no CO2 corr.~~

Figure 10~~3~~. Time anomalies of deseasonalized CA, CAEH and CAEL over the globe. In the case of CA, additional values are shown without calibration of spectral atmospheric transmissivities for changes in atmospheric CO_2 concentration.

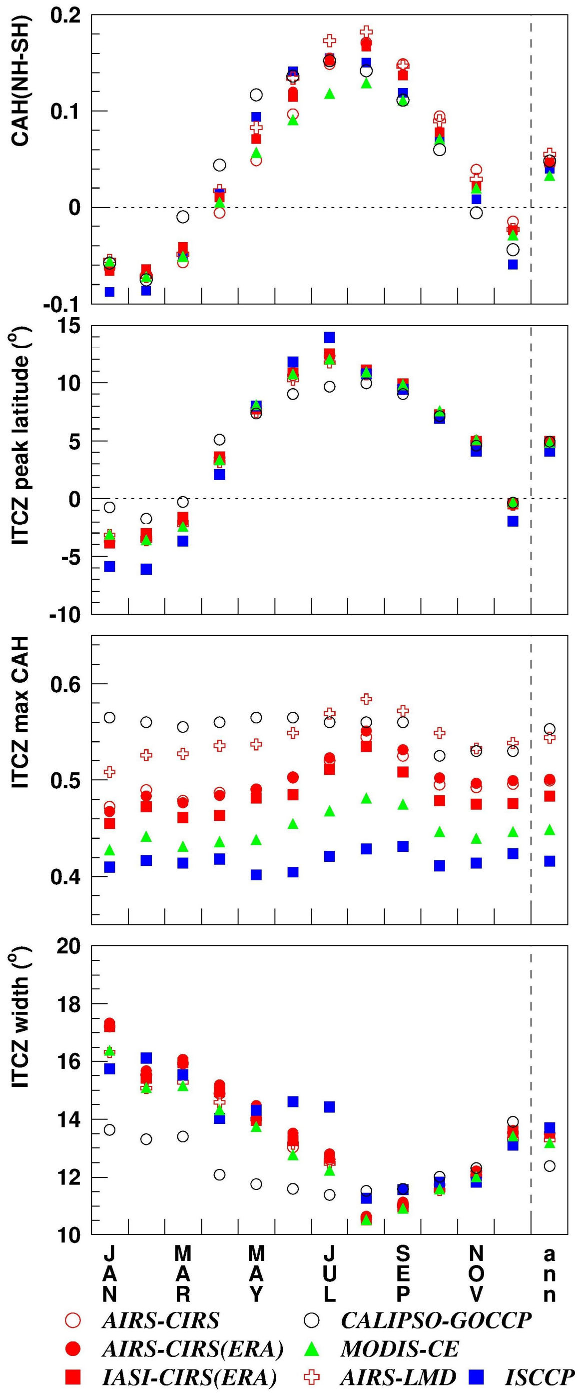

Figure 11~~2~~.~~5~~ Seasonal cycle / annual average of (1) CAH differences between NH hemisphere (0°-60N) and SH hemisphere (~~60N~~0°-60S),~~;~~ ~~seasonal cycle / annual average of~~(2) ITCZ peak latitude, (3) maximum CAH within ITCZ and (4) width of ITCZ~~ width~~.

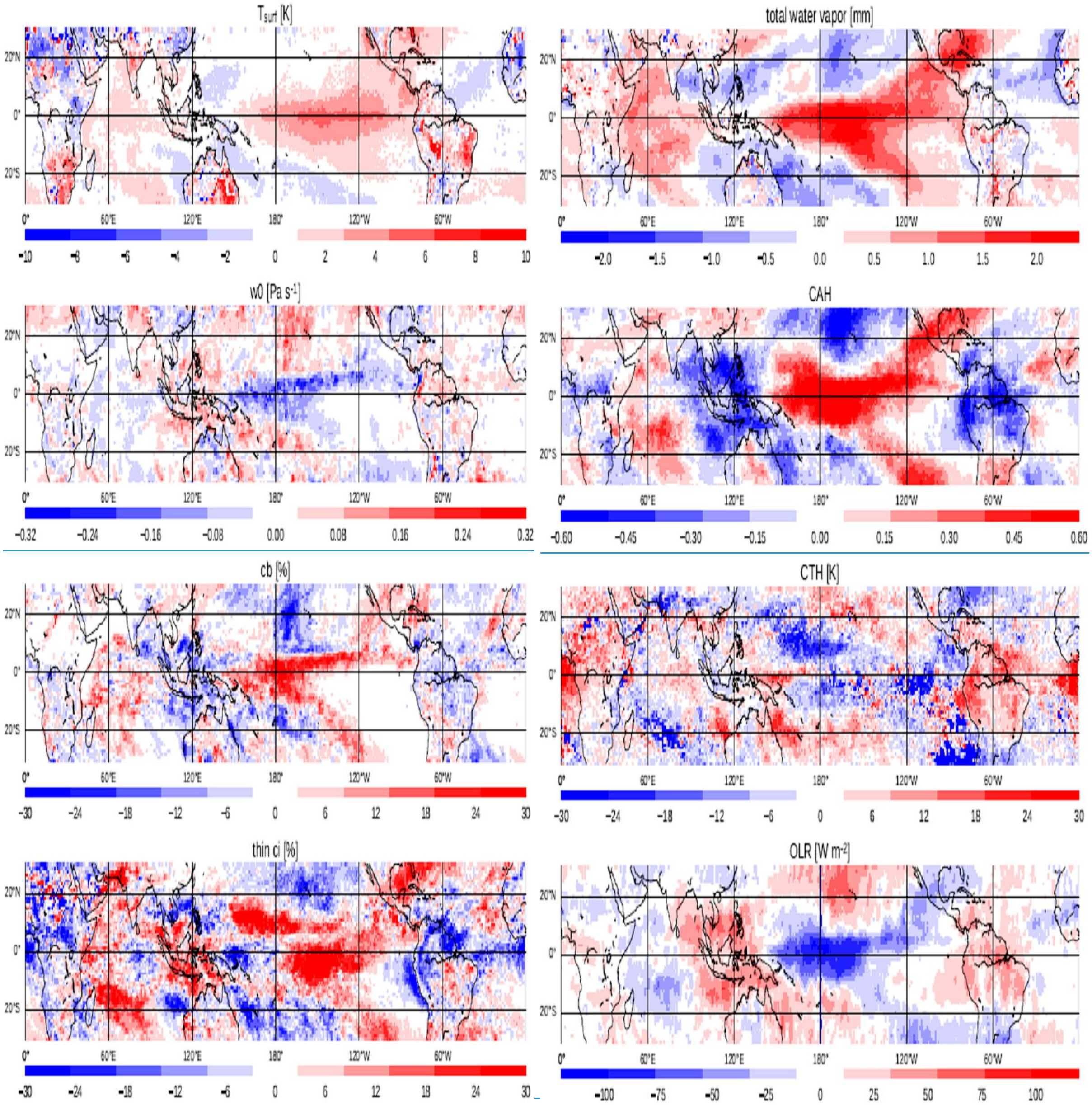

~~Figure 16. Differences between December 2015 and 2010, corresponding to El Niño and La Niña, respectively, in T_{surf}, (1. Panel, left), total atmospheric water vapour (1. Panel, right) and vertical wind at 500 hPa (2. Panel, left) from ERA-Interim, in CAH (2. Panel, right), fraction of Cb (3. Panel, left), cloud temperature of high-level clouds (3. Panel, right) and fraction of thin cirrus (4. Panel, left) from AIRS-CIRS, and OLR (4. Panel, right) from AIRS- NASA.~~

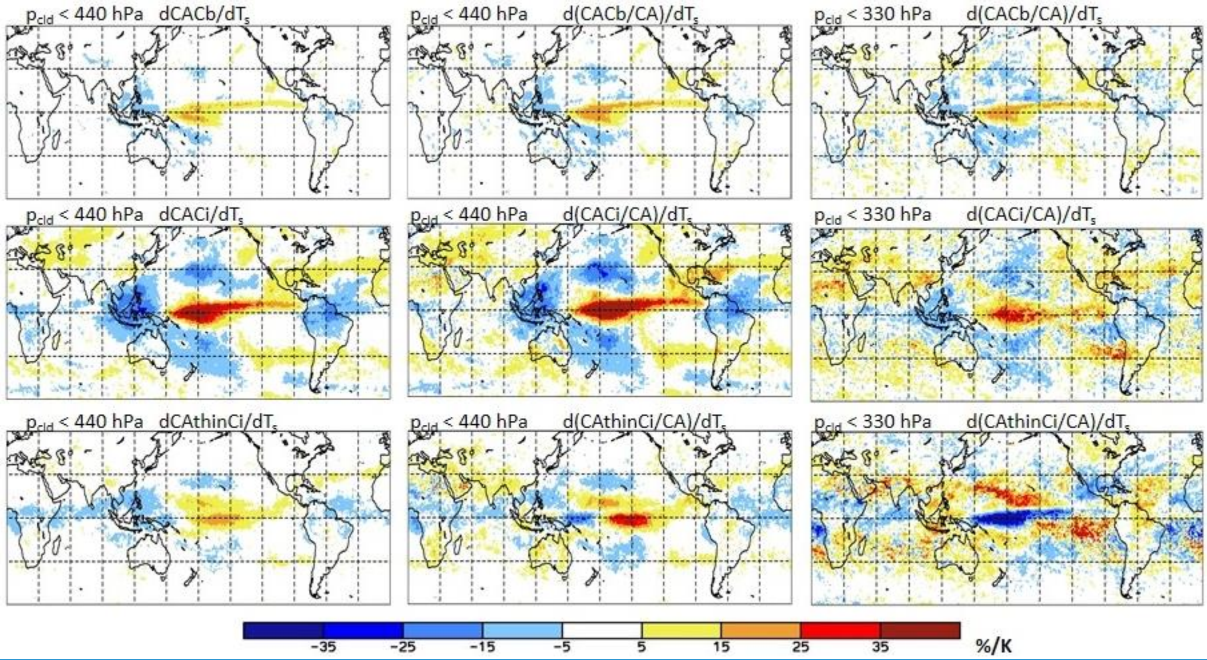

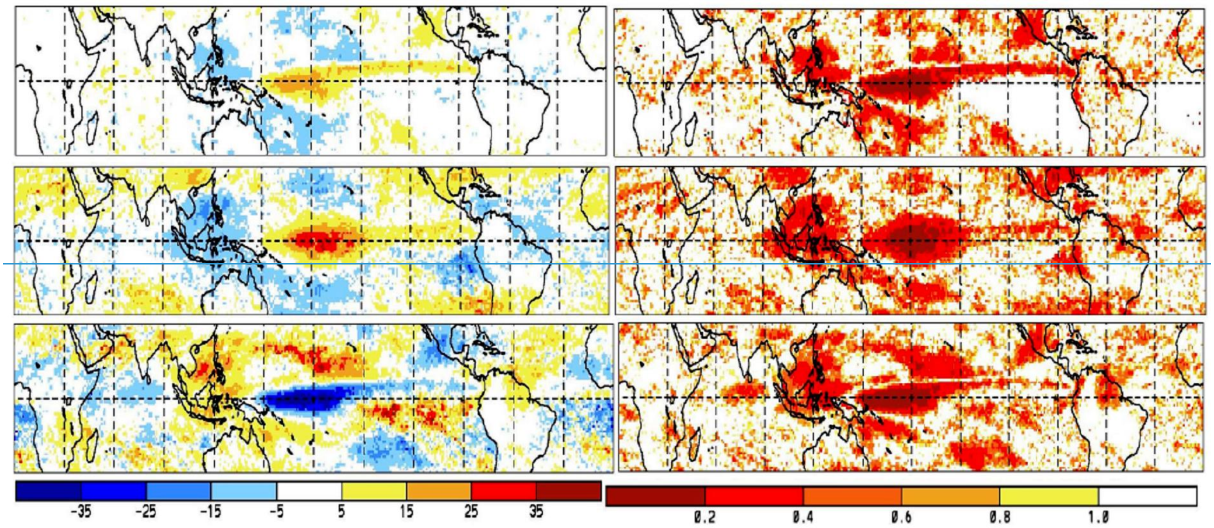

Figure 123~~7~~. ~~Left:~~ Geographical maps of linear regression s~~S~~lopes ~~of~~ between ~~change~~ monthly mean anomalies in amount of Cb (ε_{cld} > 0.95, top row), ~~cirrus~~ Ci (0.95 > ε_{cld} > 0.4, middle row) and thin ~~cirrus~~ Ci (0.4 > ε_{cld} > 0.1, bottom row) ~~amount~~ from AIRS-CIRS ~~in % per °C of tropical~~and global mean surface temperature anomalies ~~warming (20°N – 20°S)~~from ERA-Interim; left: p_{cld} < 440 hPa, middle: relative cloud amount,~~;~~ right: p_{cld} < 330 hPa and relative cloud amount. Results using ~~slope uncertainty for Cb (top), cirrus (middle) and thin cirrus (bottom) amount change per °C~~ of ~~tropical warming. Results using upper tropospheric (p_{cld} < 330 hPa) cloud type anomalies from AIRS-CIRS and surface temperature anomalies from ERA-Interim of~~ 156 months during the period 2003-2015.